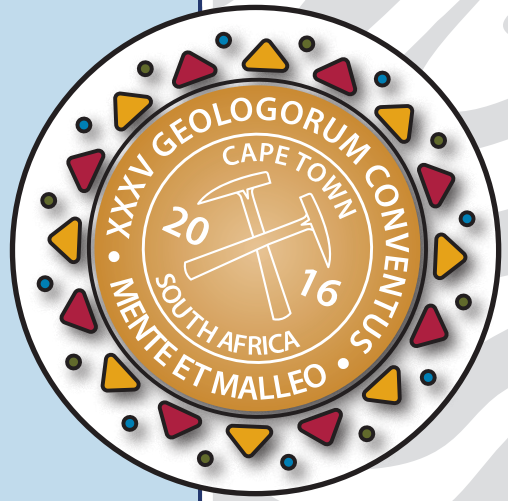


35th International Geological Congress
Field Trip Guide

THE PERMO–TRIASSIC BOUNDARY IN THE KAROO BASIN

Johann Neveling¹, Robert A. Gastaldo², John W. Geissman³



¹ Council for Geoscience,
Pretoria, South Africa

² Colby College, Waterville,
ME, USA

³ University of Texas at Dallas,
Richardson, TX, USA



The Caledon River meandering past Late Permian rocks exposed near the town of Bethulie.

22–27 August 2016
Field Trip Guide
Pre3



PERMO–TRIASSIC BOUNDARY IN THE KAROO BASIN

by **Johann Neveling¹, Robert A. Gastaldo², John W. Geissman³**

¹Council for Geosciences, Pretoria, South Africa

²Colby College, Waterville, ME, USA

³University of Texas at Dallas, Richardson, TX, USA

Field Trip Guide PRE 3
22–27 August 2016



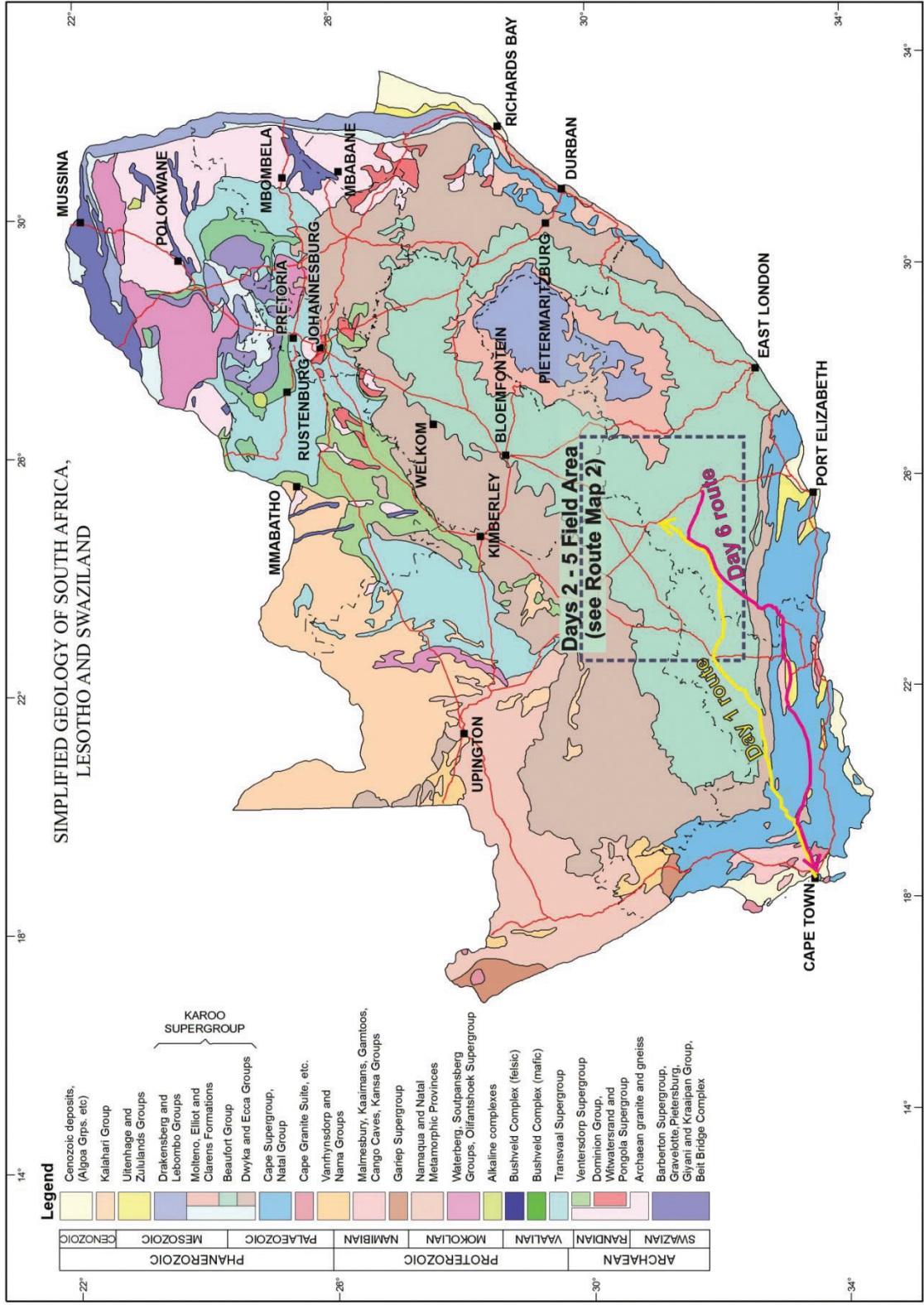
CONTENTS

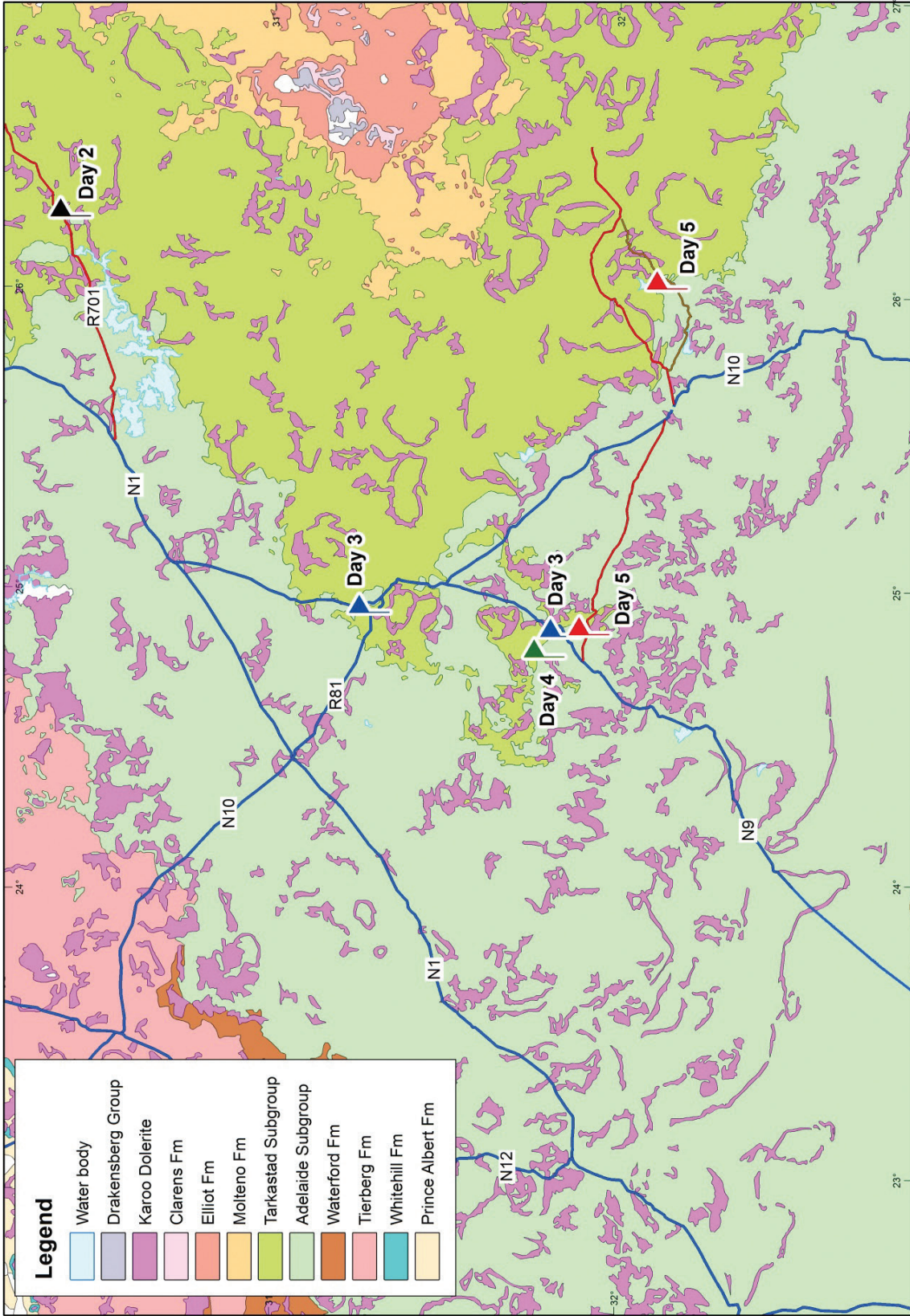
Safety in the field	7
1. Introduction	9
1.1 Basin Setting	9
1.2 Lithostratigraphy	9
1.3 Vertebrate Biostratigraphy	10
2. RELATIVE AGE	12
3. ORIGIN OF AN EXTINCTION MODEL	14
4. REFINEMENT OF THE EXTINCTION MODEL	15
4.1 Stratigraphy	15
4.2. Correlation with the global record	18
4.3 Palaeoenvironmental Extinction Model	22
5. CONCERNS ABOUT THE PTB MODEL	23
5.1 Stratigraphic Resolution	23
5.2 Palaeoenvironmental Model	24
5.3 Global Correlation and Age	26
6. SUMMARY	27
7. AUGUST (DAY 1): CAPE TOWN TO MIDDELBURG	28
7.1 Timetable	28
7.2 Directions	28
7.3 Geological Background	28
7.4 Geological Features on the Route	30
7.4.1 Paarl batholith	30
7.4.2 Uitenhage Group remnant, Worcester	30
7.4.3 Hex River Anticline, De Doorns	31
7.4.4 Dwyka and Ecca groups exposures, Matjiesfontein	31



7.4.5 Laingsburg flood	31
7.4.6 Laingsburg turbidites	32
7.4.7 The Escarpment	32
8. 23 AUGUST (DAY 2): BETHULIE LOCALITY	32
8.1 Timetable	32
8.2 Directions	32
8.3 Background	32
Stop 2-1: Permo–Triassic Boundary sequence	33
Stop 2-2: Contact between dolerite sill and host rocks, palaeomagnetic results	34
Stop 2-3: Palaeomagnetic data from Bethulie	39
Stop 2-4: Lateral Lithofacies Continuity – Section 1	41
Stop 2-5: Lateral Lithofacies Continuity – Section 3	43
Stop 2-6: Review of fossil localities	43
9. 24 AUGUST (DAY 3): CARLTON HEIGHTS AND LOOTSBERG PASS	45
9.1 Timetable	45
9.2 Directions	45
9.3 Relevant Background	45
CARLTON HEIGHTS	48
Stop 3-1: Railroad Exposure	48
Stop 3-2: Section	49
Stop 3-3: Katbergia burrows, the Fungal Spike and Detrital Zircons	49
Stop 3-4: Lower Katberg Formation sedimentology	50
Stop 3-5: Multistoried Katberg Sandstones	51
LOOTSBERG PASS	52
Stop 3-6: Overview of Lootsberg Pass area	52

10. 25 AUGUST (DAY 4): OLD LOOTSBERG PASS	53
10.1 Timetable	53
10.2 Directions	53
10.3 Relevant Background	54
Stop 4-1: Orientation	54
Stop 4-2: Early Changhsingian Porcellanite	54
Stop 4-3: Interval of reversed polarity	58
Stop 4-4: Laterally Accreted Bedsets	58
Stop 4-5: Biostratigraphically derived PTB.	59
Stop 4-6: Multistoried sandstone	59
Stop 4-7: Plant Fossil Locality	59
Stop 4-8: Traverse of Katberg Formation	61
11. 26 AUGUST (DAY 5): WAPADSBERG PASS AND COMMANDO DRIFT	62
11.1 Timetable	62
11.2 Directions	63
Stop 5-1 Orientation, Changhsingian paleosols, and a <i>Glossopteris</i> megaflora	63
Stop 5-2 Geometrically Spaced, Pedogenic Nodules	66
Stop 5-3 Fine-grained Fluvial Architectural Elements	66
Stop 5-4: Commando Drift	66
12. 27 AUGUST (DAY 6): CRADOCK TO CAPE TOWN	68
12.1 Timetable	68
12.2 Directions	68
12.3 General Geology	69
13. ACKNOWLEDGEMENTS	70
14. LITERATURE CITATIONS	71





SAFETY IN THE FIELD

We hope you enjoy visiting South Africa and, especially, participating in this excursion. However, please be aware that risk is an unavoidable part of any field excursion. Although the excursion leaders will take all necessary precautions and attempt to make this excursion as safe as possible, please note that you are primarily responsible for your own safety. Consequently, please peruse the following and please adhere to the safety protocols.

General protocols

All participants have to be aware at all times of the potential dangers and injuries that could be caused by their actions. Therefore, please act responsibly. Please try to prevent accidents, not only to yourself but also to the other participants. Please observe and follow the safety instructions from the excursion leaders, and please alert the leaders to any risks that could arise.

1. Please inform the tour leaders of any potentially hazardous medical conditions (e.g. allergies, asthma, epilepsy, acrophobia, and the like). It is assumed that all participants are aware of their own allergies, have taken the appropriate precautions, and have the appropriate emergency medication at hand. Please advise your trip leader to possible serious allergic reactions that could arise (e.g. bee-stings) and the appropriate emergency response.
2. We will on several occasion stop alongside busy roads. Please be aware of the dangers of roadside stops, be alert, observe traffic movement, and warn the other participants of potential danger.

Always exit the vehicle on the left hand side and stay away from the road shoulder. Please exercise care when crossing the road. Remember that traffic might come from a direction you are not used to and therefore will not expect. It is advisable to look carefully both right and left before crossing the road. Remember that wind or other noise could obscure the audible warnings of approaching vehicular traffic. Please never assume that the driver of any vehicle, and especially of heavy trucks, would notice you in time to avoid an accident.

3. Criminal activity is of low concern in the rural areas we shall visit. However, it would be prudent to remain vigilant when we visit the larger towns in the Karoo.
4. To ensure the safety of every participant and the smooth running of logistical arrangements, please refrain from wandering off too far in the field. However, there will be sufficient opportunity to explore the outcrops on your own.
5. Outcrops in road cuts can be unstable, so do be careful and do ensure you have proper footing when you walk around. Take extra care under windy conditions, especially if the wind is gusting when you are in an exposed position. Be aware of falling stones and overhead hazards and do warn others about potential danger.

We will do lots of walking over terrain with few or no footpaths. The surface is often covered with loose stones. Please wear appropriate shoes and take care when walking over uneven terrain. Please be careful near wire fences, which could snag loose clothing. Please ask if you require assistance.

6. Look out for scorpions, spiders, or snakes that could be hiding under the rock you might be picking up. Snakes are normally inactive during the winter months, but become active again during early spring. It is best not to disturb them. In turn, they will not normally attack. Similar to other wild animals, snakes are likely to present a hazard if startled at close quarters. Therefore, watch where you place your feet and hands.
7. The fierce African sunlight can cause serious sunburn. Cloud cover is no protection against UV radiation, while conditions such as clear blue sky, midday sun, and reflection from water greatly increase such radiation. Use sunscreen with an appropriate protection factor (highest!) and wear sunglasses to protect your eyes. Ensure that you expose as little as possible skin, and remember to protect your neck and scalp.
8. The Karoo is a dry region and although our visit takes place during a cool time of the year, it is still extremely easy to dehydrate. Therefore, take along and drink enough water. Mostly, the tap water of the accommodation establishments will be safe to drink.

9. Remember that research is continuing at many of the localities that we shall visit; therefore, do not remove any fossils that we might encounter in the field. It is most important to note that according to South African law, all fossil material belongs to the state and it is illegal to collect such material without the necessary permit.
10. Do not leave any refuse behind when you depart. Do not write or make any marks on any rock surfaces. Please leave only your footprints.
11. Enjoy your time in the Karoo!

1. INTRODUCTION

“I never pay attention to anything by ‘experts.’ I calculate everything myself.”

Richard Feynman, Nobel Prize in Physics, 1965

The end-Permian mass extinction is considered to represent generally the most severe ecological upheaval in the history of life, with an estimated species diversity loss in excess of 90%. The cause of this mass extinction is still a matter of debate, but a number of environmental crises (sometimes in combination) have been proposed, including hypoxia, hypercapnia, supervolcanic activity, ocean acidification, global warming, and ozone layer destruction. Our knowledge of this extinction is based largely on the marine record where this event has been dated at ca. 251.9 Ma (Burgess *et al.*, 2014). The terrestrial expression of this extinction is not as well understood, but is considered generally to be represented by the poorly dated boundary between the *Daptocephalus* (previously *Dicynodon*; Viglietti *et al.*, 2016) and the overlying *Lystrosaurus* Assemblage Zones (AZs) in the Karoo Basin, South Africa. The palaeo-environmental models that have been developed, based on the continental stratigraphic record in the Karoo Basin, play a central role in our understanding of the terrestrial ecosystem response to the end-Permian perturbation.

There has been some debate about the proposed extinction model applicable to the Karoo. This issue has been difficult for the scientific community to resolve because of the difficulty in locating and accessing the relevant sites. Research on this boundary interval in the Karoo has been concentrated at ten localities, namely, Bethulie, Caledon, and Nooitgedacht near the town of Bethulie in the Free State Province, and Carlton Heights (Middelburg, Eastern Cape Province), Commando Drift (close to Cradock, Eastern Cape Province), Ripplemead, Old Wapadsberg Pass, (East) Lootsberg Pass, Tweefontein, and Old (West) Lootsberg Pass (all close to Graaff-Reinet, Eastern Cape Province). This field trip will provide delegates with the opportunity of visiting and assessing some of the significant boundary localities.

1.1 Basin Setting

Any assessment of the reported Permo–Triassic Boundary (PTB) localities in the Karoo Basin needs to be done in context of their basinal and stratigraphic setting. For this purpose, a brief overview of the basin setting and stratigraphy is provided.

Several depositional basins formed in southern Gondwana during the late Paleozoic, as the result of the unique combination of tectonic stresses associated with shortening and accretion along the southern margin of Gondwana, together with extensional stresses propagating southward from the divergent Tethyan margin (Wopfner, 2002). The most extensive of these depositional basins is the Karoo Basin, named after the semi-desert region in the southern hinterland of South Africa. The Karoo Basin contains a sedimentary record that stretches from the Late Carboniferous to the Middle Jurassic (Johnson *et al.*, 2006). This basin formed to the north of the Cape Fold Belt, which borders the southern rim of the continent and is considered the source of much of the sediment that filled the basin (Rubidge, 2005). Most workers interpreted the Karoo Basin as a foreland basin (Johnson, 1991; Cole, 1992; Catuneanu *et al.*, 1998; Catuneanu *et al.*, 2002; Johnson *et al.*, 2006), but alternative interpretations have been proposed. These include a transtensional foreland system (Tankard *et al.*, 2009), a thin-skinned fold belt that developed because of collisional tectonics and more distant subduction to the south (Lindeque *et al.*, 2011), and a hypothetical mantle-plume related model (Turner 1999).

1.2 Lithostratigraphy

The dominantly sedimentary fill succession, referred to the Karoo Supergroup, crops out over the central and eastern parts of South Africa and is highly asymmetrical. The thickest sedimentary sequence is in the southwest part of the basin and this thins rapidly to the northeast. The supergroup contains four main sedimentary lithostratigraphic subdivisions, namely, the Dwyka, Ecca, Beaufort, and (informal) Stormberg groups, capped by Middle Jurassic basalts of the Drakensberg Group. The sedimentary units represent a general shift from cold and semi-arid conditions during the Late Carboniferous—earliest Permian interval, to warmer and eventually hot climates in the Jurassic. The Dwyka and Ecca groups consist primarily of sediments derived from glacial processes transported to a marine-to-coastal setting, whereas the Beaufort and Stormberg groups represent deposition in a fully continental setting. Johnson (1966, 1976) subdivided the fluvial Beaufort Group into a lower Adelaide and upper Tarkastad Subgroup. Separate formations are recognised for the Adelaide Subgroup exposed in the southwest, southeast, and north (Keyser and Smith, 1978; S.A.C.S., 1980; Groenewald, 1989), with the Koonap, Middleton, and Balfour formations recognised in the southeast (Fig. 1). Lithological variation in the Balfour Formation enabled the elucidation of five lithostratigraphic members, namely, Oudeberg, Daggaboersnek, Barberskrans, Elandsberg, and Palingkloof. The uppermost Palingkloof Member is characterised by the red colour of its mudstones, compared with the greenish-grey coloured mudstones of the preceding Elandsberg Member (Johnson, 1976; S.A.C.S., 1980).

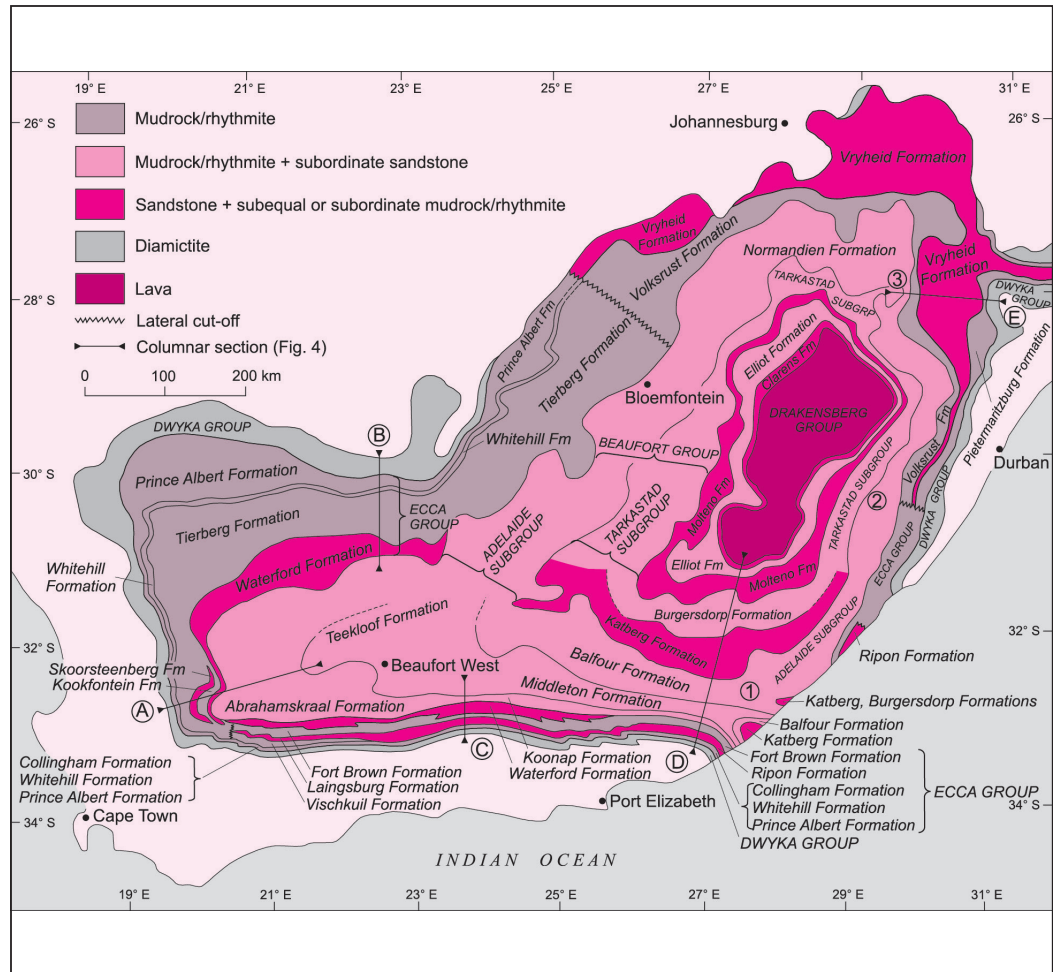


Figure 1. General map showing the distribution of the lithostratigraphic units of the Karoo Supergroup currently accepted by the South African Committee for Stratigraphy (S.A.C.S., Johnson *et al.*, 2006).

The overlying Tarkastad Subgroup, which is absent in the western half of the Karoo Basin (Keyser and Smith, 1978; S.A.C.S., 1980), consists of the Katberg and Burgersdorp formations. The Katberg Formation forms the lower unit of the Tarkastad Subgroup and is currently defined as an arenaceous unit, with varying amounts of red and olive-yellow mudrock (Groenewald, 1996). The occurrence of thick sandstone bodies, often exposed along roadways and associated with reddish mudstone, along with other field characteristics that include grain size differences, a reduced mudrock component, and a low scatter of palaeocurrent indicators (Johnson *et al.*, 2006), separate the Katberg strata from the underlying units. The placement of the Balfour–Katberg boundary is problematic because the sandstone content in the Katberg Formation decreases in a northward direction, and, north of latitude S 32° sandstone does not always predominate in the Formation (Johnson, 1976). In addition, the Palingkloof Member of the Balfour Formation coarsens upward (Smith, 1995). Consequently, this contact could manifest as either a conformable surface or a transitional boundary (Johnson, 1976). Because of the common occurrence of gradational contacts in the Eastern Cape Province, Groenewald (1996) proposed to define the base of the Katberg Formation as the point where the sandstone:mudstone ratio increases abruptly.

1.3 Vertebrate Biostratigraphy

The Beaufort Group, the thickest and most extensive of the lithostratigraphic units of the Karoo Supergroup, is particularly rich in fossils. This attribute has afforded an opportunity to establish an internationally recognised biozonation for Middle Permian to Middle Triassic terrestrial tetrapods (e.g. Lucas, 2010). The current biozonation scheme is based largely on a biostratigraphic subdivision proposed by Broom (1906), who established a six-fold biozonation. This was the standard for nearly 75 years until the first revisions were made by Kitching (1971, 1977), with subsequent modification by Keyser and Smith (1978). The biostratigraphic systems of Keyser and Smith (1978) and Keyser (1979) were accepted by the South African Committee for Stratigraphy (S.A.C.S., 1980) as formal nomenclature, but were modified by Rubidge *et al.* (1995) after a comprehensive review. The latter authors added a new biozone at the base of the Beaufort Group (Rubidge *et al.*, 1995), increasing the number of biozones to eight (Fig. 2), of which all are still currently recognised.

Some clarification is needed on the naming convention for the biozone, often considered to represent the latest Permian. The *Daptocephalus* Zone of Kitching (1971, 1977) was renamed the *Dicynodon lacerticeps* AZ by Keyser and Smith (1978), because the former taxon was considered to represent a junior synonym of *Dicynodon lacerticeps*. Subsequently, this biozone has been referred to as the *Dicynodon* AZ in PTB studies (Smith, 1995; Ward *et al.*, 2000, 2005; Smith and Botha-Brink, 2014), following the scheme of Rubidge *et al.* (1995). The systematic nomenclature of these vertebrates was revised with the work of Kammerer *et al.* (2011), who conducted a comprehensive taxonomic review of the *Dicynodon lacerticeps*, the index taxon of the *Dicynodon* AZ. However, Kammerer *et al.* (2011) have decided to resurrect the genus *Daptocephalus* and have expressed uncertainty about the stratigraphic ranges of the remaining *Dicynodon* species. Angielczyk and Kurkin (2003) have cautioned against the use of the latter genus to correlate successions in other widely separated basins.

Recently, Viglietti *et al.* (2016) reassessed the stratigraphic range of *Dicynodon* and redefined the *Dicynodon* AZ as the *Daptocephalus* AZ. In addition, these authors have subdivided the assemblage zone into upper and lower intervals. Currently, the lower unit is characterised by the first appearance of *Daptocephalus leoniceps* and *Theriongnathus microps*, whereas the upper part of the biozone is characterised by the presence of *Lystrosaurus maccaigi*, a species considered absent from the *Lystrosaurus* AZ (Smith and Botha, 2005; Botha and Smith, 2007; Viglietti *et al.*, 2016). In general, the lower part of the *Daptocephalus* biozone shows greater faunal biodiversity than the upper part. Maintaining the current paradigm, all the references to the *Daptocephalus* AZ in this guide include references to the *Dicynodon* AZ by previous workers.

Kitching (1995) reported that the *Daptocephalus* (*Dicynodon*) AZ occupied the larger part of the Balfour Formation in the southeastern sector of the basin, which roughly equates with the Teekloof Formation in the southwest. He placed the base of the biozone at the top of the arenaceous Oudeberg Member of the Balfour Formation, and the top of the biozone in the middle of the Palingkloof Member. Viglietti *et al.* (2016) moved the base of the biozone down to the middle of the Oudeberg Member (Fig. 3), based on revised stratigraphic ranges for *Daptocephalus leoniceps* and *Theriongnathus microps*. With the loss of what are considered latest Permian taxa, the overlying *Lystrosaurus* AZ is held to mark the earliest Triassic, with the advent of two taxa, *L. declivus* and *L. murrayi*.

Other than *Lystrosaurus declivus* and *L. murrayi*, common forms of the *Lystrosaurus* AZ include several cynodonts (*Thrinaxodon* and *Galesaurus*), an archosaur (*Proterosuchus*), and amphibians (e.g. *Lydekkerina* and *Micropholis*). *Lystrosaurus*, *Thrinaxodon*, *Procolophon* and the amphibian *Lydekkerina* are found frequently as articulated skeletons preserved within calcareous nodules (Groenewald and Kitching, 1995), whereas fossils of the first three genera have been found also associated with vertebrate burrows (Groenewald, 1991, 1996).

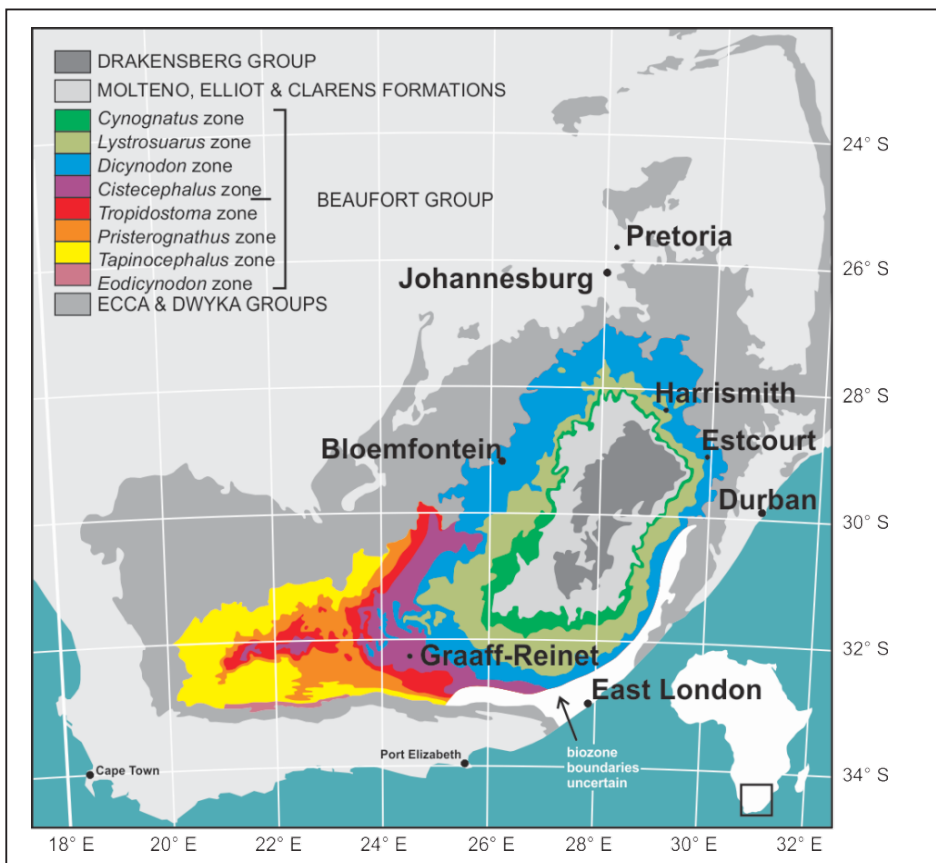


Figure 2. Map showing the distribution of the vertebrate biozonation in the Beaufort Group (Karoo Basin, South Africa).

AGE	LITHOSTRATIGRAPHY		BIOZONES	U-Pb Zircon Age	
TRIASSIC	BEAUFORT GROUP	Burgersdorp Fm.	<i>Cynognathus</i>		
		Katberg Fm.	<i>Lystrosaurus</i>		
PERMIAN	BEAUFORT GROUP	Balfour Fm.	Palingkloof Mb		
			Elandsberg Mb		
			Baberskrans Mb	<i>Daptocephalus</i>	← 253.5 Ma*
			Daggaboersnek Mb		
			Oudeberg Mb		← 255.2 Ma**
			Middleton Fm.	<i>Cistecephalus</i>	← 256.25 Ma**
		Koonap Fm.	<i>Tropidostoma</i>	← 259.26 Ma** ← 260.41 Ma**	
		<i>Pristerognathus</i>	← 261.24 Ma**		
		<i>Tapinocephalus</i>			
		<i>Eodicynodon</i>			
		arenaceous unit			

Figure 3. Lithostratigraphy, biostratigraphy, and chronometric ages of the Beaufort Group (note that the stratigraphic unit thicknesses are not to scale). Stippled line 1 in column one represents the previously reported position of the PTB (Smith and Botha-Brink, 2014). Stippled line 2 represents the hypothesised position of the PTB proposed by Gastaldo *et al.* (2015). The position of the base of the *Daptocephalus* AZ is based on Viglietti *et al.* (2016). The white arrows in the last column depict the stratigraphic positions of volcanic ash beds that yielded the U-Pb ID-TIMS ages reported by Gastaldo *et al.* 2015 (*) and Rubidge *et al.*, 2013 (**). The stippled, red, double arrow depicts the position of the boundary interval described in the literature (Smith and Ward, 2001; Smith and Botha-Brink, 2014). The blue, solid, double arrows depict the approximate stratigraphic distance from the porcellanite reported by Gastaldo *et al.* (2015) to the base (~440 m) and top (~60 m) of the *Daptocephalus* AZ.

Traditionally, the *Lystrosaurus* AZ has been considered to span the Katberg Formation, extending into the superjacent lithostratigraphic units (Groenewald and Kitching, 1995). The first elements of the *Lystrosaurus* AZ fauna appear in the Palingkloof Member of the Balfour Formation (Keyser and Smith, 1978; Stavakis, 1980), and traditional views hold that the uppermost *Lystrosaurus* AZ continues up into the lower third of the Burgersdorp Formation (Keyser and Smith, 1978; Groenewald and Kitching, 1995). However, Neveling *et al.* (2005) demonstrated that the overlying *Cynognathus* AZ correlates with the entire Burgersdorp Formation in South Africa, which means that the *Lystrosaurus* AZ is restricted to the Palingkloof Member of the Balfour and Katberg formations (Fig. 3).

The primary focus of this field trip will be on the exposures of the Elandsberg and Palingkloof members (Balfour Formation), and the base of the Katberg Formation that encompasses the upper *Daptocephalus* and lower *Lystrosaurus* AZs. Accordingly, the transition from the latest Permian to earliest Triassic and, therefore, the Permian–Triassic boundary, as currently held, will be evaluated.

2. RELATIVE AGE

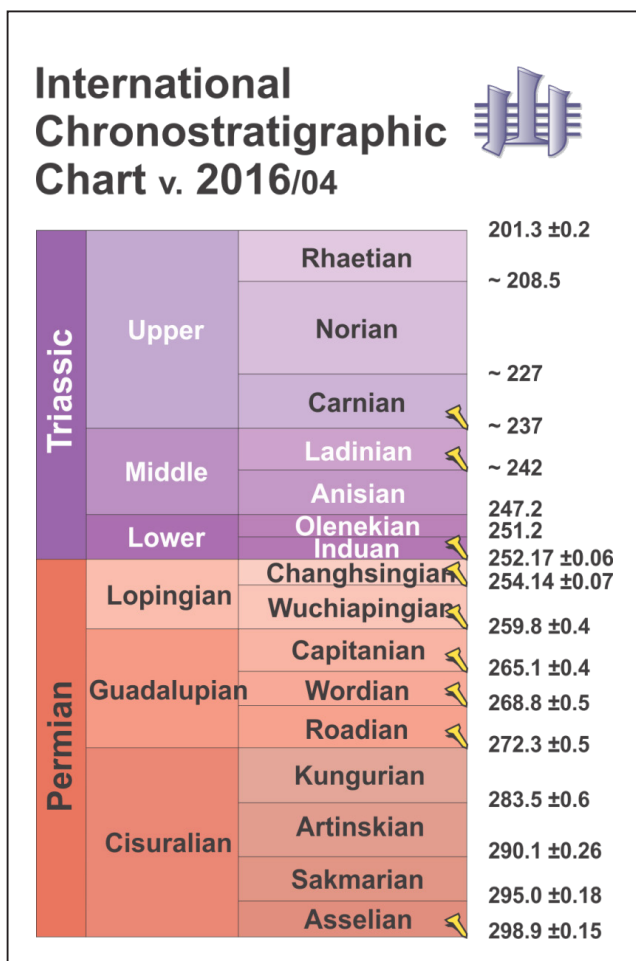
Until recently, relative ages were assigned to the various biozones of the Beaufort Group because of a lack of horizons that could be dated by geochronometric methods. Broom (1906) first assigned the *Lystrosaurus* Zone to the Triassic, and the underlying biozones, including the interval encompassing the *Daptocephalus* AZ, to the Late Permian. The logic and reasoning for these age assignments are unstated in the literature and may have reflected the prevailing assumption at the time. The Permian age for the *Daptocephalus* AZ remained unchallenged for more than a century, seemingly based on strong biostratigraphic correlation of the underlying *Cistecephalus* AZ (Smith and Kitching, 1995) with better-dated sequences in India (Kutty, 1972), South America (Keyser, 1981), and Russia (Boonstra, 1969), as well as by linking sedimentary sequences in the Karoo with dates obtained for tectonic events in the Cape Fold Belt (Halbich, 1983). The Permian age was confirmed by the publication of Guadalupian to Lopingian (Fig. 4) U-Pb ID-TIMS age estimates for the Adelaide Subgroup strata (Fig. 3) by Rubidge *et al.* (2013). Until recently, though, no marker horizons that could be dated by geochronometric methods have been reported for either of the uppermost two biozones of the Beaufort Group. In view of these constraints, relative ages have been assigned to the *Lystrosaurus* AZ based on palaeontological correlations. Biostratigraphic correlation with vertebrate assemblages in other basins has placed

the age of the *Lystrosaurus* AZ in close association with the age assigned to the overlying *Cynognathus* AZ. This correlation has been accepted because the latter assemblage zone contains a greater number of cosmopolitan taxa that allowed for correlation with the type sequences of the Triassic exposed in Europe and North America.

The *Lystrosaurus* Zone was assigned initially to the Early Triassic (Broom, 1906; 1932), but its placement was not accepted unreservedly by all workers. Subsequently, the Early Triassic assignment of the assemblage zone was questioned by several workers. For example, Watson (1942) assigned the *Cynognathus* AZ to the Lower Triassic, based on the similarities of its amphibian fauna with the Middle Bunter Sandstone (Buntsandstein) in central Europe and the Russian Zone VI (Efremov, 1940). In this age assignment, the preceding *Lystrosaurus* AZ was considered of Permian age. Cosgriff (1965) correlated the *Cynognathus* AZ with the Blina Formation of Western Australia and the *Posidonomya* beds of Spitzbergen (Norway). Cosgriff's correlation was based on the taxonomic affinities of the rhytidosteid amphibian *Rhytidosteus*, then (1965) still assigned to the *Cynognathus* AZ (Broom, 1907, 1909), with *Deltasaurus* (Australia) and *Peltostega* (Spitzbergen). In the mid-20th Century, the *Posidonomya* beds of Spitzbergen were assigned to the Scythian (Lower Triassic), based on the rich ammonite fauna it contained, and a similar age was assigned to the *Cynognathus* AZ. Since Cosgriff (1965) considered the amphibian fauna of the *Lystrosaurus* AZ more primitive than that of the *Cynognathus* AZ, he placed the *Lystrosaurus* AZ in the Late Permian.

Subsequently, the stratigraphic position of the amphibian genus *Rhytidosteus* was reassigned to the *Lystrosaurus* AZ (Kitching, 1978; Cosgriff and Zawiski, 1979; Groenewald and Kitching, 1995), suggesting that the assemblage zone should be reassigned to the early Scythian. Therefore, Cosgriff (1984) abandoned his earlier view and correlated the amphibians of the *Lystrosaurus* AZ with amphibians found in the early Scythian assemblages elsewhere in the world. Marine invertebrates associated with tetrapod fossils in various Scythian assemblages indicate that this biozone should be placed in the Induan or lower Olenekian (Cosgriff, 1984).

The concepts used by Cosgriff (1965, 1984) followed the earlier work of Romer (1966, 1969), Cox (1967), and Colbert (1969) who all reviewed the continental vertebrate faunas of the Triassic. They placed the *Lystrosaurus* AZ in the Lower Triassic, based on the co-occurrence of amphibian taxa in this biozone and Greenland, and on the occurrences of *Lystrosaurus* in Asia (Romer, 1969). After the discovery of *Lystrosaurus* in rocks in Russia, assigned to the Lower Triassic (Scythian) based on a conchostracan fauna (Kalandadze, 1975), most workers accepted an Early Triassic age for the *Lystrosaurus* AZ (Anderson and Cruickshank, 1978; Battail, 1993; Groenewald and Kitching, 1995). The only dissenting voice at the time was that of Cooper (1982).



Cooper (1982) reassigned the *Lystrosaurus* AZ to the Permian, based on an Induan age he had proposed for the *Cynognathus* AZ. His Induan age for the *Cynognathus* AZ was based on a correlation of the amphibian genera from the *Cynognathus* AZ with taxa recovered from the Andavakoera Formation of northern Madagascar and the Vetluga and Baskunchak Series of the Russian Platform. The age assignment of the Malagasy rocks was based on ammonite biostratigraphy. However, the Madagascar assemblages used by Cooper (1982) were poorly known at the time and subsequent research indicated that he had mixed and correlated dissimilar assemblages (Ochev and Shishkin, 1989). In consequence, by the beginning of the 1990s, when more focussed research on the end-Permian extinction commenced, an Early Triassic age for the *Lystrosaurus* AZ was widely accepted.

The exact position of the PTB in the Karoo Basin continued to be a matter of debate. Turner (1979) placed the PTB in the base of the *Lystrosaurus* Zone, contrasting with the approach of Anderson

Figure 4. Chronostratigraphic chart for the Permian and Triassic. (Modified from the chronostratigraphic chart released by the IGC in April 2016).

and Cruickshank (1978), who were the first to correlate the first occurrence of the dicynodont genus *Lystrosaurus* with the end-Permian extinction. Dingle (1978) and Hiller and Stavrakis (1984) placed the PTB at the first appearance of *Lystrosaurus*, which they associated with the base of the Palingkloof Member. This position continued to gain acceptance into the late 20th Century.

3. ORIGIN OF AN EXTINCTION MODEL

Smith (1995) first described a Permo–Triassic boundary section from what has been referred to in the literature as the Bethulie locality in the Free State Province (Day 2). At that time, the stratigraphic ranges of the *Daptocephalus* and *Lystrosaurus* AZ faunas were thought to be non-concurrent (Keyser and Smith, 1978), even though Hotton (1967) previously had reported overlap in the stratigraphic ranges of the index taxa. The latter observation was confirmed by the biostratigraphic ranges presented by Smith (1995, his fig. 3). These ranges showed a sharp turnover at the contact between the *Daptocephalus* and *Lystrosaurus* AZs, with the exception of the genus *Lystrosaurus*, showing an overlap of 25 m with the former biozone (Fig. 5). Although acknowledging that the Permo–Triassic boundary was not defined clearly, Smith (1995) interpreted the apparently sharp faunal turnover as representing the end-Permian extinction event in order to maintain uniformity with the more severe extinction recorded in the marine realm. Accordingly, the boundary was correlated with "...the uppermost occurrence of the *Dicynodon* (*Daptocephalus*) AZ fauna. ..." (Smith, 1995, p. 86), placed near the base of the Palingkloof Member. However, such assignment, contradicts later claims (Smith and Ward, 2001; Ward *et al.*, 2005) that the base of the *Lystrosaurus* AZ was associated traditionally with the base of the Katberg Formation.

From a sedimentological perspective, the succession in which the *Daptocephalus* AZ fauna is preserved is reportedly dominated (~80%) by greyish (bluish grey, dark-grey, greenish-grey) and even some purple siltstones, in which fine-grained single story (4–8 m) and multistory (10–25 m) ribbon sandstones and thin sand sheets are enveloped. Most workers agree with Smith's interpretation that these sediments accumulated in a meandering fluvial setting. However, it should be pointed out that the meander belt exposures on which Smith (1995, p. 87, his fig. 5) based this interpretation, crop out at the Reiersvlei locality, which exposes a section at a lower stratigraphic position in the Beaufort Formation and is geographically situated more than 400 km to the southwest (Smith, 1987). A colour change to reddish brown characterises

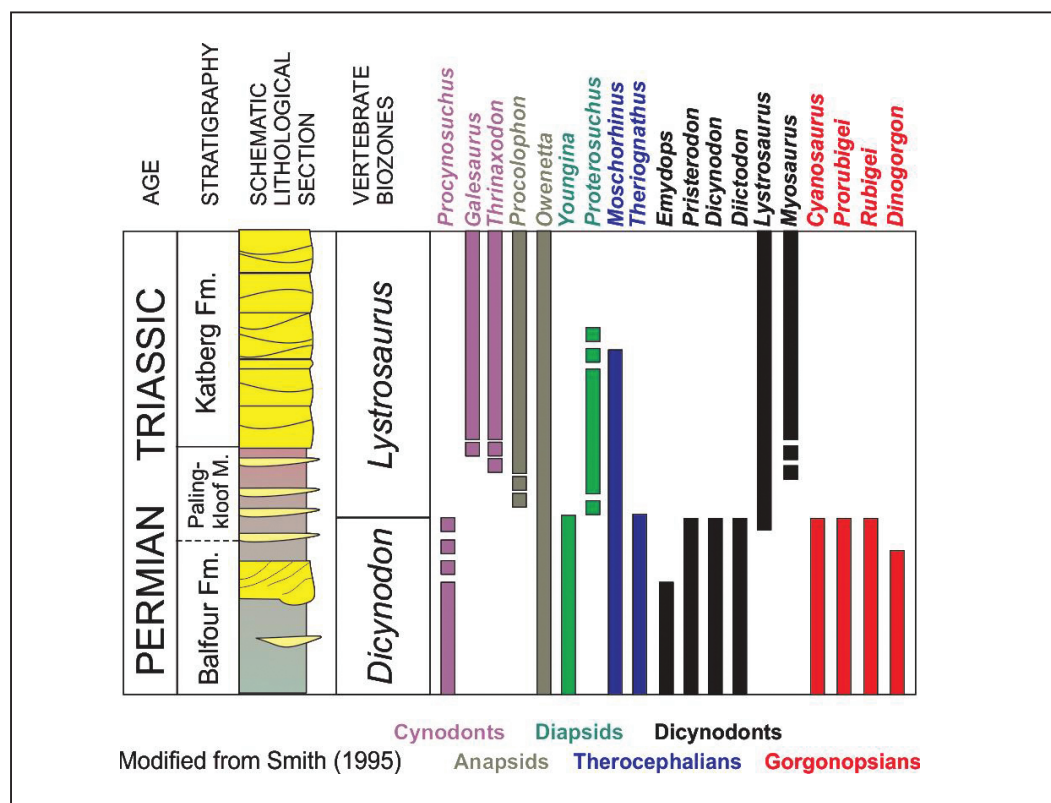


Figure 5. The traditional lithostratigraphy, predominant lithologies, biostratigraphy model, and faunal ranges associated with the *Dicynodon* (*Daptocephalus*)–*Lystrosaurus* AZ contact. (Figure from article published in *Palaeogeography, Palaeoclimatology, Palaeoecology*, v. 117, Smith, Changing fluvial environments across the Permian-Triassic boundary in the Karoo Basin, South Africa and possible causes of tetrapod extinctions, pp. 81–104, Copyright Elsevier, 1995).

the siltstones of the Palingkloof Member (reportedly more than 40 m thick) at Bethulie, with this change being combined with an increase in the frequency and thickness of sheet sandstones. The sandstone bodies are <5 m thick, and are reported to contain upper flow-regime sedimentary structures, which include gullied bases draped by matrix-supported intraformational conglomerate. The conglomerate consists of siltstone, pedogenic nodular (glaebules) clasts, and bone fragments. The latter could occur also as isolated lenses in the siltstone. This interval was interpreted to have been deposited in wide, shallow, ephemeral streams that were the precursors of the braidplains associated with Katberg sedimentation (Smith, 1995).

The pedogenic features associated with the greenish-grey siltstone of the *Daptocephalus* AZ from this interval were interpreted to reflect soil formation under a warm climate and strong seasonality, with an overall high water table. In contrast, the rubified calcic soil horizons of the overlying *Lystrorhynchus* AZ, together with an increased frequency of articulated vertebrate remains, were believed to be associated with warm, semi-arid climatic conditions. In this document, 'rubified' describes the colour changes, versus the process of *in situ* transformation of yellowish, amorphous ferric oxides under well-drained soils conditions exposed to a marked alternation of humid and pronounced dry seasons (Stoops, 1989). Following Hiller and Stavrakis (1984), Smith (1995) deemed both tectonic and climatic factors to have been responsible for the changes in the fluvial style across this interval, but considered tectonic processes to have been the primary driving force. A change from high to low-sinuosity fluvial environment was attributed to a pulse of tectonism in the Cape Fold Belt. The initiation of regional aridification over southern Gondwana was associated with this tectonic pulse and was linked to a decline in tetrapod diversity during the latest Permian. In this initial model, the tectonically induced change in fluvial regime introduced basinward migration of dry floodplain environments, which allowed the dry-adapted *Lystrorhynchus* communities to colonise the central parts of the basin to the detriment of the *Daptocephalus* AZ fauna that lived there. These communities were considered to have co-existed for a short period until a combination of shrinking habitat and competition resulted in the disappearance of the latter (*Daptocephalus*) fauna.

4. REFINEMENT OF THE EXTINCTION MODEL

4.1 Stratigraphy

Using the previous work of Smith (1995), Ward *et al.* (2000) introduced a sedimentologic model for the boundary interval, in which these authors delimited three distinct lithofacies associations (Fig. 6), linked with the pre-extinction, the boundary event, and the post-extinction

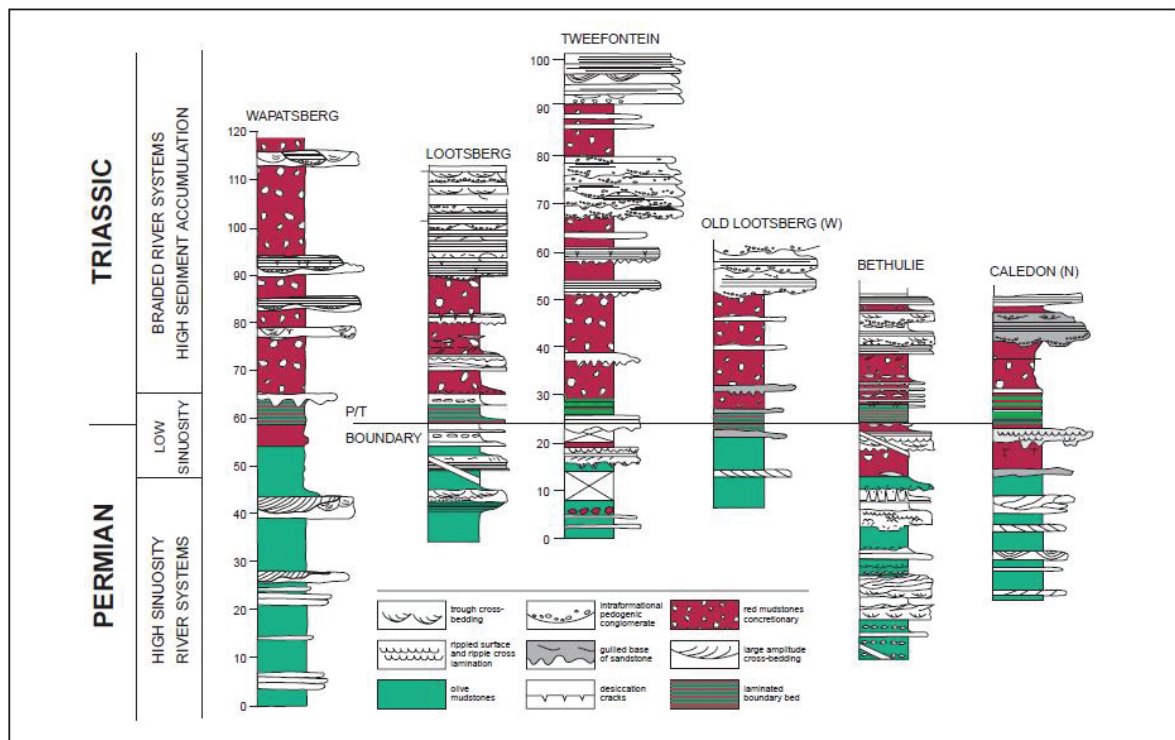


Figure 6. Proposed correlation of PTB localities reported by Ward *et al.* (2000, their fig. 1), based on the reported presence of a “unique” interval of laminated siltstone at each of these sections. (Figure from Ward *et al.*, 2000, Altered River Morphology in South Africa Related to the Permian-Triassic Extinction. *SCIENCE*, 289:1740. Reprinted with permission from AAAS).

landscapes. Subsequently, the model evolved to encompass five distinct lithofacies associations, with this work primarily based on two sections near Bethulie (Day 2; Free State Province) and five sections near Lootsberg Pass (Days 3–5; Eastern Cape Province; Ward *et al.*, 2000; Smith and Ward, 2001). Later, these localities were augmented by data reported from Carlton Heights (Day 3; Retallack *et al.*, 2003; Ward *et al.*, 2005), Commando Drift (Day 5; De Kock and Kirschvink, 2004; Ward *et al.*, 2005), and Ripplemead (Smith and Botha-Brink, 2014). Recently, a new boundary locality was described from the farm Nooitgedacht 68 in the Free State Province (Botha-Brink *et al.*, 2014). The boundary sequence, from bottom to top, can be summarised as follows.

The base of the succession (**lithofacies association A**) is characterised by massive, greenish-grey siltstone that predominates, with subordinate, thick, single-storied sandstone bodies (Ward *et al.*, 2000). Based on the lithofacies sequence evident in these sandstones and the presence of low-angle (10–15°) lateral accretion surfaces (Day 4) that typically extend throughout the thickness of the channel sandstone and into the overlying siltstone deposits (Ward *et al.*, 2000), this interval has been interpreted to represent meandering fluvial deposits (Smith and Ward, 2001; Smith and Botha-Brink, 2014). Lithofacies association A contains the largest diversity of vertebrate fossils belonging to the *Daptocephalus* AZ (Smith and Ward, 2001).

Overlying lithofacies association A is an interval (**lithofacies association B**) of massive, mottled maroon and greenish-grey mudrock, with thin, tabular sandstone bodies that display distinctive ‘gullied’ basal contacts (Smith and Ward, 2001; Smith and Botha-Brink, 2014). In past model versions, lithofacies association B was part of the first lithofacies association (Ward *et al.*, 2005; Smith and Botha, 2005; Botha and Smith, 2006). Smith and Ward (2001) reported a single horizon of “large brown-weathering calcareous nodules” from the uppermost siltstone of this interval, which they considered the lithological expression of the PTB (Day 2). Subsequently, the uppermost concretion-bearing siltstone was referred to as the “End-Permian Paleosol” (EPP; De Kock and Kirschvink, 2004), but the concept appears to have been abandoned in nearly all subsequent papers (see Coney *et al.*, 2007, who continued to use this concept). Fossil remains of the *Daptocephalus*

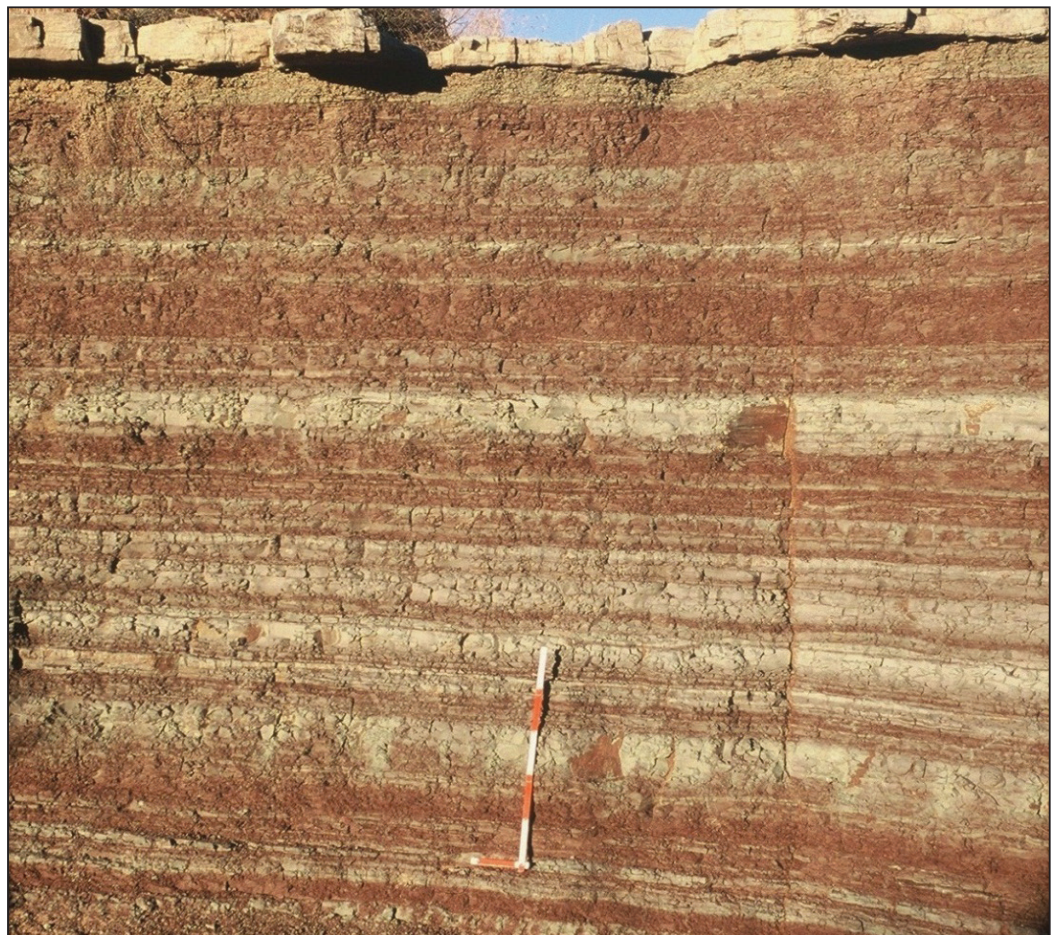


Figure 7.

Very thin bedded siltstones (lithofacies association C), interpreted by some to represent an “event bed” associated with the end-Permian extinction on land. This exposure was documented at a locality in the Tussen-die-Riviere Game Park, south of the Caledon River, reported by Retallack *et al.* (2003, their fig. 3B). Less than 10 m of section is exposed at this locality and it is bounded at the base by a rare, normal fault.

AZ are comparatively rare in this second unit (Smith and Botha, 2005), while the ichnogenus *Katbergia* (Gastaldo and Rolerson, 2008) reportedly makes its first appearance in this interval (Smith and Botha-Brink, 2014).

The third lithofacies association (**lithofacies association C**) was introduced first by Ward *et al.* (2000) and has been associated subsequently by many workers with the Permo–Triassic Boundary (PTB) itself (Days 2–3). It is described as a laminated mudrock interval (Fig. 7), 3–5 m thick (Smith and Ward, 2001; Ward *et al.*, 2005; also refer to Retallack *et al.*, 2003; Coney *et al.*, 2007; Botha-Brink *et al.*, 2014) that consists of dark reddish–brown (2.5YR 3/4; 2.5YR 2.5/4) and olive-grey (5Y 5/2; Smith and Botha, 2005; Botha and Smith, 2006) siltstone–mudstone couplets, each 1–3 cm thick (Smith and Ward, 2001; Smith and Botha-Brink, 2014). These very thin beds have a sharp, flat basal bounding surface, fine upwards (Smith and Botha-Brink, 2014), and contain very thin laminae (i.e., light–dark alterations), interpreted as varves (Retallack *et al.*, 2003; Smith and Botha, 2005). Their upper surfaces commonly display oscillation ripples and textures reminiscent of algal mat impressions (Smith and Botha-Brink, 2014). Smith and Botha-Brink (2014) considered a single horizon of large, brown-weathering calcareous nodules, now reported from the top of this interval (Smith and Botha, 2005), to represent a workable lithologic marker of the end-Permian in the southern Karoo Basin. This lithofacies association has been considered unique, with rooting structures, *Katbergia* burrows, and nodules being the only evidence of pedogenesis. In addition, Retallack *et al.* (2003) described a 10 cm thick claystone breccia from the laminated interval, but the presence of this facies has not been corroborated by subsequent publications. A dearth of vertebrate remains recovered from this facies association led previous workers to place the PTB at the base of this interval (Smith and Ward, 2001; Ward *et al.*, 2005). Subsequently, the vertebrate-defined PTB was moved to the top of this lithofacies association when prospecting yielded an impoverished *Daptocephalus* AZ in this interval.

The appearance of lithofacies association C has been termed an “event” by various workers (Smith and Ward, 2001; Ward *et al.*, 2005; Smith and Botha, 2005; Smith and Botha-Brink, 2014) and the characteristics of this interval have been used by many as the definitive PTB marker (Botha-Brink *et al.*, 2014; Viglietti *et al.*, 2016; Rubidge *et al.*, 2016). The “event bed”, described at Bethulie, Lootsberg Pass, and other localities was not used initially in a time connotation. Instead, it was used to describe rapid and widespread environmental change, which Ward *et al.* (2005) correlated, using bio-, magneto- and chemostratigraphy, with the global Permo–Triassic boundary (Ward *et al.*, 2012). However, Gastaldo *et al.* (2009) were unable to trace this lithostratigraphic unit at the same stratigraphic level across a <1 km distance at Bethulie (Day 2). Their field data, developed in a stratigraphic framework, resulted in the rejection of the boundary bed concept, which continues to be debated (Ward *et al.*, 2012; Gastaldo and Neveling, 2012) and propagated in the literature (Smith and Botha-Brink, 2014; Botha-Brink *et al.*, 2014; Viglietti *et al.*, 2016).

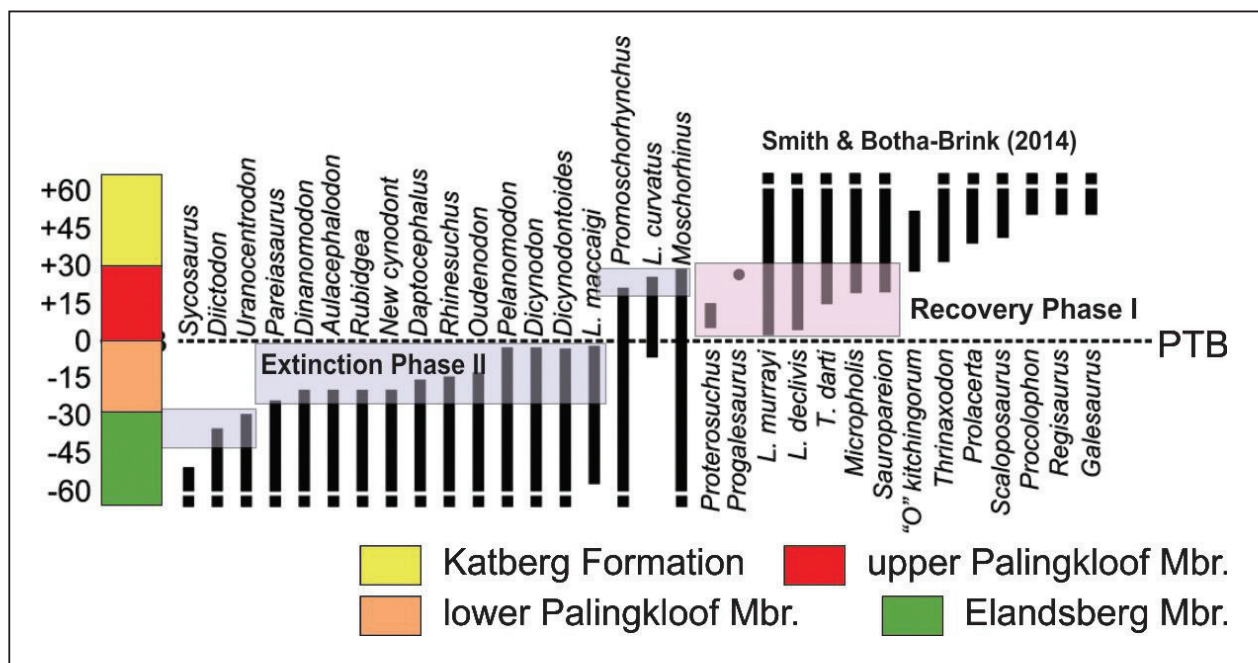


Figure 8.

Vertebrate biostratigraphic ranges reported from above and below the *Daptocephalus*–*Lystrosaurus* AZ contact by Smith and Botha-Brink (2014). Based on these data, these authors recognised two extinction phases leading up to the first appearance of the *Lystrosaurus* AZ fauna (associated with Recovery Phase 1). The third extinction phase refers to the disappearance of two *Daptocephalus* AZ taxa and *L. curvatus*. (Figure adapted from an article published in *Palaeogeography, Palaeoclimatology, Palaeoecology*, v. 396, Smith and Botha-Brink, Anatomy of a mass extinction: Sedimentological and taphonomic evidence for drought-induced die-offs at the Permo–Triassic boundary in the main Karoo Basin, South Africa: p. 99–118, Copyright Elsevier, 2014).



A succession characterised by massive maroon and olive-grey siltstone, in which the *Lystrosaurus* AZ fauna is preserved, overlies the last-appearance datum of the *Daptocephalus* AZ in lithofacies association C. **Lithofacies association D** contains minor thin, gullied sandstone sheets (Smith and Ward, 2001; Smith and Botha, 2005; Botha and Smith, 2006; Smith and Botha-Brink, 2014; Botha-Brink *et al.*, 2014) without the reported presence of fluvial channel-form bodies. A greater abundance of desiccation features and a slightly lighter colour (2.5 YR 3/6), compared with the dark reddish-brown (2.5 YR 2.5/4) of the lower facies, are reported as recognition criteria for this lithofacies association.

The boundary interval is capped by the sandstone-dominated Katberg Formation (**lithofacies association E**). The Katberg Formation is composed of vertically stacked and multistoried (5–10 m thick) tabular, olive-grey to greyish-yellow, fine- to medium-grained sandstone bodies, separated by intervals of light olive-grey and dark-red mudstones (Ward *et al.*, 2000; Smith and Ward, 2001; Ward *et al.*, 2005; Smith and Botha-Brink, 2014). A distinctive feature of these sandstones is the common occurrence of irregular disconformities, lined with lenses of intraformational conglomerates composed of mudrock pebbles, reworked bone fragments, and numerous spheroidal pedogenic pisoliths that can exhibit internal septarian shrinkage cracks (Botha and Smith, 2006; Smith and Botha-Brink, 2014). These sandstone bodies, containing elements of the *Lystrosaurus* AZ fauna are interpreted to represent deposition by wide, shallow, low-sinuosity, “braided” rivers (Ward *et al.*, 2005; Smith and Botha-Brink, 2014).

As the field collection of new fossils continued, the biostratigraphic ranges were refined; accordingly, Smith and Ward (2001) first extended the range of the genus *Lystrosaurus* downward, overlapping the *Daptocephalus* AZ by more than 41 m (recall that Hotton, 1967), first reported the biostratigraphic range overlap). In 2007, Botha and Smith proposed that the majority of these lower occurrences of *Lystrosaurus* could be assigned to the species *L. maccaigi* and that this taxon was restricted to the *Daptocephalus* AZ.

The co-occurrence of *Lystrosaurus maccaigi* with *Daptocephalus* AZ faunal elements, as reported by Smith and Botha-Brink (2014), was continued by Viglietti *et al.* (2016), who consider this species to be the index taxon of the Upper *Daptocephalus* AZ. In addition, a second species of *Lystrosaurus*, *L. curvatus*, was reported to have a restricted biostratigraphic range, occurring in the uppermost *Daptocephalus* and basalmost *Lystrosaurus* AZs. Based on the overlap of an additional three taxa (*Moschorhinus*, *Tetracynodon*, *Ictidusuchoides*) with *L. curvatus* and other *Lystrosaurus* AZ fauna, Smith and Botha (2005) distinguished between extinction, survivor, and recovery faunas. Following taxonomic and stratigraphic revision (Smith and Botha-Brink, 2014; Viglietti *et al.*, 2016) the composition of the survivor taxa have changed and decreased in number (Fig. 8). Yet, vertebrate ranges are considered still sufficient for the identification of three extinction phases and one ‘early recovery’ phase in the boundary interval (Fig. 8).

4.2. Correlation with the global record

An important question in the debate about a turnover in vertebrate biozones is whether the faunal changeover reported from strata in the Karoo Basin can be considered correlative with the end-Guadalupian (ca. 260 Ma; Fig. 4) and younger PTB marine extinctions. An answer to this question will help to determine whether there is synchrony or diachroneity of the marine and terrestrial events. However, such correlation is not simple because there are no stratigraphic sections that contain terrestrial tetrapods that also can be correlated unequivocally directly to the marine record across the PTB. Similarly, until very recently, there has been a dearth of geochronologic data in the Karoo successions to validate the hypothesised and widely held, correlation. Therefore, previous authors had to rely on isotope chemostratigraphy, magnetostratigraphy, and palynostratigraphy to correlate the non-marine and marine records across the rocks that represent the PTB.

The first attempt at correlating the non-marine record of the Karoo Basin with that preserved at the IGCP (International Geoscience Programme) section at Meishan, China, was based on stable isotope chemostratigraphy. MacLeod *et al.* (2000) reported trends in $\delta^{13}\text{C}$ obtained from pedogenic carbonate nodules (and supported by a smaller excursion from vertebrate tusks), with the interval of biostratigraphic overlap (i.e. the uppermost 15 m of the *Daptocephalus* AZ). Here, they demonstrated a negative $\delta^{13}\text{C}$ excursion, which they correlated with the negative $\delta^{13}\text{C}$ excursion reported from just below the marine-defined PTB (Wang *et al.*, 1994). Subsequently, Tabor *et al.* (2007) demonstrated that $\delta^{13}\text{C}$ values from many of the pedogenic nodule cements reflected calcite precipitation under saturated sediment, rather than precipitates influenced and reflective of atmospheric gas concentrations. As such, the trends reported by MacLeod *et al.* (2000) cannot be correlated with those in the marine record. Furthermore, Lucas (2009) noted that the stable isotopic data reported by Ward *et al.* (2005; Fig. 9) are difficult to follow and that their interpretations are contradicted by the data provided in the figures. More recently, Gastaldo *et al.* (2014) have shown that $\delta^{13}\text{C}$ values obtained from calcite (micrite and microspar) cement in concretions at two stratigraphic sections at Wapadsberg and Old Wapadsberg Pass (Day 5) reflect mineral precipitation either under well-drained sediment (paleosol) conditions or under saturated conditions. These authors reproduced the $\delta^{13}\text{C}$ trend reported by MacLeod *et al.* (2000) $\delta^{13}\text{C}$ from concretions that formed under conditions of saturated sediment and concluded that there was no evidence for the unidirectional aridification trend as had been interpreted previously. To date, few palynological assemblages have been recovered from Karoo rocks in the uppermost *Daptocephalus* and lowermost *Lystrosaurus* AZs, leaving correlations with other basins rudimentary. Palynological records from Gondwana continents originate from sections in Antarctica (Askin, 1998; McLoughlin *et al.* 1997; Collinson *et al.*, 2006; Awatar *et al.*, 2014), India (e.g., Jha, 2006), and Australia, with the Australian palynostratigraphic zones serving as the standard biostratigraphic classification for Gondwana. The Australian palynozones are defined according to the first or consistent appearance of spores and pollen taxa in the Western (e.g., Helby *et al.*, 1987; Mory and Backhouse,

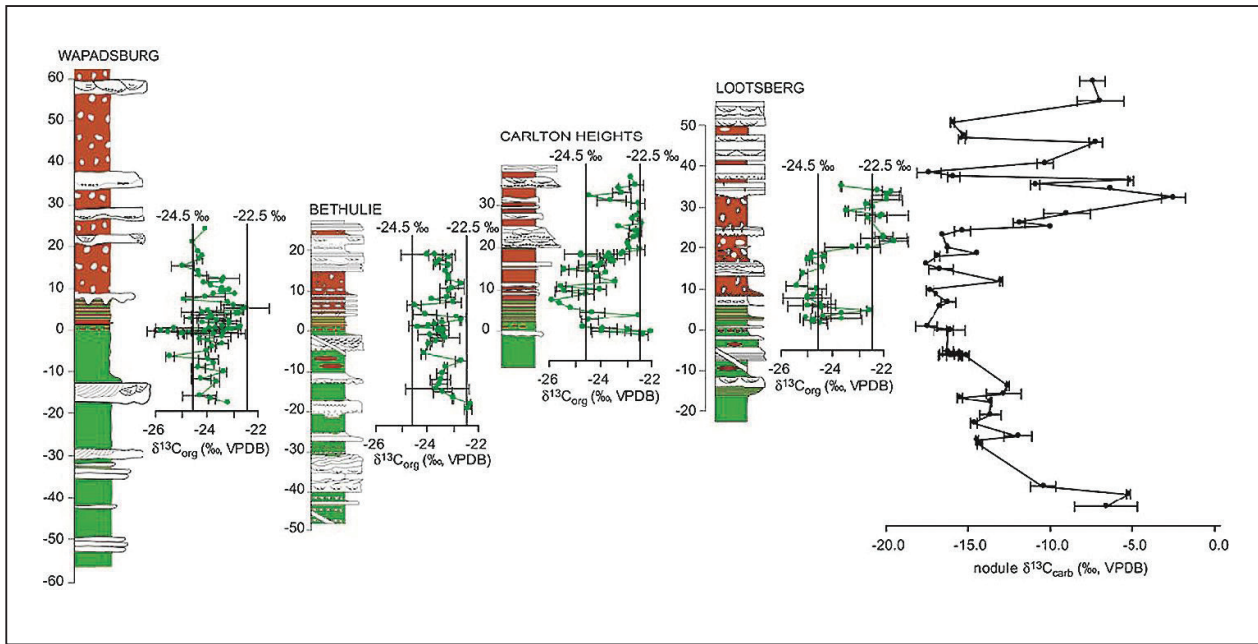


Figure 9.

Soil and bulk sediment $\delta^{13}\text{C}$ records reported from four boundary sections by Ward *et al.* (2005, their fig. 2). These authors considered the isotopic record from Wapadsberg and Bethulie to have been influenced by Jurassic dolerite intrusions, and a negative excursion, near the top of their laminated interval at Carlton Heights and Lootsberg, to resemble isotope trends obtained from the marine record. (From Ward *et al.*, 2005, Abrupt and Gradual Extinction among Late Permian Land Vertebrates in the Karoo Basin, South Africa: *SCIENCE*, 307:709-714. Reprinted with permission from AAAS).

1997) and Eastern Australian basins (e.g., Foster, 1982; Price, 1997). These biozones are calibrated against independently dated marine invertebrate zones (Foster and Archbold, 2001; Metcalfe *et al.*, 2008), carbon-isotope stratigraphy, and geochronometric dates (Metcalfe *et al.*, 2008, 2015). Palynoassemblages from the Karoo are often diagenetically influenced by thermochemical processes associated with the emplacement of the early Middle Jurassic Karoo dolerites. To date, the few published studies from the uppermost *Daptoccephalus* AZ all exhibit typical Late Permian, *Glossopteris*-dominated assemblages, with an admixture of pollen taxa thought to represent the post-extinction recovery flora (Prevec *et al.*, 2010; Gastaldo *et al.*, 2015). Palynofloras from Old Lootsberg Pass (Day 4; Gastaldo *et al.*, 2015) and Wapadsberg Pass (Day 5; Prevec *et al.*, 2010) are assigned a Changhsingian age, and correlative with the *Protohaploxylinus microcorpus* biozone of Western (Price, 1997) and Eastern Australia (Morante, 1995; Metcalfe *et al.*, 2015).

The magnetostratigraphic record in the Karoo across the *Daptoccephalus* and *Lystrosaurus* AZs (Kirschvink and Ward, 1998; De Kock and Kirschvink, 2004; Ward *et al.*, 2005) has been used as the basis for correlating with the estimated geomagnetic polarity time scale (e.g., Ward *et al.*, 2005; Glen *et al.*, 2009; Lucas, 2009). Over the past two decades of research, a growing volume of documentation has developed on the time interval associated with several events associated with the Permian–Triassic transition, indicating all the events took place during a single normal polarity chron (e.g., Opdyke and Channel, 1996). More recently, the detailed work by Szurlies on Western and Central European strata (summarised by Szurlies, 2013) has demonstrated convincingly that this normal polarity chron is approximately 700 ka in duration, and that the reverse to normal polarity transition into this chron took place some 200 ka before the actual PTB (Fig. 10).

According to Ward *et al.* (2005, their fig. 3), the PTB in South Africa (as defined by vertebrate biostratigraphy and the presence of the event bed) is placed in the lower part of what they labelled as their N1 magnetozone (Fig. 11). The presence of the inferred normal polarity magnetozone is reported to be consistent between the northern (Carlton Heights and Bethulie) and southern (Lootsberg and Wapadsberg Pass) parts of the basin, although Ward *et al.* (2005) reported that the magnetic polarity record of both Wapadsberg and Bethulie had been affected by thermochemical processes associated with intrusions of the early Middle Jurassic Karoo Large Igneous Province (LIP). Earlier, De Kock and Kirschvink (2004) published a magnetic polarity stratigraphy for the section exposed at Kommandodrifdam (= Commando Drift; Day 6). They noted that the PTB was situated in an interval of red mudstone (the End Permian Paleosol; EPP) that exhibits a polarity pattern assigned to what they labelled as their R1 magnetozone. Notably, these workers provided no documentation through orthogonal demagnetisation diagrams to illustrate progressive demagnetisation results in the isolation of bona fide reverse polarity magnetisations in these strata. As we elaborate later in the document, the essential issue in establishing a magnetic polarity stratigraphy in Beaufort strata anywhere in the Karoo Basin is the separation of a magnetisation acquired during early Middle Jurassic Karoo magmatism from magnetisation of Late Permian to Early Triassic age, if such magnetisations even exist. For example, Ballard *et al.* (1986) demonstrated the widespread re-magnetisation in Jurassic time of Permian strata in the northern flank of the Cape Fold Belt.



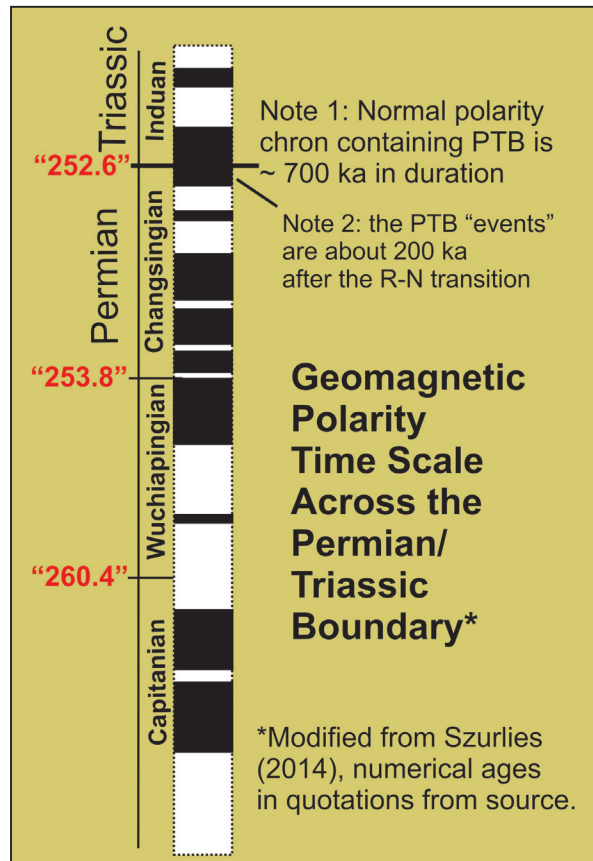


Figure 10. Estimated geomagnetic polarity time scale across the Permian–Triassic boundary. Black denotes normal polarity chrons, and white denotes reverse polarity chrons. (Modified from Szurlies, 2013).

De Kock and Kirschvink (2004, p. 177) first associated the Last Appearance Datum (LAD) of *Daptocephalus* with an EPP horizon (Smith and Ward, 2001, and others) that coincides with the top of their R1 reversed polarity interval, but, subsequently, reassigned it to exposures they associated with the “event bed” of Ward *et al.* (2000), outcropping some ~6 m higher and within their overlying N2 normal polarity interval (De Kock and Kirschvink, 2004, p. 180). At this stratigraphic position, the biozone boundary is 6 m to 12 m above the polarity reversal (R1 to N2 magnetozone), but about 100 m below the polarity change from N2 to R2 when correlated with data from Lootsberg Pass (Ward and Kirschvink, 1998). Based on the global magnetic polarity stratigraphy then available, De Kock and Kirschvink (2004, p. 180) concluded that it could be assumed that, “. . . at least 12 m of older normally magnetised strata, or a minimum of 100 m of younger normally magnetised strata separates the extinction of mammal-like reptiles from the mass extinction event as seen in the marine realm.” In addition, De Kock and Kirschvink (2004, p. 181) argued that the contact between the green and first red mudstones (~6 m below the “EPP”) represented the PTB (interpreted to represent a change from wet-to-dry climate conditions) and that the event was associated with a reverse magnetic polarity chron. Coney *et al.* (2007) followed the interpretation of De Kock and Kirschvink (2004) and identified both a palaeontological (0 m; their fig. 3) and a palaeomagnetic boundary (+5.2 m; their fig. 3), with the palaeontological boundary placed within the De Kock and Kirschvink (2004) R1 magnetozone. Although Ward *et al.* (2005) eventually showed the end-Permian interval to lie within a normal polarity magnetozone (Fig. 11), which differed from the data set presented by De Kock and Kirschvink (2004), Lucas (2009) interpreted their pattern as evidence that this biozone contact predated the marine extinction. More recently, the overall polarity pattern of Ward *et al.* (2005) for Old Lootsberg Pass could not be repeated by Gastaldo *et al.* (2015). In passing, we note that the Commando Drift section lies directly above a Karoo dolerite sill that can be traced for kilometres.

As noted above, the PTB marine extinction took place during a relatively long interval of normal magnetic polarity that is well documented in several marine sections (Ogg, 2004; Steiner, 2006). More recently, these early interpretations have been documented better through extensive work in Western and Central Europe by M. Szurlies and colleagues and, most recently, were summarised by Szurlies (2013). An interpreted interval of normal polarity in the Karoo Basin encompasses the highest occurrence of *Daptocephalus* and is part of the stratigraphically thick (~60 m) interval of low $\delta^{13}C$ values (Schwindt *et al.*, 2003; De Kock and Kirschvink, 2004; Ward *et al.*, 2005; Steiner, 2006; Fig. 5). If viable, these magnetostratigraphic data indicate the lowest occurrence of *Lystrosaurus* in a reverse polarity magnetozone older than the PTB (as already suggested by King and Jenkins, 1997, and Botha and Smith, 2007, among others). If true, the highest occurrence of *Daptocephalus* (*Dicynodon*) based on Smith and Both-Brink’s data is closer to the PTB (Fig. 5). Therefore, the statement by Retallack *et al.* (2003) that “biostratigraphy, palaeomagnetic stratigraphy, and isotope chemostratigraphy indicate that the P–T boundary is within a 7-m-thick sequence of laminated purple to grey beds”, the “event bed” of Smith and Ward (2001), which approximates the highest occurrence of *Daptocephalus*, is possible but not precisely demonstrable on the basis of current data.

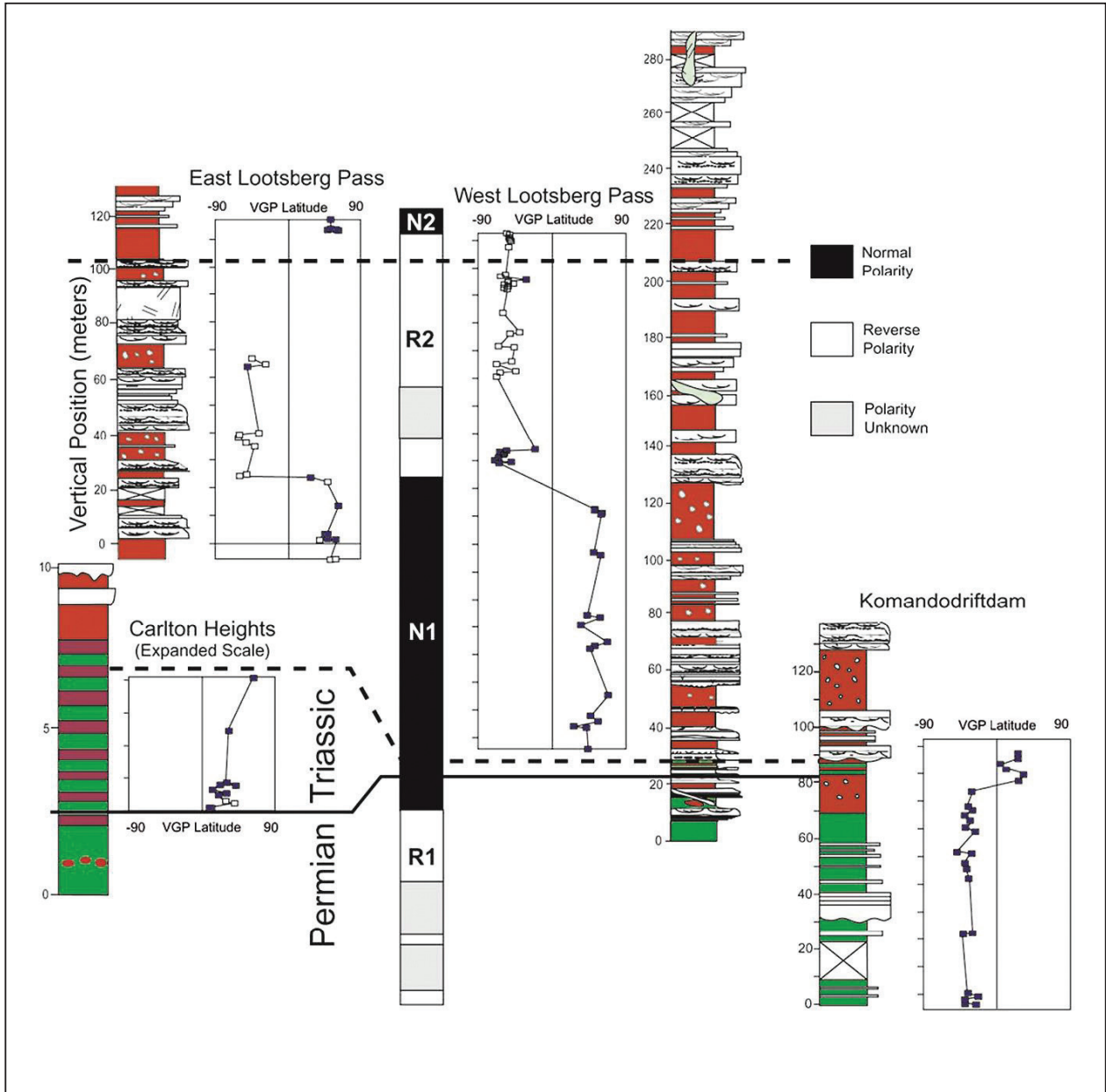


Figure 11.

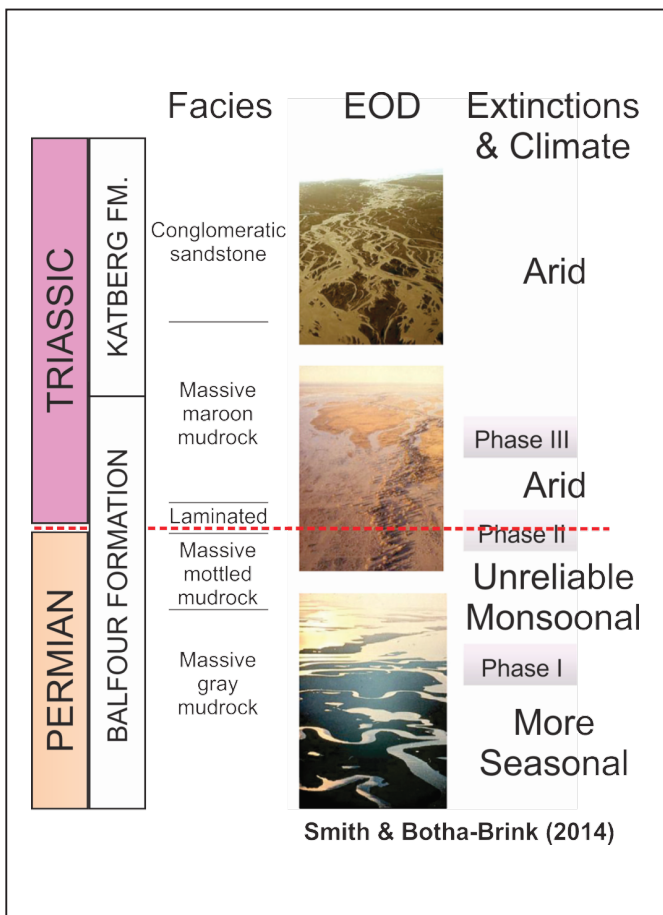
Magnetostratigraphic correlation of three Karoo sections by Ward *et al.* (2005, their fig. 1). They reported an interval of reversed polarity that ended approximately five metres below their laminated interval (~8 to 10 m below the biozone contact). This contact is situated in an interval of normal polarity extending up into the lower Katberg Formation, and correlated with magnetozone SN1 of the German Trias record. (Figure from Ward *et al.*, 2005, Abrupt and Gradual Extinction among Late Permian Land Vertebrates in the Karoo Basin, South Africa: *SCIENCE*, 307:709–714. Reprinted with permission from AAAS).

Using the data available at the time, Retallack *et al.* (2003, p. 1147) envisioned, "... a pronounced and geologically abrupt extinction of vertebrates at the Permian–Triassic boundary, with a diversity minimum in the poorly fossiliferous laminites [event bed]". However, the stratigraphic range data of Ward *et al.* (2005, their fig. 3) and Botha and Smith (2006, their fig. 6) indicate an evolutionary turnover of tetrapod taxa that is more prolonged and that begins below the lowest occurrence of *Lystrorhynchus* and extends through the base of the Katberg Formation, a stratigraphic interval of approximately 60 m (Fig. 5). Given that the PTB level at Meishan is approximately one-third of the way up into a normal magnetozone (but recall that the Meishan section is considered a condensed marine interval), Steiner (2006) suggested that the correlation between Meishan and Karoo Basin strata places the purported fungal abundance spike (Day 3) in the Karoo close to the defined PTB (and the epilogue extinction). However, this is not a straightforward correlation, given the differences in sedimentary completeness and accumulation rates between the marine (Meishan) and non-marine (Karoo) sections.

4.3 Palaeoenvironmental Extinction Model

Smith (1995) interpreted the change in the fluvial environment of Karoo strata near the PTB as coincident with the vertebrate turnover. At the time, this interpreted change in depositional setting was thought to be the result of tectonics affecting the basin. A switch occurred from a Karoo landscape dominated by alluvial plains, traversed by a few large, highly meandering rivers, to a distributary channel network that eventually widened and separated into a braided pattern. The changeover is assumed to have occurred through a transitional stage when the rivers straightened and branched, with braidplains developed in response to increased sediment load from the Cape Fold Belt. Later, Ward *et al.* (2000) discarded the role of basin tectonics in the sedimentologic change across the Balfour–Katberg formational contact because an appropriately dated paroxysm in the Cape Fold Belt could not be identified (Hälbich, 1983; Gresse, 1992). As an alternative, Ward *et al.* (2000) proposed the fluvial change as the result of a dramatic increase in sediment load caused by widespread vegetation die-off, in response to regional drying and drought. Based on the change in fluvial style and reddening (rubification) of floodplain soils, supported by taphonomic data, Smith and Ward (2001) considered the boundary interval to reflect increased aridification. This interpretation has been retained by subsequent workers (e.g., Smith and Botha, 2005; Scheffler *et al.*, 2006; Coney *et al.*, 2007; Smith and Botha-Brink, 2014; Rubidge *et al.*, 2016; Viglietti *et al.*, 2016).

In contrast, Retallack *et al.* (2003), using pedogenic data, proposed that the Permian palaeoclimate was strongly seasonal and arid in the latest Permian, changing to a less seasonal, semi-arid to subhumid Triassic paleoclimate. In part, the interpretation was based on the depth to pedogenic calcic horizons in all paleosols with nodules, regardless of whether calcite precipitated in equilibrium with atmospheric gas pressures, or because of microbial decay of organic matter (Tabor *et al.*, 2007). The former conditions are requisite for a valid interpretation of climate. This paradigm was reviewed by Smith and Botha (2005; Botha and Smith, 2006) who considered the increased depth to pedogenic calcic horizon and the introduction of sandstone sheets, which display basal gullying, draped by lenses of intraformational conglomerate containing pedogenic nodules, to be indicative of ephemeral discharge. Their explanation (Fig. 12) centered on an interpreted increase in mean annual temperature, combined with the onset of a highly seasonal, but unreliable (monsoonal) rainfall regime. Together with an increased frequency of desiccation features, rubification of soils, and taphonomic data, which include an increase in observed vertebrate-fossil articulation, increasing aridity into the Triassic was interpreted up-section (Smith and Ward, 2001; Smith and Botha, 2005; Botha and Smith, 2006, 2007). A new interpretation of the thick red siltstones above the biozone contact as aeolian deposits (first suggested by Smith, 1995) was proposed and used to support the presence of a semi-arid climate, with a short, but intensive wet season for the post-extinction landscape (Smith and Botha-Brink, 2014).



In general, the current paleoclimate models for the Beaufort—Katberg transition mirror that of Smith (1995). An overall trend of increasing aridification (Fig. 12), modified by Ward *et al.* (2005), is assumed, with a prolonged period of environmental stress (upper Elandsberg and lower Palingkloof members) punctuated by a short interval of even greater perturbation, associated with biozone contact. In this context, the “event bed” laminites, generally considered to constitute a single, synchronous and mappable horizon (Smith and Botha, 2005; Botha and Smith, 2006; Smith and Botha-Brink, 2014), were interpreted as representing turbidite deposition in playa lakes. Deposition took place during a short period when the Karoo Basin was almost devoid of vegetation and soil-forming processes had been suspended (Retallack *et al.*, 2003; Botha and Smith, 2005; Smith and Botha-Brink, 2014). These unusual circumstances were interpreted as the result of the catastrophic drought, responsible for the demise of the *Daptocephalus* AZ, caused by CO₂-induced aridification (Smith and Botha-Brink, 2014).

Figure 12. Generalised section showing the proposed facies sequence of the extinction interval, with proposed modern analogues for the interpreted development of the Karoo palaeo-environment. EOD = Environment of Deposition. (Figure adapted from an article published in *Palaeogeography, Palaeoclimatology, Palaeoecology*, v. 396, Smith and Botha-Brink, Anatomy of a mass extinction: Sedimentological and taphonomic evidence for drought-induced die-offs at the Permo–Triassic boundary in the main Karoo Basin, South Africa, Copyright Elsevier, 2014).

5. CONCERNS ABOUT THE PTB MODEL

The current terrestrial PTB model for the Karoo Basin represents more than two decades of published research. This model is widely accepted and plays a central role in our global scale interpretation of extinction and recovery dynamics on land during and after the event (e.g., Benton and Newell, 2014; Roopnarine and Angielczyk, 2015; Botha-Brink *et al.*, 2016). However, the litmus test for any hypothesis is whether the detail that leads to a proposed model could be verified repeatedly by independent study. We assert that many aspects of the model are not repeatable, which has raised questions about the validity and utility of the terrestrial end-Permian extinction model for Karoo Basin successions.

5.1 Stratigraphic Resolution

Stratigraphers have long recognised that continental successions are notorious for being incomplete (for references see Gastaldo and Demko, 2011). Sediment supply to a basin is periodic, controlled by variations in climate, is a function of the fluvial gradient active in any part of that basin, and is associated with the rate and scale of tectonic processes (e.g., Connell *et al.*, 2012; Straub *et al.*, 2013; Reitz *et al.*, 2015). In the majority of basins throughout geologic history, the sediment transported into them ultimately arrived at a coastal–marine interface, where nearly all detritus was distributed and deposited in the ocean (base level). However, the deposition in the Beaufort Group of the Karoo Basin was different because there was no coastal–marine setting anywhere in the area during the latest Permian and Early Triassic. The transition from the Ecca Group to the Beaufort Group at the contact with the Waterford Formation (Rubidge *et al.*, 2012) marks a full regression in the basin during which sedimentation became restricted to a terrestrial setting. This is a unique circumstance, as few fully enclosed continental basins of this magnitude are recognised in the geologic record and only one fully enclosed continental basin is known currently on Earth (Eyre Basin, Australia; Nanson *et al.*, 1986; Tooth and Nanson, 1995; Alley, 1998). Therefore, as factors controlling sediment supply and deposition varied over time, the stratigraphic record became an amalgamation of aggradational and degradational landscapes over various spatial scales (Gastaldo and Demko, 2011). This view contradicts the descriptions of the Beaufort stratigraphy that claim it to be stratigraphically complete (Ward *et al.*, 2005; Smith and Botha, 2005; Smith and Botha-Brink, 2014).

If the stratigraphic record of the uppermost Adelaide Subgroup and lowermost Katberg Formation were indeed comprised of both aggradational and degradational landscapes, representing a discontinuous record (Pace *et al.*, 2009; Gastaldo *et al.*, 2015), then the biostratigraphic patterns identified in the tetrapod record had to be evaluated within such a context. Similarly, taphonomic processes responsible for the preservation of biological remains are controlled by these landscape patterns, which also operate over space and time (Behrensmeyer *et al.*, 2000). Therefore, the resultant fossil record of any basin represents a small fraction of the biodiversity of the Earth (Plotnick *et al.*, 2016) at the time of sediment supply, biologic burial, and early diagenetic fossilisation. The record is limited even further by the spatial extent of fossiliferous rocks that are exposed at the time of their discovery and collection. To compensate for the incompleteness of the record, statistical methods have been developed in an attempt to predict a First and Last Appearance Datum for taxa below and above the stratigraphic position of collected specimens that is more realistic (e.g., Signor and Lipps, 1982; Marshall, 1990). Statistical models are routinely applied to marine successions, albeit generally without consideration of sequence stratigraphic context (however, refer to Holland and Patzkowsky, 2015; Holland, 2016). Stratigraphic patterns are exaggerated in continental rocks because of the interplay between aggradational, static, and degradational landscapes (Gastaldo and Demko, 2011). Nevertheless, such models, based on the more complete marine record, have been applied to vertebrates of the Karoo Basin.

Ward *et al.* (2005) recognised the inherent difficulty in correlating between fluvial sections and have relied on magnetostratigraphic data (see below) and stable carbon isotopic excursions (see above), aligned with a purportedly unique boundary interval (Smith and Ward, 2001; lithofacies association C of Smith and Botha-Brink, 2014) for broad correlation. They concluded that their Unit II (laminated mudrock) represented a contemporaneous interval because of the occurrence of the uppermost biozone indicator, *Dicynodon laceriteps* (i.e. *Daptocephalus leoniceps*), which served as a datum against which the ranges of vertebrate taxa were evaluated. Confidence intervals were calculated on stratigraphic ranges of fossil taxa by using Marshall's (1990) approach. The conclusion was that vertebrate biodiversity loss occurred in stepwise fashion in the latest Permian, with the final event being coincidental with Unit II of Ward *et al.* (2005) and Smith and Ward's (2001) "event bed." Marshall (2005) first demonstrated that an alternative conclusion could be reached by using the same biostratigraphic dataset of Ward *et al.* (2005). In addition, Marshall found that these data supported the following hypotheses (1) taxa interpreted to have disappeared before the base of the Triassic could have continued up-section; (2) there was no evidence for an accelerated background extinction pattern well before the top of Unit I (lithofacies association B of Smith and Botha-Brink, 2014); (3) data for all uppermost Permian taxa were consistent with a simultaneous extinction scenario, rather than a step-wise, phased pattern; and (4) taxa that appeared in the Triassic probably originated in Unit III. Marshall (2005, p. 1413b) noted that the "...accuracy of the relative positions of the fossil horizons depicted in the composite section..." ultimately would control the validity of the calculated confidence intervals. These concerns led Lucas (2009) to caution against the indiscriminate use of statistical methods of stratigraphic range estimation to analyse extinctions. Further concerns have been raised about the resolution of this dataset.



As Marshall (2005) recognised, the resolution of the three-phase end-Permian extinction model previously advanced for the Karoo necessitated a highly accurate stratigraphy and stratigraphic framework. This is especially relevant in a fluvial setting that displays significant lateral variation. The laminated interval (Unit II of Ward *et al.*, 2005; lithofacies association C of Smith and Botha-Brink, 2014) plays a critical role in the correlation between sections, some of which could be as much 200 km apart. This laminated interval has been considered, "... a stratigraphically unique unit. . ." (Smith and Ward, 2001, p. 1148; also refer to Ward *et al.*, 2000) that is, "... sufficiently different from those above and below to be used as a mappable unit. . . and a datum. . ." (Smith and Botha-Brink, 2014, p. 103) to correlate between widely distributed sections (Smith and Botha-Brink, 2014, p. 110). The stratigraphic position of each logged, in situ vertebrate fossil was reported relative to this datum and used to assign it a stratigraphic distance (in metres) below or above the PTB (Smith and Botha-Brink, 2014, p. 101, supplementary data). Yet, the correlative utility of this datum has never been proven.

The laminated interval, or "laminated facies" of Smith and Ward (2001), is reported not only from several localities in the Karoo Basin but also from other Gondwanan continents at various stratigraphic positions. For example, Retallack *et al.* (2003) have reported the presence of laminated beds below the *Daptocephalus* (*Dicynodon*)–*Lystrorhynchus* biozone boundary from exposures in the KwaZulu-Natal Province in the northeastern part of the basin. Yet, Botha-Brink *et al.* (2014) have used this as the criterion to identify the PTB in two isolated exposures of vertebrate-bearing successions on the farm Nooitgedacht 68 in the Bethulie District of the Free State Province. Their continued reliance on this lithofacies association is in contrast to the findings of Gastaldo *et al.* (2009) who, in a detailed stratigraphic investigation at Bethulie, demonstrated that this facies association was neither unique nor isochronous. This fact had been subsequently acknowledged by Ward *et al.* (2012) who stated that their data, "... indicate 'laminites' at, above, and below the boundary." The very thinly bedded or laminated fine-grained rocks were recorded at multiple horizons at Bethulie (Day 2; Gastaldo *et al.*, 2009), Old Lootsberg Pass, and Old Wapadsberg Pass (Day 4; Neveling *et al.*, 2016) and have a well-established lateral association with low-sinuosity channel deposits. Nevertheless, the presence of thinly bedded fine-grained rocks in upper Permian Antarctic strata led Retallack *et al.* (2003) to claim that the unique facies could be correlated across continents.

Another datum often used for stratigraphic correlation of widely spaced sections in this part of the Karoo Supergroup is the base of the Katberg Formation (Smith and Botha-Brink, 2014, p. 110). Research on Old Lootsberg Pass (Day 4; Neveling *et al.*, 2016) demonstrates that the base of the Katberg Formation, as well as its characteristics, stratigraphically vary over tens of metres over a short geographic distance. The emplacement of fluvial channels, with features diagnostic of the formation, is encountered at many different stratigraphic positions that reflect the temporal variation of when a fluvial facies was established on a spatial scale. This observation, alone, disqualifies the Katberg Formation as a key correlation tool among sections in the basin. In general, an assessment of lateral facies relationships demonstrates that it is impossible to correlate accurately successions between different localities, or even between outcrops at a single locality, without tracing boundary surfaces in the field and the development of a detailed stratigraphic framework.

The field relationships among discontinuous formational contacts and lithofacies distribution within members raise substantial questions regarding the accuracy of the biostratigraphic data and extinction model on which it is based. For example, when the *Daptocephalus*–*Lystrorhynchus* biozone boundary is extrapolated from the reported locations of vertebrates (using the Smith and Botha-Brink [2014] database, with GPS coordinates for specimens on which the model is constructed, provided by R.M.H. Smith on 19 February 2014) at Old (West) Lootsberg Pass and stratigraphic sections measured on the farm Blaauwater 65 and Lucerne 70 (Tweefontein), **none** of the horizons at which vertebrate turnover was reported to occur corresponded with a 3–5 m thick, laminated interval (Day 4; Neveling *et al.* 2016; Gastaldo *et al.*, in review). Similarly, Battifarano *et al.* (2015) identified significant variance between the reported and actual stratigraphic positions of specific vertebrate-collection sites relative to the inferred PTB at Bethulie (Day 2). A similar field-based review of reported fossil localities at the Old Wapadsberg locality (Day 5) suggests much greater overlap between elements of the *Daptocephalus* AZ specimens and *Lystrorhynchus murrayi*, of the *Lystrorhynchus* AZ, than advanced by the current model (Neveling *et al.*, 2016). Without established confidence in the accuracy of the biostratigraphic data, the validity of the three-phased faunal turnover (Smith and Botha-Brink, 2014) and ecological models (Roopnarine and Angielczyk, 2015) remain in question.

5.2 Palaeoenvironmental Model

The environmental model of drought-induced extinction, associated with an aeolian component (Smith, 1995; Smith and Botha-Brink, 2014) was developed in the absence of palaeobotanical data. This was at a time when the plant-fossil record for the central and southern parts of the basin for this interval was considered almost barren. This interpretation was predicated on an underlying, widely held assumption that an absence of plant fossils in a stratigraphic succession had to be a consequence of an absence of vegetation during sediment accumulation. However, we now understand that the absence of plant remains is a function of taphonomy (refer to DiMichele and Gastaldo, 2008). Subsequent studies demonstrated the presence of macrofossil plants and palynomorphs where they were once considered absent (Gastaldo *et al.*, 2005; Prevec *et al.*, 2009, 2010; Gastaldo *et al.*, 2015), and a taphonomic model was proposed to account for the paucity of plant remains in the *Daptocephalus* and *Lystrorhynchus* AZs (Gastaldo *et al.*, 2005). Since then, the discovery of several glossopterid floras and pollen assemblages from the uppermost *Daptocephalus* AZ (Prevec *et al.*, 2010; Gastaldo *et al.*, in review) and lowermost *Lystrorhynchus* AZ (Gastaldo *et al.*, 2015) have indicated that moist soil conditions prevailed across the biozone boundary interval. This conclusion is corroborated by pedogenic data.

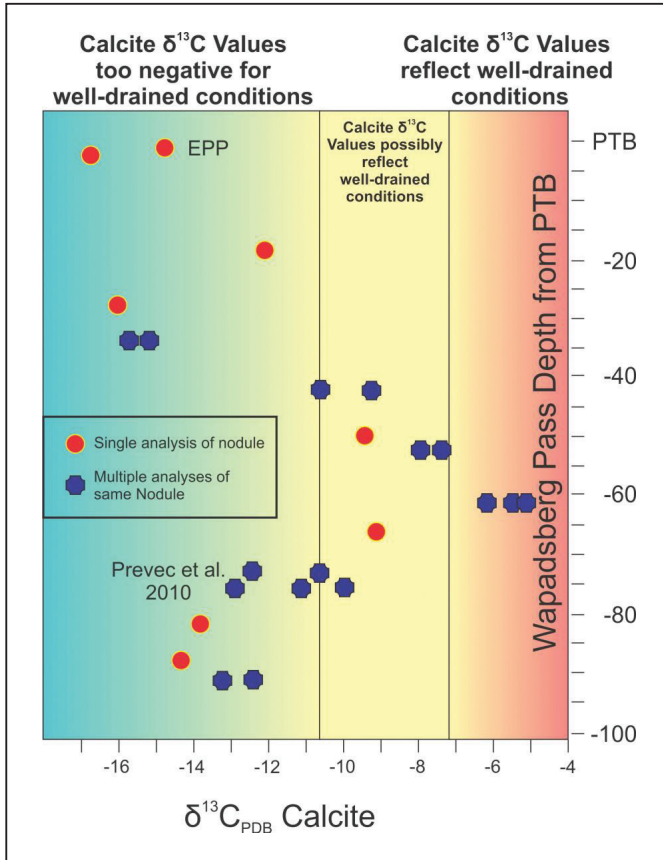


Figure 13. The stratigraphic position and $\delta^{13}\text{C}$ values obtained from pedogenic nodules in the uppermost *Daptocephalus* AZ at New Wapadsberg Pass. Black circles represent paleosol profiles from which only one paleosol nodule $\delta^{13}\text{C}$ value was determined, whereas grey plaques represent paleosol profiles where multiple (i.e., $n = 2$ or 3) paleosol nodule $\delta^{13}\text{C}$ values were determined. Fields in which $\delta^{13}\text{C}$ values reflect crystallization under well-drained or wetland conditions are plotted, indicating that most carbonate nodules precipitated under closed, wet sediment conditions (adapted from Gastaldo *et al.*, 2014).

An increasing proportion of reddish-grey mudrock from the Elandsberg through Palingkloof members and into the Katberg Formation, and the occurrence of carbonate-cemented concretions (nodules) in this part of the Karoo, has been assumed evidence to support the prevalence of a seasonally dry, semi-arid to arid climate (Smith, 1995; Ward *et al.*, 2005) at the time of, and following, vertebrate turnover. Siltstone colouration is thought to be a function of $\text{Fe}^{2+}/\text{Fe}^{3+}$ in the sediment, and is believed by many to reflect the oxidising potential of the depositional

environment (Coney *et al.*, 2007; Smith and Botha-Brink, 2014). Greenish-grey colouration, thought to result from an abundance of Fe^{2+} , is associated with a moist climate and high water table that insulates iron in subaerial sediments from oxidation by atmospheric oxygen. Reddish-grey colouration, on the other hand, is interpreted to represent a high proportion of Fe^{3+} oxidised by direct contact with air in a dry climate, with low water table (Coney *et al.*, 2007). Although other researchers have reported that colouration of Permian rock is not correlated with climate (Sheldon, 2005), this relationship continues to be applied in the Karoo succession. In addition, to reinforce the climate model, the massive reddish-grey siltstone of the lowermost *Lystrosaurus* AZ has been interpreted as being, in part, of loessic origin (Smith and Botha-Brink, 2014). To date, there is little evidence to support an aeolian origin for these rocks (Gastaldo and Neveling, 2016; Neveling *et al.*, 2016).

MacLeod *et al.* (2000) reported stable isotopic trends by from concretions at Wapadsberg Pass, which were used to justify an increasing aridity in the section (Ward *et al.*, 2005), and it was assumed that their cements had formed in response to atmospheric CO_2 flux into soils, where water tables fluctuated from seasonal wet to dry conditions. Calcite cement-binding mudrock, in the form of concretions, can be precipitated either in response to atmospheric CO_2 influx, or as a consequence of CH_4 and CO_2 microbial genesis as an effect of organic matter decay under saturated conditions (Cerling, 1991). Using carbon isotopic values of organic matter in conjunction with values obtained from micritic calcite cement, Tabor *et al.* (2007) were able to evaluate the soil-drainage conditions of boundary-straddling concretions at Carlton Heights (Day 3). They observed that the nodular paleosols throughout the sequence and exposed at Carlton Heights display isotopic values indicative of poorly drained conditions (all $\delta^{13}\text{C}$ values below -10.6‰), where cementation was promoted in anoxic conditions near or below the local groundwater table. The data of Tabor *et al.* (2007) parallel those published by MacLeod *et al.* (2000); however, Tabor *et al.* (2007) offer a different conclusion. Therefore, the majority of pedogenic horizons above and below the reported vertebrate biozone boundary represent seasonally to perennially wet soils, rather than soils developed under well-drained conditions.

Evidence for dry floodplain conditions, however, is available from the stable isotopic data obtained from some paleosol nodules. For example, Gastaldo *et al.* (2014) found that one stratigraphic interval at Wapadsberg Pass (Day 5) was characterised by calcite precipitation under well-drained soil conditions (Fig. 13). These nodules lie ~ 60 m below the level at which the boundary is placed by others (Ward *et al.*, 2000, 2005; Smith and Botha-Brink, 2014), indicating their formation was not coincident with the vertebrate-defined PTB (Day 5; Gastaldo *et al.*, 2014), where more seasonally dry conditions are believed to have prevailed. Other evidence of seasonally dry interfluvial floodplains is seen, especially as the erosional remnants of palaeo-calcic Vertisols contained in lenses of reworked nodule conglomerate (Pace *et al.*, 2009; Gastaldo *et al.*, 2013). The presence of better-drained soil conditions in the basin is mirrored by the preservation of palynofloral elements considered better adapted to drier conditions (e.g., conifers and peltasperms; Prevec *et al.*, 2010; Gastaldo *et al.*, 2015, in review), preserved together with a wetland glossopterid flora in the lowermost *Lystrosaurus* AZ. Together with pedogenic data, these features suggest a

gradual trend of increasing seasonality over time. However, conditions in the uppermost *Daptocephalus* and lowermost *Lystrosaurus* AZs were not as dry as portrayed.

The current interpretation of the laminated boundary beds (Unit III of Ward *et al.*, 2005; lithofacies association C of Smith and Botha-Brink, 2014) assumes sedimentation of this interval under processes that operated in a playa lake environment. These sediments are portrayed as representing “. . . a rapid and widespread environmental change. . .” (Smith and Botha-Brink, 2014, p. 100), linked to a die-off of the *Glossopteris* flora (Ward and Smith, 2000; Ward *et al.*, 2005; Smith and Botha, 2005). Note that the latter assertion cannot be substantiated any longer with the presence of glossopterids documented at multiple horizons in the lowermost *Lystrosaurus* AZ (Gastaldo *et al.*, 2015, in review). Primary sedimentary and biogenic structures (Gray *et al.*, 2004; Newbury *et al.*, 2007), along with geochemical data of vertical and lateral samples (Battifarano *et al.*, 2015) in laminated intervals at Bethulie and Old Lootsberg Pass (Li *et al.*, 2015) are indicative of physical and chemical processes that did not operate under evaporative climatic conditions. The occurrence of this lithofacies at multiple horizons (Gastaldo *et al.*, 2009; Ward *et al.*, 2012) and their well-established, lateral association with channel deposits suggest that these successions represent channel-fill, fining-up sequences associated with avulsion (Gastaldo *et al.*, 2009; Gastaldo and Neveling, 2012). Therefore, an increasing seasonal drying, alone, cannot explain the faunal change, if that exists at all.

5.3 Global Correlation and Age

The chemo- and magnetostratigraphic records from the Karoo that were used previously to correlate the *Daptocephalus*–*Lystrosaurus* biozone contact with the global PTB boundary have received pointed criticism that has largely been ignored. For example, Lucas (2009) criticised the approach that Ward *et al.* (2005) used in their interpretation of the stable carbon isotope data, and pointed out several inconsistencies between the data provided in the text and in the figures. The $\delta^{13}\text{C}$ trend reported by MacLeod *et al.* (2000) from carbonate-cemented nodules (see above) shows a relatively low value of -7‰ throughout the section, with a negative excursion to -18‰ at the highest occurrence of *Daptocephalus* (*Dicynodon*), which was correlated with the negative excursion just below the marine-defined boundary. In 2005, Ward *et al.* presented a different trend through the PTB interval that showed a significant drop of 10‰ $\delta^{13}\text{C}$ some stratigraphic distance below the highest reported position of *Daptocephalus*, and just below the first appearance of *Lystrosaurus* (in the *Daptocephalus* AZ). Therefore, Lucas (2009, p. 499) noted, “. . . there is no unambiguous correlation to the point in the marine isotope curve that corresponds to the PTB.” In addition, he pointed out (Lucas, 2009) that the negative excursion at the biozone boundary indicated by MacLeod *et al.* (2000) and Ward *et al.* (2005) looked like natural variation when compared with the generally low $\delta^{13}\text{C}$ values reported by Retallack and Krull (2006) for a much longer Permian section from the Karoo. In addition, Lucas (2009) acknowledged the contribution of Tabor *et al.* (2007) to the argument, based on their stable isotopic studies at Carlton Heights, that the carbonate-cemented nodules formed under saturated sediment conditions and not in equilibrium with atmospheric pCO_2 . Similar to Gastaldo *et al.* (2014), Lucas concluded that the $\delta^{13}\text{C}$ record published to date could not be correlated with that across the marine PTB at Meishan and elsewhere. Therefore, these data do not represent a viable* chemostratigraphic correlation with the global record, which, in turn, leads to the conclusion that variation in the data obtained from fossil material is inconclusive and compromised by uncertainty about biostratigraphic resolution.

According to the magnetostratigraphic records in the marine realm, the duration over which the end-Permian extinction occurred is positioned in an interval of relatively long normal magnetic polarity. An interval of normal polarity is reportedly associated with the *Daptocephalus*–*Lystrosaurus* AZ turnover above an underlying interval of reverse polarity (Ward *et al.*, 2005; Steiner, 2006), in which the first appearance of *Lystrosaurus* is recognised (King and Jenkins, 1997; Botha and Smith, 2007). Lucas (2009) interpreted this pattern as evidence that this biozone contact predated the marine extinction. At the time of his assessment, Lucas (2009) determined that the proposed magnetostratigraphic correlations between the Karoo Basin and sections at Meishan were consistent with the available data. Recently, though, the overall magnetostratigraphic polarity pattern reported from key localities (i.e. Old Lootsberg Pass; Gastaldo *et al.*, 2015) could not be repeated. Regardless of using the magnetostratigraphic record for correlation, the addition of high-resolution geochronology represents the best opportunity for understanding the palaeontological and stable carbon isotopic trends in the basin.

Until recently, bio-, magneto-, and chemostratigraphic correlations have been attempted in the Karoo successions across the vertebrate-defined PTB, in the absence of volcanogenic deposits that could be used for geochronometric constraint of these rocks. Rubidge *et al.* (2013) first demonstrated the presence of the volcanic ash in the Adelaide Subgroup strata and, using high-resolution U-Pb ID-TIMS analyses of single zircon crystals from silicified ash and devitrified claystone, placed several time constraints on the Beaufort Group. These ages, though, are reported outside of any published lithostratigraphy or stratigraphic framework. Dated ash beds occur at various positions, including (1) 1 230 m above the Ecça–Beaufort contact, (2) 30 m below a prominent sandstone which, “. . . could be the lowermost sandstone of the Middleton Formation, . . .”, (3) 375 m above the base of the Middleton Formation, (4) 220 m below the Middleton–Oudeberg contact, and (5) from within the arenaceous Oudeberg Member. All are reported either as chert (siliceous siltstone) or ash (presumably devitrified claystone), but measured stratigraphic sections or details about these deposits are not provided. The relative position of each sample allowed Rubidge *et al.* (2013) to estimate the base of the, then, *Dicynodon* AZ to be ca. 255.22 ± 0.16 Ma. Up to that time, this estimate was the only geochronometric constraint in the Balfour Formation, 500 m below the *Daptocephalus*–*Lystrosaurus* boundary (Kitching, 1995). Ward *et al.* (2005) and Erwin (2006) commented that other methodologies were needed (see

above) to constrain the end-Permian event because of an absence of volcanic deposits in the *Daptocephalus* AZ. However, this is not the case.

Several silicified siltstone (porcellanite) and devitrified claystone (tuffite) horizons are in close proximity to the vertebrate-defined PTB in the Lootsberg and Wapadsberg Pass areas. Recently, Gastaldo *et al.* (2015) have reported a U-Pb ID-TIMS age of 253.48 ± 0.15 Ma from a silicified ash bed situated ~60 m below the reported *Daptocephalus*–*Lystrosaurus* AZ boundary. This maximum depositional age determination is early Changhsingian, clearly younger than the Wuchiapingian (255.22 ± 0.16 Ma) age reported from the base of the *Daptocephalus* AZ (Rubidge *et al.*, 2013). Given the reported biozone thickness for the *Daptocephalus* AZ (Viglietti *et al.*, 2016) and high stratigraphic position of the ash bed within this biozone, Gastaldo *et al.* (2015) concluded there was an extremely low probability that the faunal turnover between the *Daptocephalus* and *Lystrosaurus* AZs actually represented the end-Permian terrestrial expression of the marine mass extinction event. This conclusion is supported by the magnetostratigraphic data presented by these authors. These data indicate that the upper part of the *Daptocephalus* AZ, with the exception of one thin reverse polarity magnetozone immediately above the silicified bed, together with the lower part of the *Lystrosaurus* AZ, to be located in normal polarity magnetozones. Such pattern is correlated more readily with an early Changhsingian polarity time scale than the global polarity reversal pattern close to the PTB (Szurlies, 2013).

6. SUMMARY

The response of the biosphere to the end-Permian extinction event serves as one of several deep time models used to predict how ecosystems can react to a global, unidirectional warming trend as a consequence of climate change. Currently, this model envisions a coeval collapse in both marine and terrestrial ecosystems (Benton and Newell, 2014), both of which were pushed past a series of physico-chemical thresholds (Knoll *et al.*, 2007) from which most organisms at various taxonomic levels never recovered. Phased extinction in the ocean basins (Song *et al.*, 2013; Payne and Clapham, 2012) occurred over approximately 61 ± 41 ka (Burgess *et al.* 2014, linked to the start of pulsed eruptions associated with the Siberian Traps (Kamo *et al.*, 2003; Burgess and Bowring, 2015). The onset and timing of maximum-marine extinction are dated at 252.2 ± 0.12 and 251.907 ± 0.067 Ma, respectively (Burgess and Bowring, 2015). The events in the marine realm are well documented biostratigraphically, placed in a high-resolution chemostratigraphic (Erwin *et al.*, 2002; Payne *et al.*, 2004; Hermann *et al.*, 2010; Horacek *et al.*, 2010) and magnetostratigraphic (Steiner, 2006; Szurlies, 2007; Glen *et al.*, 2009) framework, and well constrained by geochronometric ages (Shen *et al.*, 2011; Burgess *et al.*, 2014). In contrast, the events in the terrestrial record are based on a biostratigraphic hypothesis proposed over a century ago of vertebrate systematic turnover in the Karoo Basin, South Africa, (Broom, 1906, 1911), that has been extrapolated to other southern hemisphere regions (Retallack *et al.*, 2003) and the palaeo-mid-latitudes of Russia (Benton and Newell, 2014).

The model of “the Great Dying” is based on the replacement of the *Daptocephalus* AZ (Keyser and Smith, 1978; Rubidge, 1995) (formerly the *Dicynodon* AZ, but is still considered the latest Permian [Viglietti *et al.*, 2016]) by the *Lystrosaurus* AZ, considered as earliest Triassic. Phased turnover and vertebrate-extinction patterns are interpreted as the result of landscape devegetation (Smith and Ward, 2001; Smith and Botha-Brink, 2014), because of increasing aridity and environmental perturbation. The extinction and turnover is argued to have occurred over the same period as the marine event (Smith and Botha-Brink, 2014). This hypothesis and its purported correlation with the marine crisis is the result of a claimed unique lithostratigraphic horizon (Ward *et al.*, 2000) being fitted into a very coarse chemostratigraphic (MacLeod *et al.* 2000; Ward *et al.*, 2005) and magnetostratigraphic (De Kock and Kirschvink, 2004; Ward *et al.* 2005) framework, in the absence of precise isotopic ages (Erwin, 2006). To date, our results in the Karoo Basin demonstrate that there is little reliability to either the lithostratigraphic, biostratigraphic (Gastaldo *et al.*, 2015), chemostratigraphic (Gastaldo *et al.*, 2014), magnetostratigraphic, or palaeoecologic (Gastaldo *et al.*, 2015) models. However, these currently invoked and widely accepted (Rey *et al.*, 2015; Viglietti *et al.*, 2016) models form the basis on which the response of the terrestrial ecosystem to the “Mother of Mass Extinctions” is modelled (e.g., Roopnarine and Angielczyk, 2015). Recently, we have demonstrated that the probability that the timing of vertebrate turnover was coincident with the events in the oceans was extremely low. Our data indicate that the *Daptocephalus*–*Lystrosaurus* AZ boundary preceded the marine extinctions by at least more than 1 Ma (Gastaldo *et al.*, 2015) and, therefore, was unrelated to the volcanic activity associated with the Siberian Traps. Although the Karoo Basin model is untenable, it continues to be used (Viglietti *et al.*, 2016). Where is the Permian–Triassic transition in the Karoo Basin? Is it preserved (Hancox *et al.* 2002)? What is the response across the landscape, if any, to the perturbation in the marine realm? If we are to use deep time events as models for potential future responses to perturbed earth systems, these models have to be accurate.



7. AUGUST (DAY 1): CAPE TOWN TO MIDDELBURG

Day 1 is predominantly a day of travel, during which the field party will cross the Cape Fold Belt and traverse the plains and smaller mountains of the southern Karoo.

7.1 Timetable

Depart from Cape Town	08:00
Laingsburg	10:30
Beaufort West (lunch)	13:00
Depart Beaufort West	14:00
Graaff-Reinet	16:00
Middelburg (Eastern Cape)	17:00

7.2 Directions

Travel north from Cape Town on the N1 to Beaufort West. Major towns on this route include Paarl, Worcester, De Doorns, Touws River, and Laingsburg. At Beaufort West (~457 km), turn right (east) onto the R81 to Aberdeen (~135 km to the east). At Aberdeen, turn left (north) onto the N9 to Graaff-Reinet (56 km). Continue through Graaff-Reinet on the N9 to Middelburg (106 km), where we will overnight at the Karoo Country Inn.

7.3 Geological Background

The landscape that we will travel across on Day 1 is the result of four main geological events:

1. Accumulation of the Cape Supergroup in a passive margin setting during the Early Ordovician to Early Carboniferous.
2. Permo–Triassic Cape Orogeny that formed the Cape Fold Belt, which was the main sedimentary source for the Karoo Supergroup to the north.
3. Early Middle Jurassic (ca. 184 Ma) formation of the Karoo Large Igneous Province that preceded the continental breakup of Gondwana during the Mesozoic.

Late Proterozoic to early Palaeozoic extension, related to the breakup of greater proto-Gondwana, formed an extensive passive margin along the southern edge of South Africa (De Wit and Ransome, 1992). A wedge-shaped succession of clastic, shallow-marine, deltaic and nearshore fluvial strata (e.g. the Cape Supergroup) accumulated in this continental margin setting during the Early Ordovician to Early Carboniferous (Thamm and Johnson, 2006). This basin extended east–west for more than 1 000 km, and palaeocurrent data, thickness

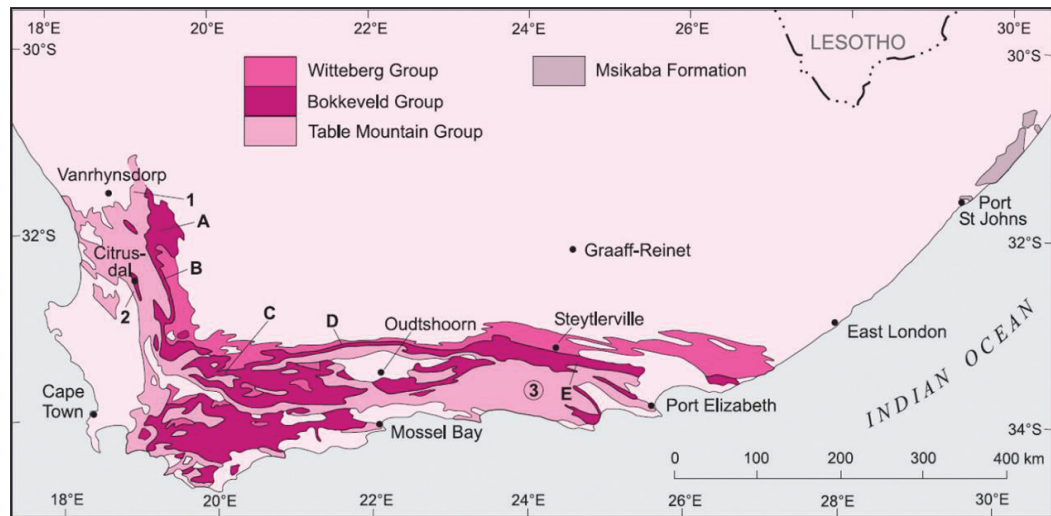


Figure 14.

Map showing the distribution of the three lithostratigraphic groups comprising the Cape Supergroup (from Thamm and Johnson, 2006).

changes, and grain-size variation all indicate that the main sediment source areas were located to the north and northwest of the basin (Thamm and Johnson, 2006).

Three groups are recognised in the Cape Supergroup (Fig. 14). The quartzites of the Table Mountain Group crop out at the base, are overlain by the argillaceous fine-grained sandstones of the Bokkeveld Group, and topped by the shales and subordinate sandstones of the Witteberg Group. A maximum thickness of almost 8 000 m was recorded for the Cape Supergroup succession near the coast (Thamm and Johnson, 2006). The Supergroup thins to the north and extends underneath the Karoo Supergroup, forming part of the upper crust, to a point north of the present-day escarpment, north of the town of Beaufort West (Lindeque *et al.*, 2011).

Deformation during the Permian–Triassic Cape orogeny formed the Cape Fold Belt (Newton *et al.*, 2006), while the associated crustal loading created the Karoo Basin to the north (Johnson *et al.*, 2006; Lindeque *et al.*, 2011). The Cape Fold Belt is considered generally to have formed part of a regionally extensive mountain belt that developed along the southern margin of Gondwana. This belt is traceable from the Sierra de la Ventana in Argentina to the Pensacola Mountains of the Trans-Antarctic Mountains (Newton *et al.*, 2006). The Cape orogeny had limited influence on the southernmost part of the low relief Karoo Supergroup (Hälbich and Swart, 1983; Stankiewicz *et al.*, 2007), with intense deformation occurring to the south of the Karoo Basin, where the rocks of the Cape Supergroup form the bulk of the Cape Fold Mountains (Hälbich and Swart, 1983; Paton *et al.*, 2006). On a regional scale, two structural branches have been recognised in the Cape Fold Belt (Fig. 15), namely, a north–northwest–striking western branch north of Cape Town and an east–west–trending southern branch, with the two branches coalescing in the Cape Syntaxis (Söhnge, 1983; De Beer, 1990, 1998).

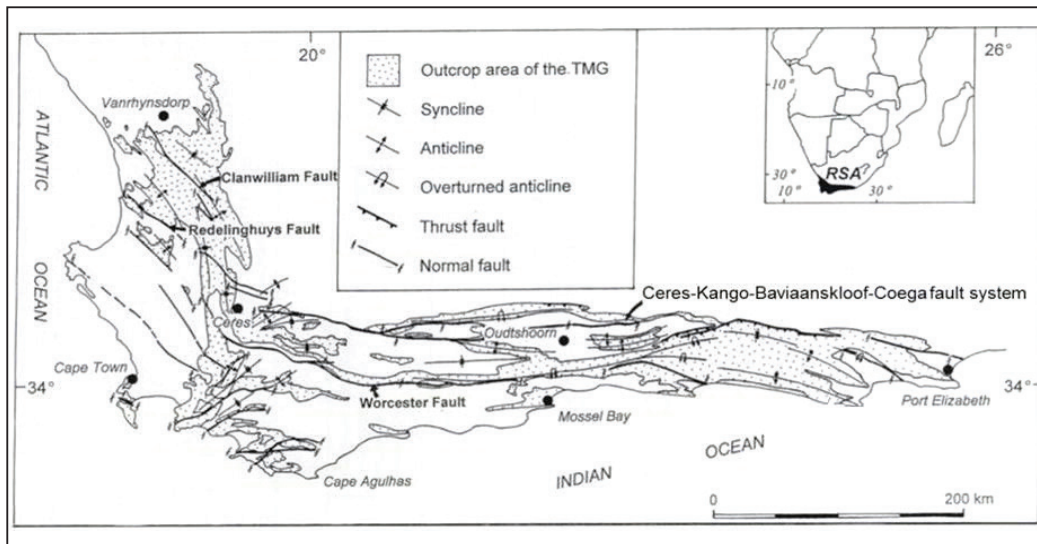


Figure 14. Map showing the two structural branches of the Cape Fold Belt (from De Beer, 2002).

The lowermost Dwyka Group of the Karoo Supergroup consists of glacial deposits that accumulated during the Late Carboniferous to Early Permian. In the south, it consists predominantly of silt-dominated diamictite with dropstones (Catuneanu *et al.*, 2005; Johnson *et al.*, 2006). It is succeeded by the rocks of the Eccca Group that record glaciofluvial deposition in the north and contemporaneous deep-water marine sedimentation in the south. The asymmetric shape of the Karoo Basin, in conjunction with the mode of origin of the Eccca Group, resulted in significant lateral facies variation within this group. This variation is reflected by the sixteen formations (Fig. 1) that have been recognised within the Eccca Group, of which eight (from base to top they are the Prince Albert, Whitehill, Collingham, Vischkuil, Laingsburg, Ripon, Fort Brown, and Waterford formations) crop out in the southern rim of the basin in the south (Johnson *et al.*, 2006). The deep-marine setting allowed the accumulation of basin-floor pelagic sediments (Prince Albert and Whitehill formations), and submarine fans (Collingham and Ripon formations; Catuneanu *et al.*, 2005). The latter two units are separated by the Laingsburg Formation, from which several turbidite systems are described (e.g. Sixsmith *et al.*, 2004). Prodelta slope mudstones of the Fort Brown Formation (Johnson *et al.*, 2006) and deltaic deposits of the Waterford Formation (Wickens, 1994) are indicative of shallower environments above the Rippon Formation.

Sedimentation in the Karoo ceased with the extrusion of the Drakensberg lavas at ca. ~183 Ma, followed shortly thereafter by the continental breakup of Gondwana. Continental breakup resulted in both uplift and subsidence, and high rates of erosion in southern Africa (Partridge and Maud, 1987; De Wit, 1999). At the southern margin of the continent, much of this sediment was deposited in a series of graben and half-graben rift basins that were superimposed onto the fold belt (Le Roux, 1983; Bate and Malan, 1992). These basins filled by an upward-fining sequence, consisting of the alluvial (Enon), fluvial (Kirkwood), and shallow-marine (Sundays River) formations of the Jurassic and

Cretaceous Uitenhage Group (Shone, 2006). Remnants of these deposits are preserved still in a number of Mesozoic inliers along the coast and throughout the Cape Fold Belt, and generally thin from east to west (Shone, 2006).

A predominantly erosional regime during the mid to late Cretaceous dissected the Karoo Basin, and this process continued during the Cenozoic. The rates of land-level change during the Cenozoic vary among different locations in southern Africa and multiple hypotheses have been presented to explain both the reason and the varying rates. The models of Palaeogene to Recent rates of land-level change and erosion can be grouped generally into two categories and requires either:

- discrete episodes of rapid uplift (e.g., King, 1962; Partridge and Maud, 1987), or
- no uplift (e.g., Gurnis *et al.*, 2000; Doucoré and De Wit, 2003), with almost continuous erosion.

Whichever model is viable, the net effect was dissection of the Karoo Basin fill, which sculpted the characteristic landscape of the Karoo. This landscape includes flat-topped koppies (hills), capped by extremely resistant dolerite sills or dikes, or comparably resistant sandstone-dominated sequences. Such a landscape is said to have influenced J.R.R. Tolkien, who had lived in Bloemfontein for three years and had seen vast expanses of grasslands punctuated by koppies, when he described his fictional universe of Middle-Earth, Mordor. At the time of continental breakup, the African palaeosurface was unequivocally high (Doucoré and De Wit, 2003), forming a marginal escarpment (Partridge and Maud, 2000). Over time, this escarpment was eroded, forming the modern Great Escarpment that occurs “as a giant rampart 20 to 200 km inland of the coast” (Partridge and Maud, 2000).

7.4 Geological Features on the Route

7.4.1 Paarl batholith

De Beer (1990) proposed that the position and development of the Cape Syntaxis was influenced by the buttressing effect of granite intrusions in the southwestern tip of the continent, together with a change in basement structural grain and southwest compression. The north-northwest orientation of the western branch of the Cape Fold Belt is the reason for the geology of Cape Town being generally unaffected by this orogenic event. It also explains why the quartzite cap of Table Mountain is essentially horizontal. The Paarl Pluton, overlooking the town of Paarl, is one of the best-known examples of these late Precambrian to Early Cambrian granites. As we travel further northeast, the effect of the orogenic processes that formed the Cape Fold Belt will become more apparent.

7.4.2 Uitenhage Group remnant, Worcester

After crossing the Du Toit’s Kloof Mountains northeast of Paarl, the N1 traverses a broad plain on the way to Worcester. Look out for a low, red hill on the right hand side of the road, approximately 5 km from Worcester, where the road splits into two separate lanes. This hill represents one of the westernmost remnants of the Enon and Kirkwood formations, which once filled the valleys in the Cape Fold Belt during an erosional phase (Cretaceous).

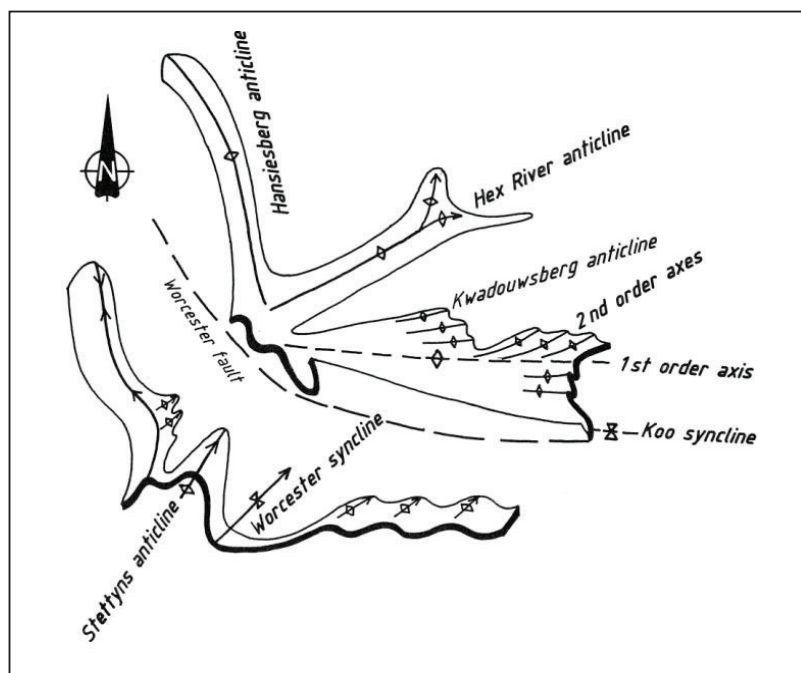


Figure 16.
A schematic interpretation of the structural geology of the syntaxial core (from De Beer, 1998).

7.4.3 Hex River Anticline, De Doorns

Folding becomes more intense to the northeast, after passing Worcester, where the N1 travels parallel to the syntaxical core (Fig. 16), which is characterised by numerous northeast-trending folds. The influence of the northeast-orientated Hex River Anticline is evident in the narrow Hex River Valley, home to the town of De Doorns. The N1 leaves the valley via the Hex River Pass to the northeast, after which the landscape flattens out somewhat. Here, *en route* to the town of Touws River, the first outcrops of the Dwyka and Ecca groups can be seen.

7.4.4 Dwyka and Ecca groups exposures, Matjiesfontein

The Dwyka Group crops out on both sides of the road at the crossing to Sutherland (left onto the R354) and Matjiesfontein (right). Approximately one kilometre farther, where the road starts to curve gently to the left, the lowermost formations of the Ecca Group are exposed on the right hand side of the road. The Prince Albert Formation (40–150 m thick) consists of dark-grey, pyrite-rich shale, with dark chert beds and phosphatic nodules. The overlying Whitehill Formation weathers to white (making it a useful marker unit), but in fresh exposures consists of black, carbonaceous (with organic carbon content of $\leq 17\%$), very thinly laminated shale. It commonly yields plant remains, palaeoniscid fish and arthropod remains. It is best known for containing the remains of the aquatic reptile *Mesosaurus*, which was instrumental in Alfred Wegener's development of the theory of continental drift, because it is also known from eastern South America. The Collingham Formation (30–70 m thick) consists of a rhythmic alternation dark-grey siliceous mudrock and soft, yellow tuff. The Matjiesfontein Chert Bed, in the lower half of this formation, weathers positively (to resemble a low stonewall), forming a distinctive local marker.

7.4.5 Laingsburg flood

In the summer of 1981, the small town of Laingsburg, situated in an arid part of the Karoo that has thin soils and very sparse vegetation, was struck by a flash flood. The Buffels River catchment area received the entire average annual rainfall (~300 mm) within a 12-hour period. On 25 January 1981, the dendritic catchment of the Buffels River concentrated the floodwaters on the town of Laingsburg. Overbank flood levels were exacerbated by the railway bridge, which created a temporary barrier and artificial dam wall (Fig. 17) downstream of the town. A second flood pulse, which arrived approximately three hours after the first maximum flood level, eroded the bridge embankments, leading to the collapse of the bridge. The maximum water depth in the channel was calculated to be 12 m at peak flow and the overbank sediments were deposited more than a kilometre from the river channel (Stear, 1985).

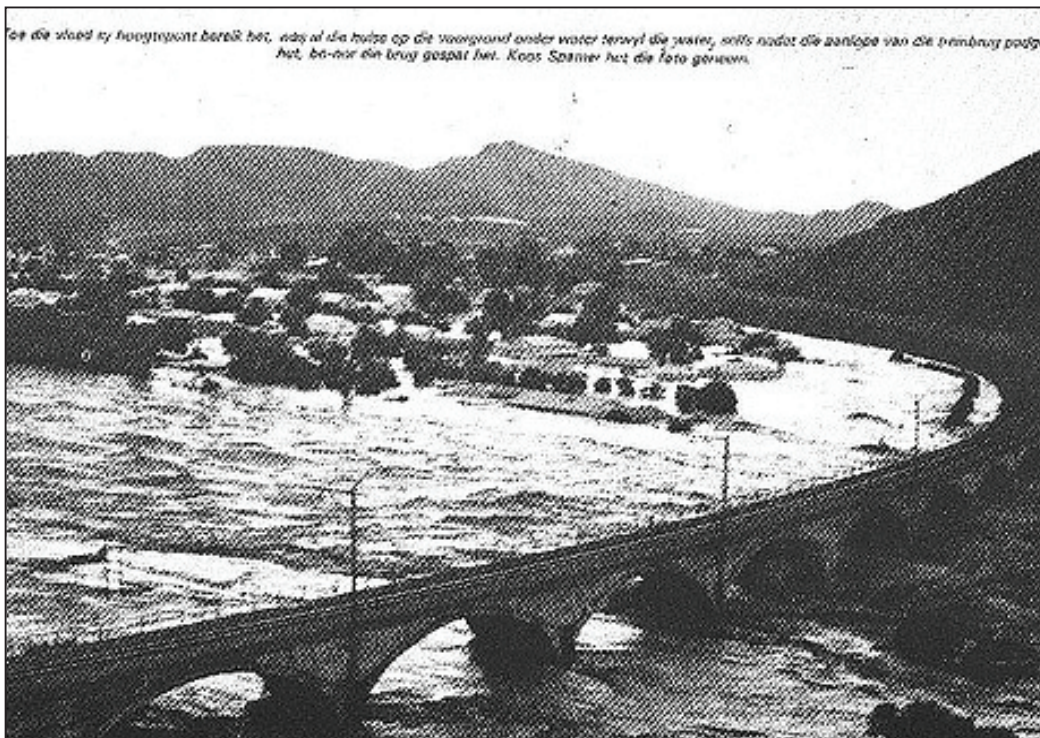


Figure 17.

Photograph of the pooling effect and resulted flooding caused by the railway bridge downstream of Laingsburg during the flood of 25 January 1981 (source unknown).



7.4.6 Laingsburg turbidites

The hills around Laingsburg belong to the Laingsburg Formation. Sixsmith *et al.* (2004) undertook a detailed investigation of the lowest of six turbidite systems described from the area and characterised these turbidites. Thick, sheet-like sandstones predominate and are separated by much thinner mudstone-dominated units, which represent both turbidite deposition and suspension-load settling. The bedded siltstones and mudstones next to the N1 show parallel or undulating laminations, with rare ripple cross-stratification. They can be separated by rare thin sandstones up to a few centimetres in thickness, and are interpreted to represent dilute turbidite deposition on the basin floor (Sixsmith *et al.*, 2004).

7.4.7 The Escarpment

At the time of breakup of Gondwana in the Mesozoic, the African land surface was high (Doucoré and De Wit, 2003), forming a marginal escarpment (Partridge and Maud, 2000). Over time, this escarpment was driven back by erosive processes, forming the modern Great Escarpment. The Great Escarpment occurs as a giant rampart 50 to 200 km inland of the coast (Partridge and Maud, 2000). On the road between Beaufort West and Aberdeen, the escarpment is visible on the left (north) side of the road.

8. 23 AUGUST (DAY 2): BETHULIE LOCALITY

Much of Day 2 will be spent away from the bus, walking over relatively rough terrain; therefore, please ensure that you wear suitable shoes, and dress for both warm and cold weather. Bring your baboon repellent!

8.1 Timetable

Depart from Middelburg	08:00
Arrive at locality turn-off, depart to Bethulie locality	10:00
Arrive at locality	10:30
Stop 2-1 to 2-3	10:30–12:00
Lunch	12:00
Stops 2-4 to 2-6	13:00
Depart from locality	15:00
Depart for the town of Bethulie	15:30
Arrive at hotel	16:00

8.2 Directions

Travel north from Middelburg on the N9, passing the town of Noupoort, joining the N1 North at Colesberg after 100 km. Continue north on the N1, crossing the Orange River and, after 44 km, take the turn-off for the R701 near Gariiep Dam village. Travel east on the R701 to the town of Bethulie (60km) and continue east past Bethulie for 27 km, at which point the road forks, with the left fork continuing as the R701 toward Smithfield. Take the right hand fork (gravel road) toward the town of Aliwal North and travel for approximately 6 km. The entrance to the farm Bethal 763 is on the right. Travel along the dirt track for approximately 4 km to the Bethulie locality. Upon leaving the locality, retrace the route to Bethulie, where we will overnight in the Bethulie Royal Hotel.

8.3 Background

The Bethulie locality is situated approximately 30 km east of the town of Bethulie, on the farms (Fig. 18) Bethel 763, Heldenmoed 677, and Donald 207 (encompassing the farm Fairydale). It is a well-known and productive fossil locality at the base of a deep valley that was discovered first by James Kitching in 1977 (Abdala *et al.*, 2006). Smith (1995) recorded the first PTB section here and his depicted measured section (Fig. 5) is featured prominently in subsequent publications. It is arguably the most important PTB locality in South Africa, having yielded the largest number of vertebrate fossils of all the sections studied (~250 fossils — see Smith and Botha-Brink, 2014, supplementary data). Sedimentological data collected at this locality have made an important contribution to the current depositional model, whereas the geochemical data obtained here have been used to propose an isotope-based global correlation.

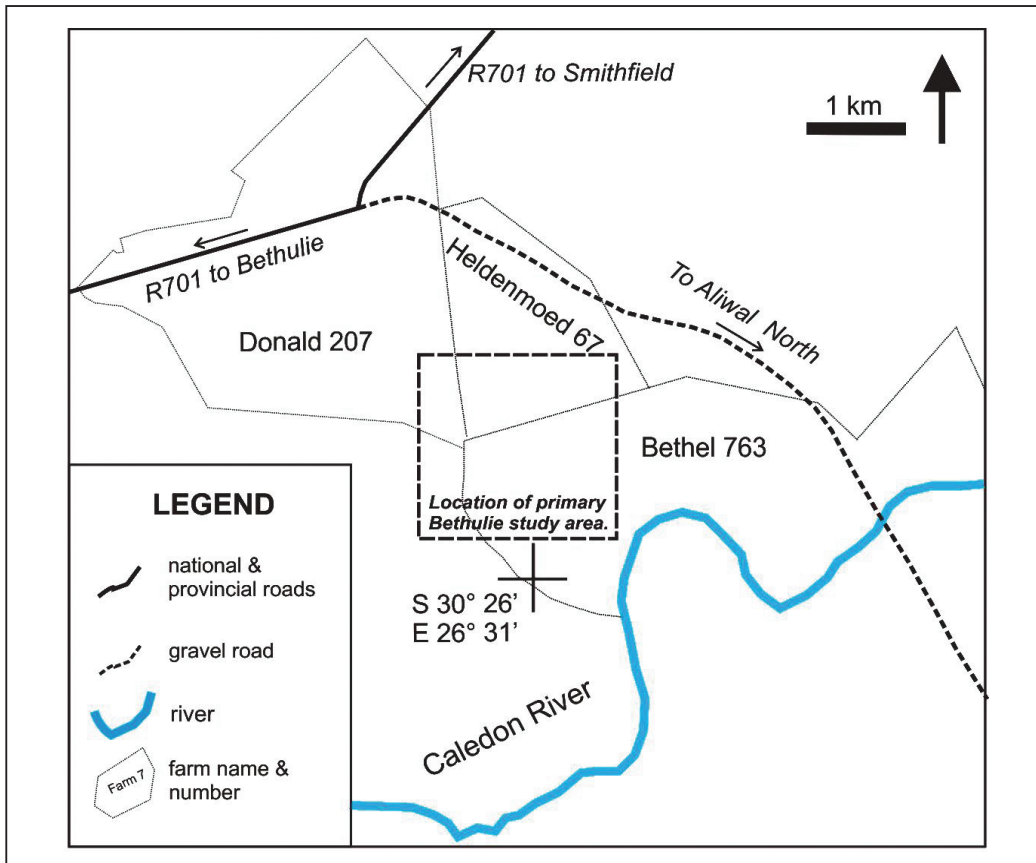


Figure 18. Map of the Bethulie locality on the farms Bethel, Heldenmoed, and Donald. The stippled block depicts the position of the valley (also refer to Fig. 27) that has been the primary focus of research in the area and will be visited during this trip.

The Caledon locality of Ward *et al.* (2000), and the photograph of the “laminare event bed” at the Bethulie locality provided by Retallack *et al.* (2003, their fig. 3B) refer to localities on the opposite side of the Caledon River (and valley) to the south-southeast. These exposures are generally of limited extent and contributed little to the development of the extinction model. When assessing the stratigraphy of the sections in the southern Free State, it should be kept in mind that the localities near Bethulie represent the northernmost (and distalmost) Upper Permian–Lower Triassic sections used in extinction studies. Therefore, these areas display stratigraphy that is more condensed than is that of the localities that will be visited on subsequent days.

We will start the exploration by traversing up the main donga used to construct the primary stratigraphic section at the locality (Smith, 1995).

Stop 2-1: Permo–Triassic Boundary sequence

No coordinates for specific PTB exposures are available from the literature, but a photograph of the boundary sequence at the Bethulie locality is provided in Botha and Smith (2006, their fig. 1) and Smith and Botha-Brink (2014, their fig. 5). Here, at least the upper four of the five described boundary lithofacies associations crop out (Fig. 19). These are (from top to bottom):

- E – Conglomeratic sandstones (Katberg Formation)
- D – Massively bedded maroon and grey siltstones
- C – Laminated siltstone–mudstone couplets
- B – Massive maroon and grey mudrock.

The PTB has been placed at the top of lithofacies association C, which, at this location, is represented by a siltstone interval that appears greyish red when viewed from a distance (Fig. 19). Delegates will have the opportunity for close-up examination of these

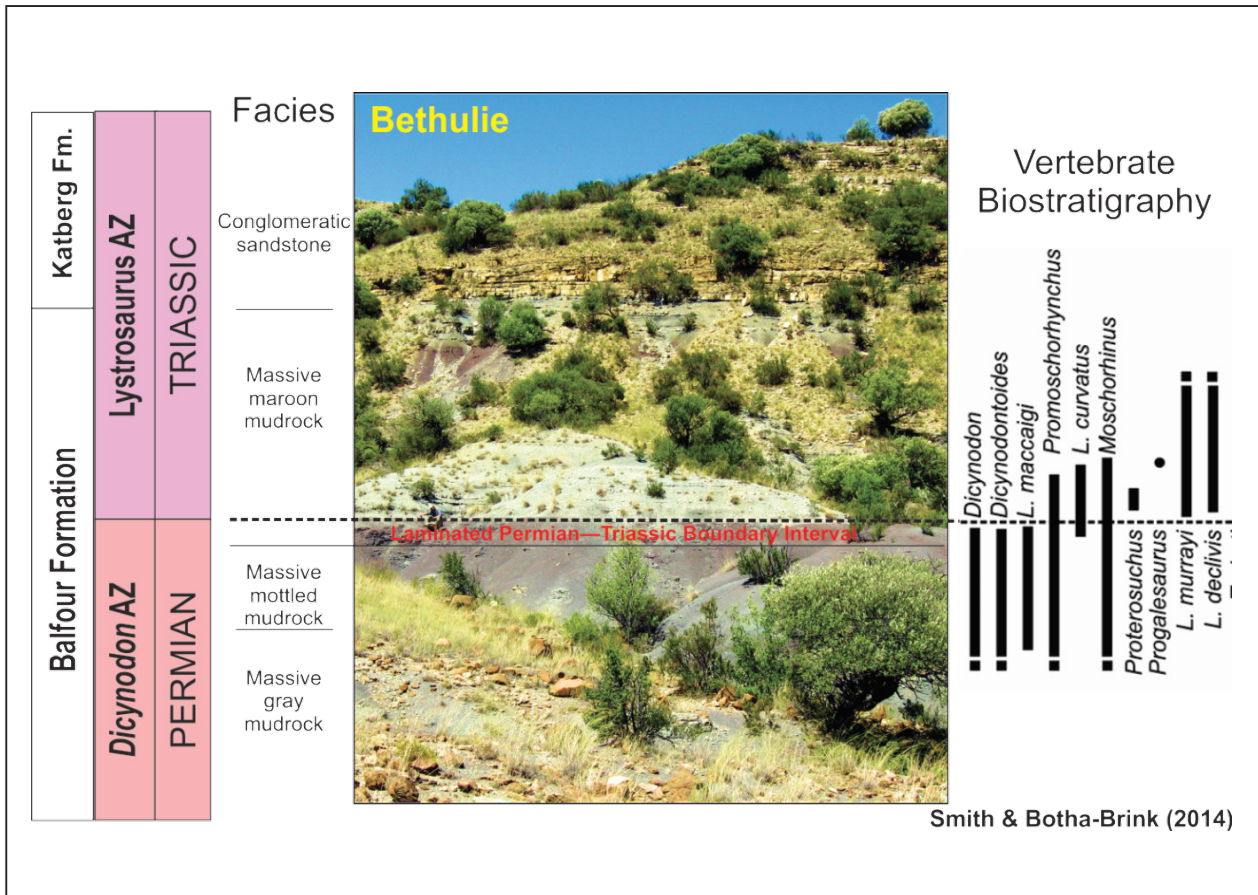


Figure 19.

Stop 2-1. The location of the PTB and facies sequence, as reported by Botha and Smith (2005) and Smith and Botha-Brink (2014). A summary of their facies sequence (as applied at this location) and general biostratigraphic tetrapod ranges are provided on the left and right of the figure respectively. (Figure adapted from an article published in *Palaeogeography, Palaeoclimatology, Palaeoecology*, v. 396, Smith and Botha-Brink, Anatomy of a mass extinction: Sedimentological and taphonomic evidence for drought-induced die-offs at the Permo–Triassic boundary in the main Karoo Basin, South Africa, p. 99–118, Copyright Elsevier, 2014).

rocks and comparison of their own observations with the descriptions in the literature. As presented above, there are two schools of thought on the genesis of these beds. In order to solve this controversy, the lateral facies relationships need to be assessed. The field party will have an opportunity to trace the laminated interval to the right (south) and study its relationship with a lenticular sandstone succession situated above Stop 2-2.

Stop 2-2: Contact between dolerite sill and host rocks, palaeomagnetic results

The attitude of Karoo strata is mainly horizontal, but the strata are dissected extensively by typical more resistant dolerites of the Karoo LIP, as interconnected networks of dikes, sills, and saucer-shaped sheets (Chevallier and Woodford, 1999). This complex of mafic intrusions is considered generally to represent the shallow feeder system for the flood basalts, exceeding one kilometre in thickness, that makes up the Drakensberg Group at the top of the Karoo Supergroup. The thermochemical sedimentary succession in the Karoo Basin has been the subject of considerable research, with a range of tentative interpretations being put forward.

The Bethulie locality we will visit has been sampled extensively for palaeomagnetic (magnetic polarity) stratigraphy study (Fig. 20). Several relatively thin (0.5 to 3 m wide) dolerite dikes are exposed at the locality. Excellent exposures of these dikes AND their thermally modified (to contact metamorphosed) host-contact strata are typical in the dongas (erosional gullies). The dike and contact rocks we will visit at this locality afford an excellent opportunity to undertake a classic palaeomagnetic “contact test”, as first described by Everitt and Clegg (1962). As you will see, the rocks here have been sampled extensively. The contact test is one of a number of field relation-based tests that have been used often to demonstrate the geologic antiquity of any ‘characteristic’

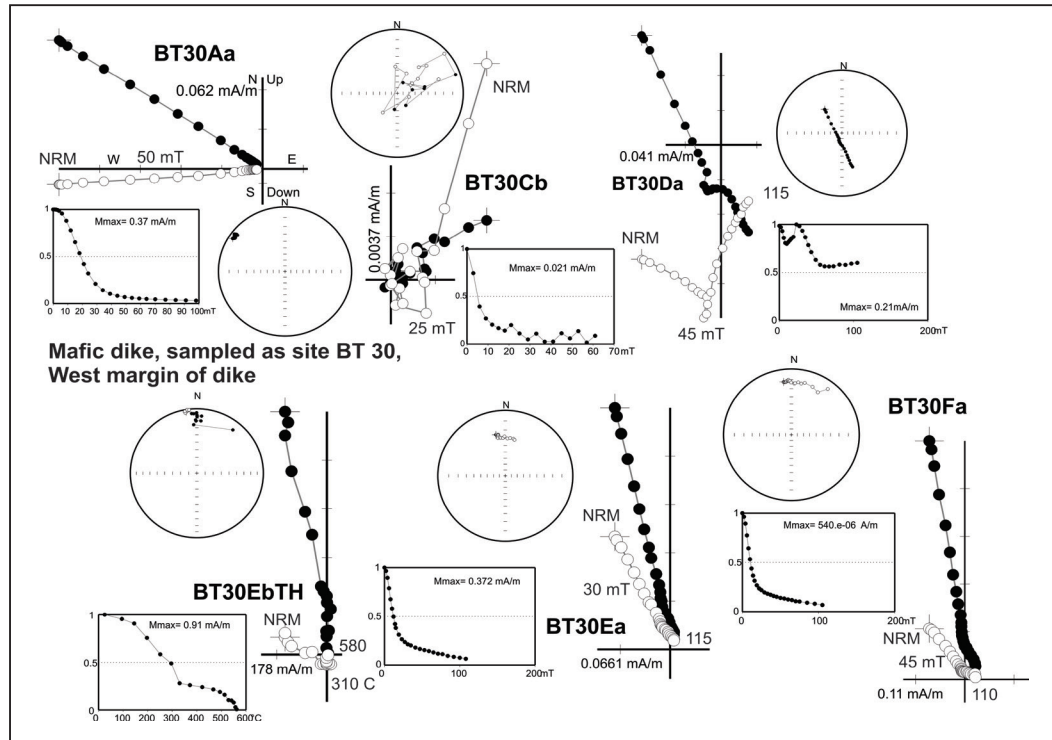


Figure 21.

Orthogonal progressive demagnetisation diagrams (Zijderveld, 1967) showing the end point of the magnetization vector plotted onto the horizontal (filled symbols) and vertical (open symbols) planes (NS–EW, EW–Up/Dn) for individual specimens from samples from site BT 30, a Karoo dolerite sill that have been subjected to alternating field (AF) or thermal demagnetisation. Also shown are normalised intensity decay plots showing response to progressive treatment and stereographic projections of the magnetisation vector measured at each step. All diagrams in geographic coordinates with identical axes orientations.

the intrusion, itself, is likely ‘primary’ and therefore associated with initial cooling and thermal ‘blocking’, and (2) remanence in the host rock that is consistent in the host rock at localities that are spatially removed from the intrusion actually predates the intrusion. For such a test to be conclusive, the remanence in the host rocks immediately adjacent to the intrusion must be directionally statistically identical to those in the intrusion, AND such remanence should decrease in overall intensity and prevalence as a function of distance from the intrusion. This trend results in the identification of remanence that is different in direction from that in the intrusion, which is well grouped and likely has different magnetisation properties (e.g. lower remanence intensity). From an historical perspective, the results of sets of baked contact tests performed in the 1950s conclusively demonstrated that the magnetic field of the Earth was capable of reversing its polarity.

The overall results obtained from the Karoo dike (sampled at BT3 and BT30) and host sedimentary rocks (sampled as BT4 and BT31) in contact with the dike at this locality are not as simple as anticipated (i.e. complicated!). Parts of the dike have magnetisation that is of east-southeast declination and moderate positive inclination, and is moderately to reasonably well isolated in progressive demagnetisation (Figs 21, 22), in that there is a defined trajectory to the origin. On the other hand, some samples yield a magnetization of north declination and shallow positive inclination, while others yield a normal polarity remanence that is more typical of that of later Karoo intrusions. The east-southeast and moderate positive inclination direction of this magnetisation characteristic of the dike is somewhat unusual, in that most Karoo intrusions are characterised as having a magnetisation of north-northwest declination and relatively steep negative inclination (~330°/-60°), which is interpreted as normal polarity remanence. Occasionally, these rocks exhibit an oppositely directed magnetisation (~150°/+60°), interpreted as reverse polarity. Therefore, the east-southeast direction in this particular dike has a more intermediate direction magnetisation. Anisotropy of magnetic susceptibility data from this dike (Fig 23) show what is often referred to as an inverse fabric for planar intrusion, in that the maximum susceptibility axis for most samples is perpendicular to the dike margin.

The host rocks sampled show a more complicated behaviour (Fig. 24, 25). Close to the dike, samples yield a magnetisation of north declination and moderately steep negative inclination. Farther from the dike, samples show an east-southeast-directed, moderate positive inclination magnetisation as their dominant remanence. In addition, these rocks exhibit remanence intensities close to an order of magnitude higher (> 50 mA/m) than those typical of the Beaufort Group strata removed from dikes. The most logical interpretation is that this magnetisation was acquired at the time of dike emplacement by thermal annealing. Host rocks farther from the dike contact, as a function of distance from the dikes, show an increasing degree of north- to north-northwest-directed magnetisation, moderate to steep negative inclination

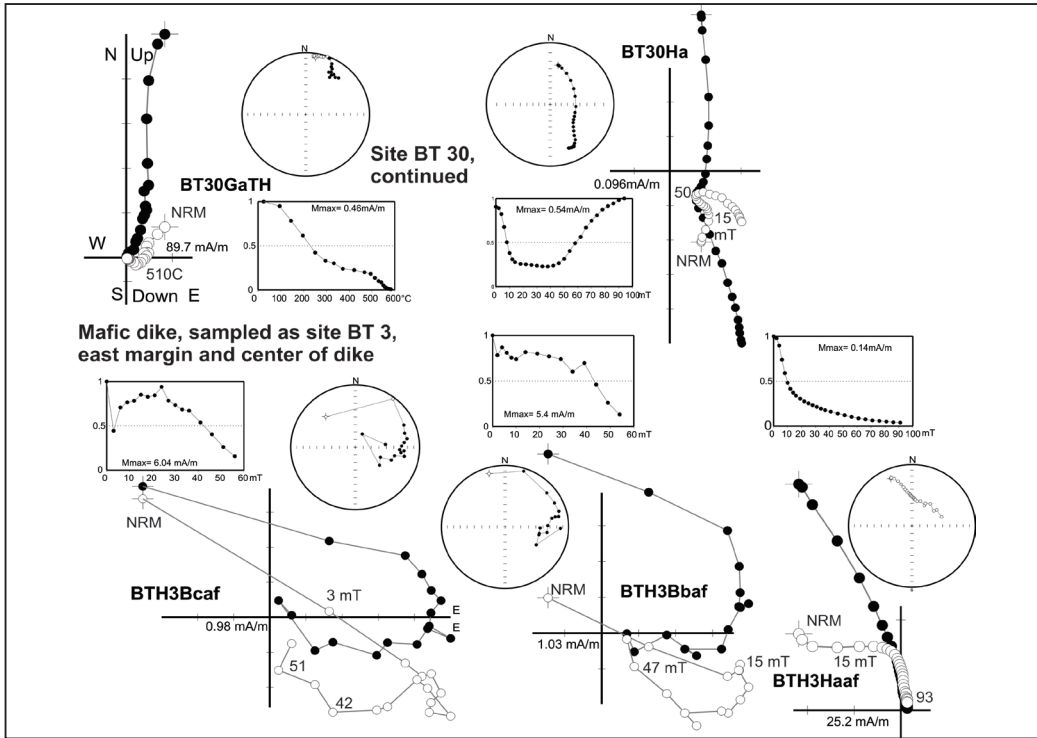


Figure 22. Orthogonal progressive demagnetisation diagrams (Zijderveld, 1967) showing the end point of the magnetisation vector plotted onto the horizontal (filled symbols) and vertical (open symbols) planes (NS–EW, EW–Up/Dn) for individual specimens from samples from site BT 30 and 3 in a Karoo dolerite dike that have been subjected to alternating field (AF) or thermal demagnetisation. Also shown are normalised intensity decay plots indicating response to progressive treatment and stereographic projections of the magnetisation vector measured at each step. All diagrams in geographic coordinates with identical axes orientations.

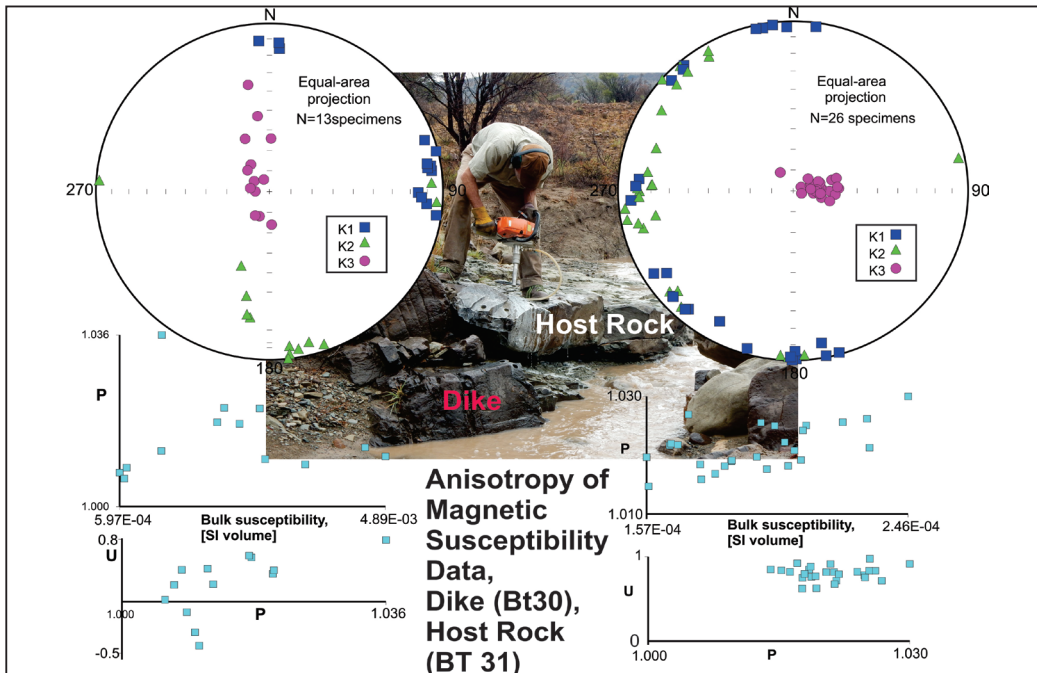


Figure 23. Anisotropy of magnetic susceptibility data from sites BT30 (Karoo dolerite dike) and BT 31 (contact host rocks). Plots of maximum, intermediate, and minimum susceptibility axes and anisotropy parameters. The Karoo dike displays well-defined foliation that is parallel to the dike contact. The host strata display extremely well-defined depositional fabric.

Figure 24.

Orthogonal progressive demagnetisation diagrams (Zijderveld, 1967) showing the end point of the magnetisation vector plotted onto the horizontal (filled symbols) and vertical (open symbols) planes (NS-EW, EW-Up/Dn) for individual specimens from samples from site BT 4, in host rock strata adjacent to a Karoo dolerite sill (site 3 and 30) that have been subjected to alternating field (AF) or thermal demagnetisation. Also shown are normalised intensity decay plots showing response to progressive treatment and stereographic projections of the magnetisation vector measured at each step. All diagrams in geographic coordinates with identical axes orientations.

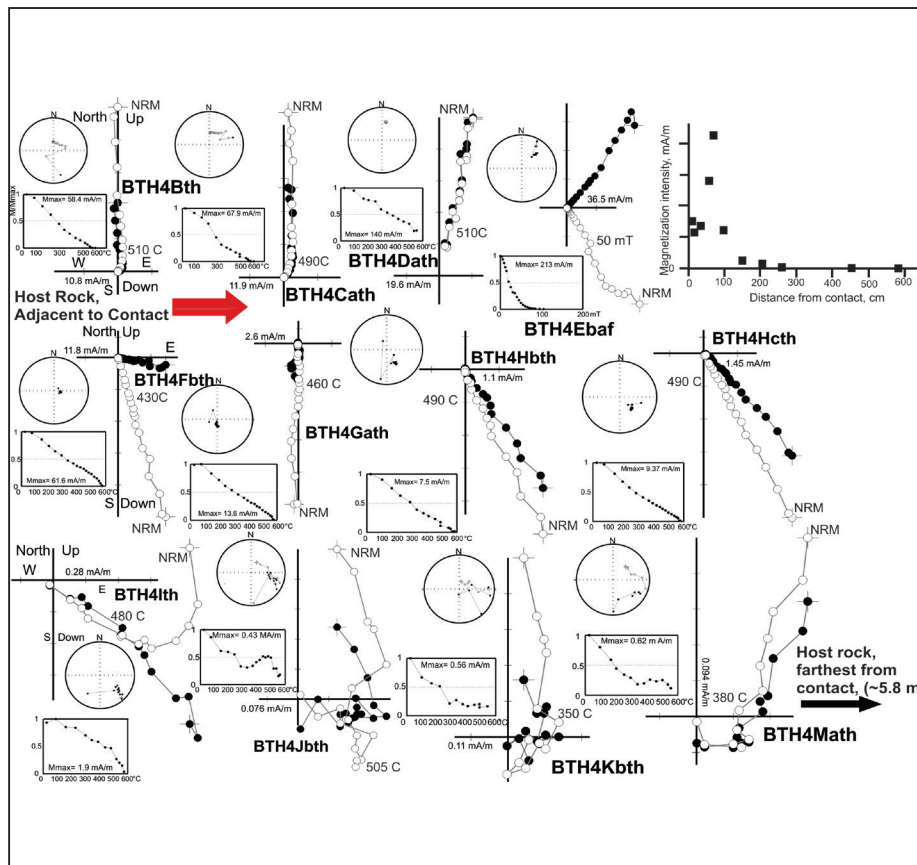
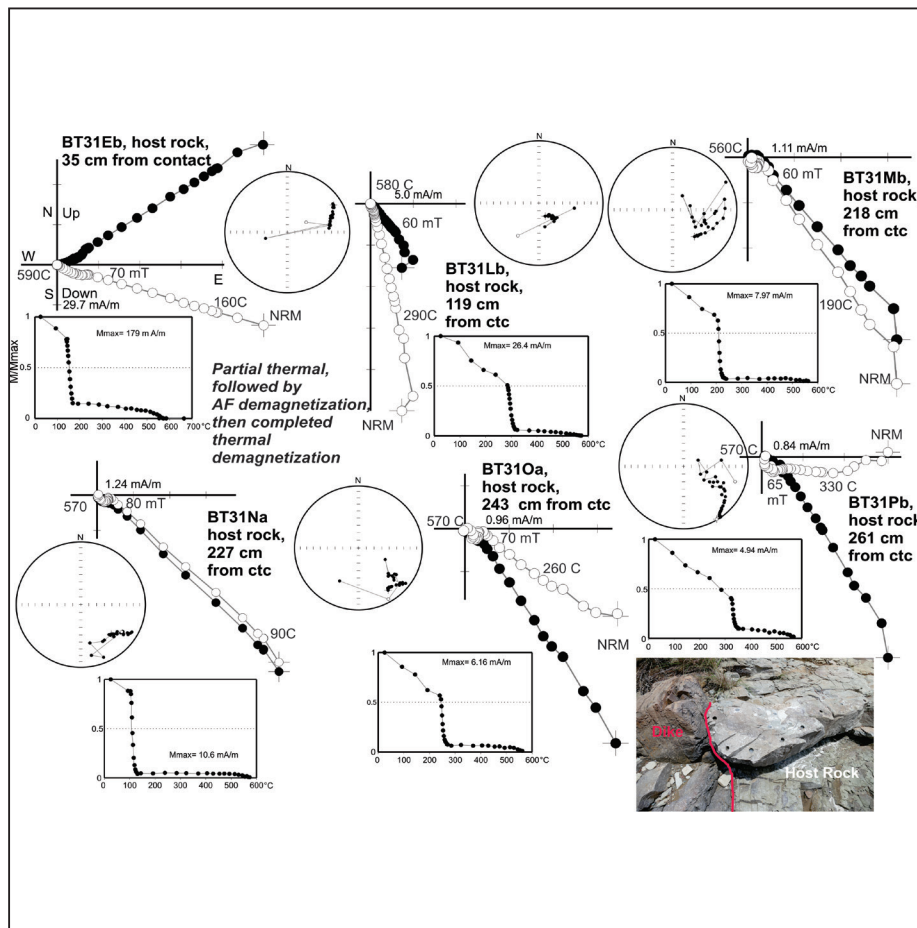


Figure 25.

Orthogonal progressive demagnetisation diagrams (Zijderveld, 1967), showing the end point of the magnetisation vector plotted onto the horizontal (filled symbols) and vertical (open symbols) planes (NS-EW, EW-Up/Dn) for individual specimens from samples from site BT 31, in host rock strata adjacent to a Karoo dolerite sill (sites 3 and 30) that have been subjected to alternating field (AF) or thermal demagnetisation. Also shown are normalised intensity decay plots indicating response to progressive treatment and stereographic projections of the magnetisation vector measured at each step. All diagrams in geographic coordinates with identical axes orientations.



magnetisation (normal polarity remanence), and considerably weaker remanence intensity. This magnetisation is superimposed on a poorly defined magnetisation of east-southeast declination and moderate positive inclination. Host rocks sampled at this locality reveal a quite straightforward magnetic anisotropy fabric typical of primary depositional fabric (Fig. 23). Based on these results, we interpret the host strata at this site to lie within a normal polarity magnetozone. As a cautionary note, the results from this dike/host rock contact test contrast greatly to those obtained from sites BT30A (mafic dike) and BT35 (host rocks) farther up the donga at the Bethulie site (refer to sampling location map, Fig. 19).

The mafic dike at this locality shows a very well-defined east-southeast declination, moderate positive inclination as its characteristic remanence, and all of the host strata within 1.5 m of the contact reveal similar magnetisation, with north-northwest declination and superimposed steep negative inclination.

Stop 2-3: Palaeomagnetic data from Bethulie

Progressing up the donga from this locality, the authors have sampled several sites in an area that shows no obvious evidence of Karoo dikes. Site BT15 (resampled as site BT21) is uniformly dominated by well-defined reverse-polarity remanent magnetisation and relatively weak, yet very distinct, superimposed normal polarity, with remanent magnetisation being fully unblocked below 400°C (Fig. 26). Our interpretation is that this stratigraphic interval is part of a reverse polarity magnetozone. The results from this site are of considerable importance in that they uniformly, from sample to sample, demonstrate that since acquisition of reverse polarity magnetisation, the effects of any subsequent processes (e.g. Karoo magmatism, young viscous remanence acquisition) could be removed in progressive thermal demagnetisation by approximately 400°C. We conclude that Beaufort Group strata at the Bethulie locality preserve early-acquired remanence, at least locally.

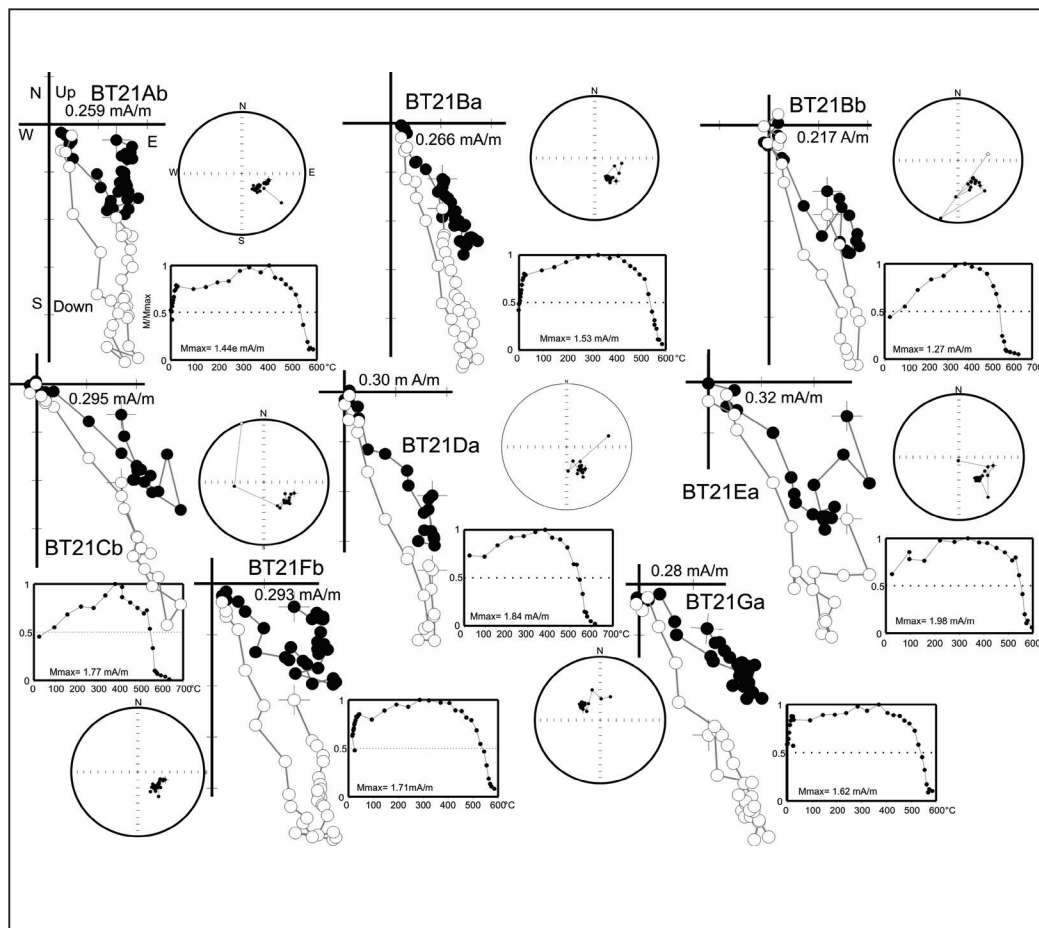


Figure 26.

Orthogonal progressive demagnetisation diagrams (Zijderveld, 1967), showing the end point of the magnetisation vector plotted onto the horizontal (filled symbols) and vertical (open symbols) planes (NS–EW, EW–Up/Dn) for individual specimens from samples from site BT 21, in host rock strata, which, based on field relations, are far removed from any Karoo dolerite sill, and have been subjected to alternating field (AF) or thermal demagnetisation. Also shown are normalised intensity decay plots showing response to progressive treatment and stereographic projections of the magnetisation vector measured at each step. All diagrams in geographic coordinates with identical axes orientations.

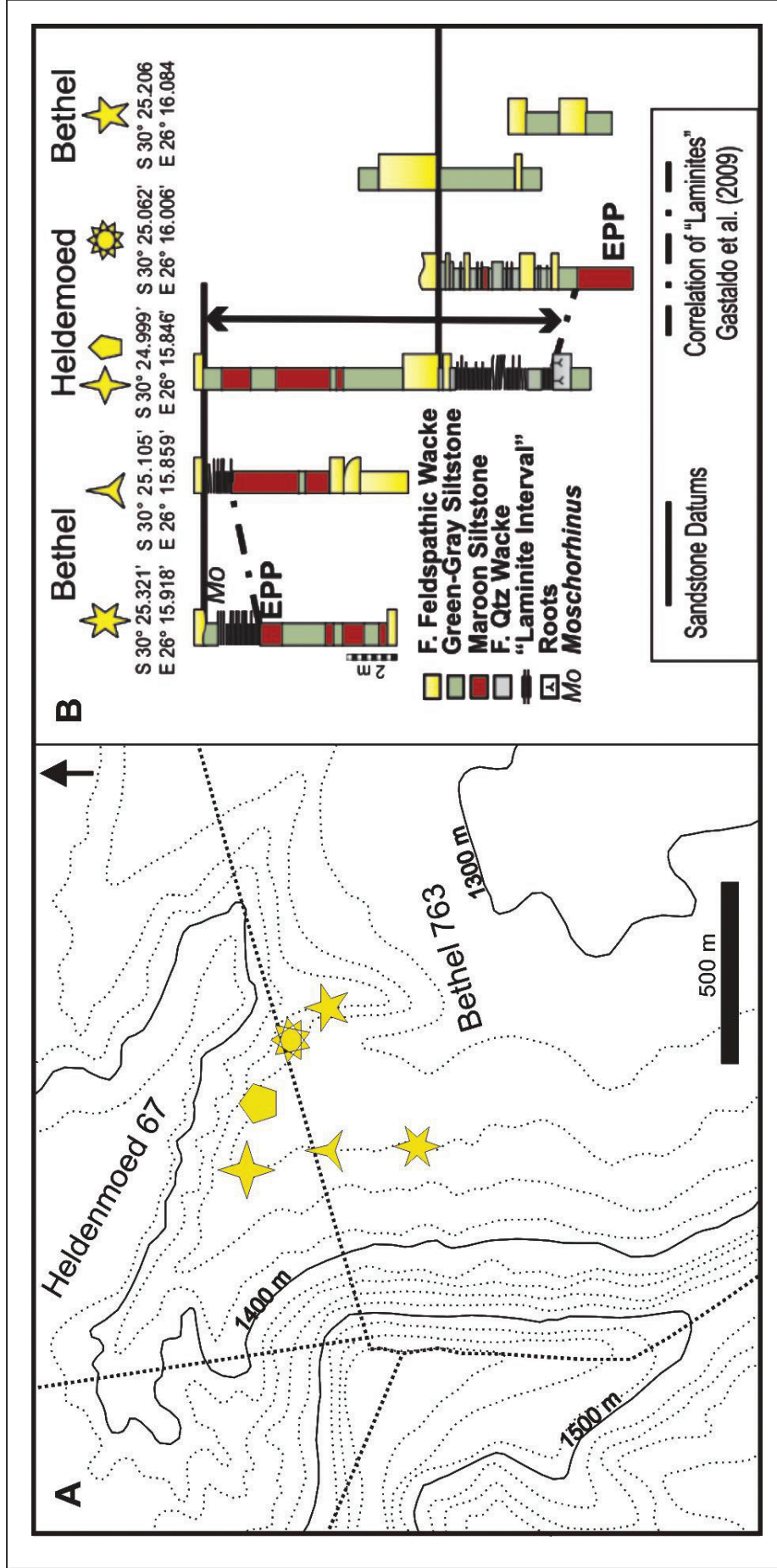


Figure 27. Topographic map (A) showing the position of six stratigraphic sections (B) measured by Gastaldo *et al.* (2009) on Bethel and Heldenmoed. The position of the map is represented by the stippled block in Fig. 18. Sections are identified by stars and were correlated by physically tracing sandstone channel-fills along the valley slopes.

Stop 2-4: Lateral Lithofacies Continuity – Section 1

The hypothesis that the ‘heterolithic’ or laminated interval (lithofacies association C) represents a single, mappable datum that could be used to correlate widely distributed sections (Smith and Botha-Brink, 2014, p. 110) implies that this ‘unique’ interval should display lateral continuity between sections, both at a single locality and between widely dispersed localities. This hypothesis was tested by Gastaldo *et al.* (2009) and the delegates will have the opportunity to trace the sections reported in this publication and compare the stratigraphy on opposite sides of the valley (Fig. 27).

At the first section (represented by a six-point star; Fig. 27), massive greyish-red to brown-grey (5YR4/1) siltstones, containing two concretionary nodule horizons, as well as invertebrate and vertebrate burrows, crop out at the base of the donga (gully) exposure. It is overlain by a very thinly bedded siltstone interval (Figs 28A, 29) that represents the datum horizon of Ward *et al.*, (2000, 2005) and Smith and Botha (2005, Botha and Smith, 2006; Smith and Botha-Brink, 2014). The reference made by Smith and Botha-Brink (2014, p. 103) to fig. 2 in Gastaldo *et al.* (2009) provides additional confirmation that the latter had identified this lithofacies association correctly. The interval consists of fining-upward couplets of centimetre-scale green-grey (4GY 4/1) very fine lithic wacke (sandstone) beds overlain by millimetre-scale greyish-red (5R 4/2) siltstone drapes. This is overlain by 0.4 m of weathered red-brown siltstone, above which are centimetre-scale beds of greenish-grey lithic wacke that fine upward to siltstone. The primary structures in the sandstone include imbricated planar beds, small-scale contorted and convoluted bedding, and ripples viewed in cross section in the wall exposure.

The red-brown siltstone is overlain by greenish-grey siltstone that contains vertebrate-bearing nodules, ~2.2 m above the laminated base. Below the nodules are sandstone-cast *Katbergia* burrows and the siltstone envelops thin lenticular sandstone beds, with ball-and-pillow structures ~0.5 m above them. Planar tabular and rippled bedsets of fine- to very fine-grained sandstone become more common up-section, where after the beds become more massive. The sandstone overlying the heterolithic interval on the Bethel farm was traced (Fig. 27) as pavement exposures across hill slopes, providing a stratigraphic datum for correlation.

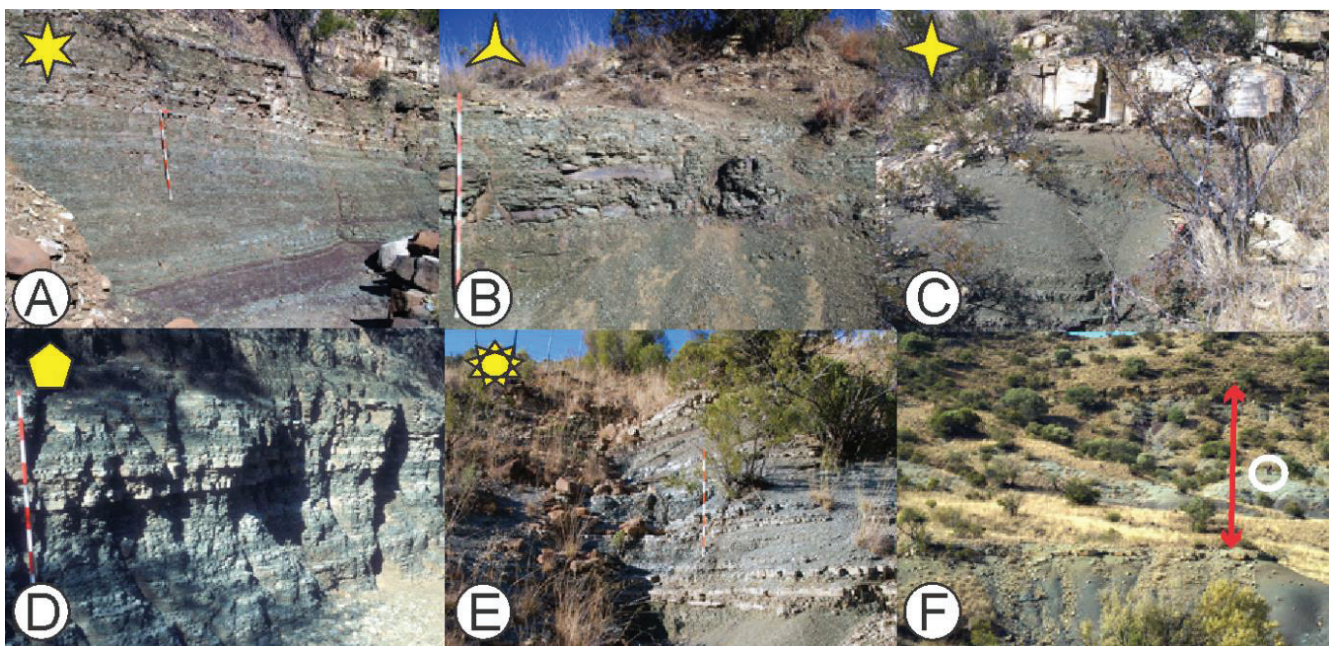


Figure 28.

Photographs of the very thinly bedded siltstones recorded in the six sections shown in Fig. 27. Sections identified by stars: A: Very thinly bedded siltstones (also referred to as laminites) on Bethel Farm (S30°25.321' E26°15.918') as described by Ward *et al.* (2000) and Smith and Ward (2001). B: Lateral correlative on the Bethel Farm (S30°25.105' E26°15.859'), where tabular and low-angle cross-bedded sandstone dominates. Scale in decimeters. C: Lateral correlative on the Heldenmoed farm (S30°24.999' E26°15.846'), where green-gray siltstone is heavily weathered and there is no evidence for sandstone-siltstone couplets. D: Bedded interval on the Heldenmoed farm (S30°25.003' E26°15.875'). Scale in decimeters. E: Lateral correlative of bedded (laminite) interval (S30°25.062' E26°16.006') on Heldenmoed farm where medium-grained tabular and planar cross-bedded sandstone are overlain by green-gray coarse siltstone. Scale in decimeters. F: The white circle shows a person standing on lithofacies D of Smith and Botha-Brink (2014). Vertical arrow indicates Early Triassic recovery faunal interval as recognized by Botha and Smith (2006). Also, see stop 2-1. (From Gastaldo *et al.*, 2009, The terrestrial Permian-Triassic boundary event bed is a nonevent: *Geology*, V. 37, p. 199-202. Reprinted with permission from GSA.)

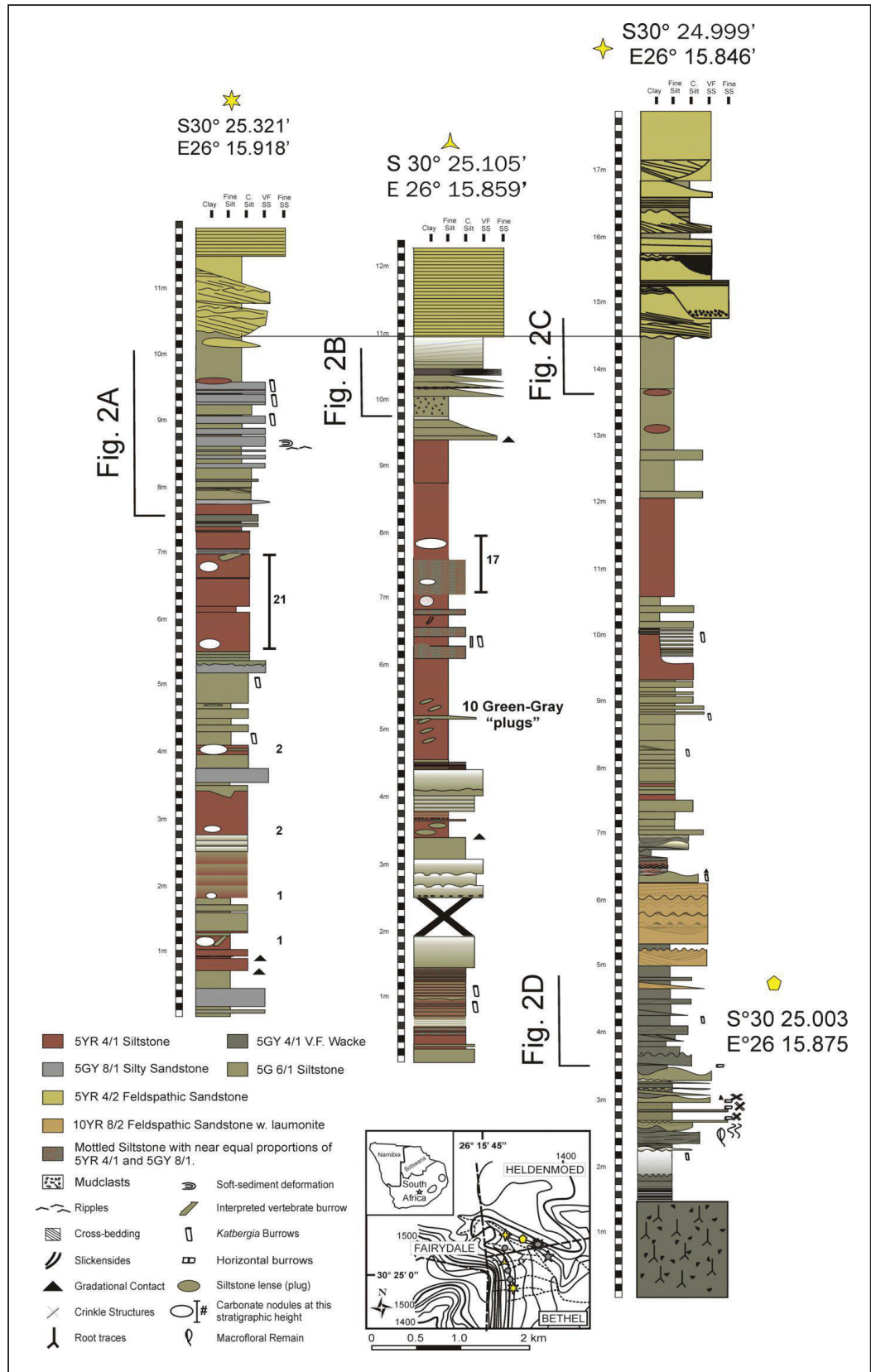


Figure 29. Detailed stratigraphic sections documented on the western side of the valley (sections represented by stars). Note multiple horizons of very thinly bedded siltstones that pinch out when traced laterally. (From Gastaldo *et al.*, 2009, The terrestrial Permian-Triassic boundary event bed is a nonevent: *Geology*, V. 37, Supplemental information. Reprinted with permission from GSA).

Stop 2-5: Lateral Lithofacies Continuity – Section 3

The laminated interval thins (Fig. 29) toward the south (see section 2; represented by a three-point star) and is completely replaced by massive greenish-grey siltstone in a longer section 3 (represented by a four-point star). From the greenish-grey and greyish-red siltstone outcropping below our datum sandstone Smith and Botha-Brink (2014, supplementary material) reported five fossil specimens localities (Fig. 30). Even though they are below the PTB, as defined in section 1, three of these fossils (k10603 – *Proterosuchus fergusi*, k10798 – *Lystrosaurus declivus*, and RS 141 – *L. murrayi*) belong to genera known from the *Lystrosaurus* AZ, and all reportedly to have been collected 1.5 m to 10 m above the boundary.

A well-developed heterolithic interval was recorded at the base of section 3 (Figs 28, 29) that differs from that observed in section 1 in having a higher sand:silt ratio and not overlying maroon concretion-bearing siltstone. Rather, this interval overlies a green-grey (5G 6/1) to light-grey (N7) rooted feldspathic wacke, containing thin (2–5 mm diameter) subvertically oriented rooting structures (Fig. 29) that are dispersed and can be branched. The ~2 m thick heterolithic interval consists of coarse green-grey siltstone and cross-bedded and rippled, centimetre to decimetre beds of feldspathic wacke organised in lenticular bedforms. Couplets are thicker and exhibit interference ripples, crinkle structures, and horizontal trails, and infilled burrows are found on the upper sandstone contacts (Gray *et al.*, 2004). These structures are exposed only at this site. Overall, the interval fines upward from coarse to fine siltstone laminae, in which *Katbergia* are preserved. The heterolithic interval is overlain by 1.2 m of fine feldspathic wacke, in which small-scale, micro-cross-stratified ripples, trough cross-beds, flute casts, and millimetre-scale angular mudclasts occur. This sandstone is useful to correlate with section 4 (represented by a complex star; Fig. 27) next to the fence.

The thick, seemingly massive greenish-grey siltstone interval below this thin sandstone can be used to correlate section 4 with the greenish-grey siltstone overlying the PTB of Stop 2-1 (represented by the five-point star; Figs 27, 28). However, caution should be exercised, as the red intervals often derive their colour from a thin scree of weathered siltstone draping green siltstones, or colour mottling, and often can hide greenish-grey siltstone intervals. However, the exercise at Stops 2-3 and 2-4 should demonstrate that the reported PTB varies by as much as 10 m on opposite sides of the valley.

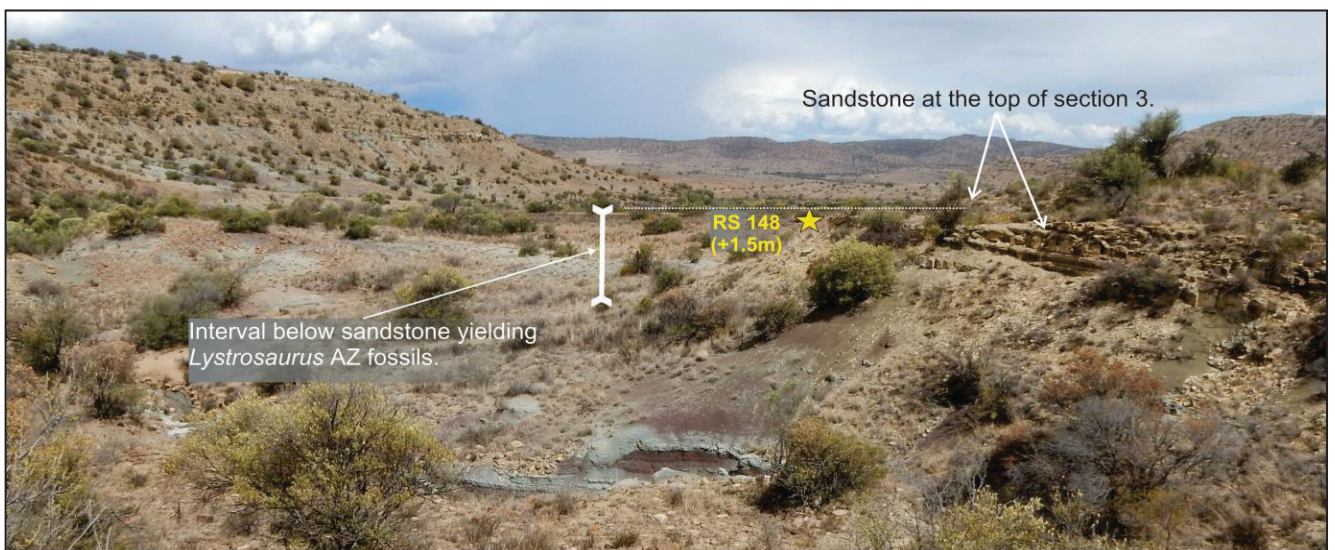


Figure 30.

Stop 2-5. Panorama of the small basin below the sandstone capping section 3 (represented by four-point star in Figs 27, 28, and 29). View is to the southeast. Stop 2-1 is located to the east-southeast, i.e. to the left of the current view. Smith and Botha-Brink (2014, supplementary material) reported several fossils assigned to the *Lystrosaurus* AZ, from the red and grey siltstones that crop out on these lower slopes below the PTB facies in section 1 (represented by a six-point star in Figs 27, 28, and 29).

Stop 2-6: Review of fossil localities

If the stratigraphic position of the lithofacies association considered to represent a datum for the PTB were at different stratigraphic positions on the opposite sides of the valley at Bethel and Heldenmoed, as demonstrated by Gastaldo *et al.* (2009), it raises serious concerns about the accuracy of the stratigraphic position of each logged fossil, as provided in the PTB biostratigraphic dataset. These concerns were confirmed when the data contained in the fossil database were reviewed in the field.

In February 2014, R.M.H. Smith forwarded his Excel spreadsheet of GPS coordinates for all the vertebrates used to circumscribe the vertebrate-defined PTB, reported in Smith and Botha-Brink (2014) to R.A. Gastaldo. The coordinates for individual fossils were reviewed and several selected localities were visited in the field. A number of obvious discrepancies were noted and one such example includes a number of fossils discovered on the slopes of the Swartberg Mountain, on the western side of the valley. Here, over a ~150 m transect, several fossils reportedly have been collected from, or directly above, the same sandstone bench, but the reported stratigraphic positions above the PTB vary greatly and inconsistently when compared with the elevation (Fig. 31).

The corroborated location of fossil RS 144 is stratigraphically above RS 215, yet is placed (Smith and Botha-Brink, 2014, supplementary material) in a stratigraphic position 70 m below the latter. Also compare the stratigraphic positions of RS 143 (+19 m), RS 144 (+17 m), RS 147 (=21 m), and k10686 (+20 m) with the positions for specimens k10373 (+90 m), RS 188 (+160 m), and k10374 (+125 m; Fig. 31). As all these fossils form part of the *Lystrosaurus* AZ fauna, the discrepancies do not have a direct impact on the biostratigraphic model; however, it suggests the need to review the stratigraphic placement of each logged vertebrate fossil, by correlating between outcrops at every locality. A reassessment of the stratigraphic position of diagnostic vertebrates relative to each other can be accomplished only by tracing and correlating the bounding surfaces of extensive sandstone bodies in the field. Without a lithostratigraphic framework in which lateral relationships are fully understood, only generalisations about palaeobiologic trends can be attempted.

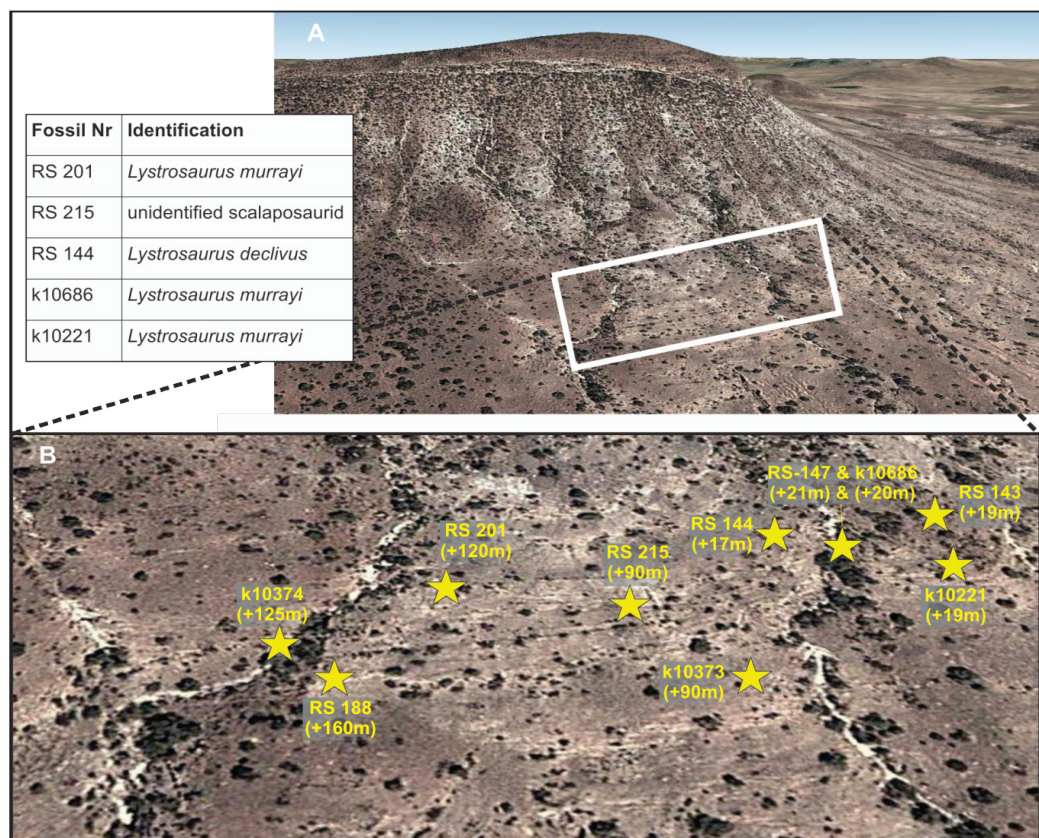


Figure 31. Google Earth images showing (A) the area studied by Battifarano *et al.* (2015) on the western slopes of the valley at Bethel. Image B shows the position (stars) of the vertebrate fossils reported by Smith and Botha-Brink (2014, supplementary material) and located by using the database provided by Smith (pers. comm. 2014). RS- and k-numbers refer to fossil numbers, while numbers in brackets refer to the reported position of each specimen above the PTB (Smith and Botha-Brink, 2014, supplementary material). RS 147 and k10686 have the same locality.

9. 24 AUGUST (DAY 3): CARLTON HEIGHTS AND LOOTSBERG PASS

Day 3 will be predominantly a day of travel, with two roadside stops. At the first locality, we will scale a fence and traverse rough terrain. Please ensure that you wear suitable shoes and dress comfortably.

9.1 Timetable

Depart from Bethulie	08:30
Arrive at Carlton Heights	10:00
Stop 3-1	10:15
Stop 3-2	10:30
Stop 3-3	10:45
Stop 3-4	11:15
Stop 3-5	11:45
Depart Carlton Heights	12:00
Lunch at Middelburg	12h30
Depart Middelburg	14:00
Arrive at Lootsberg Pass (Stop 3-6)	14:45
Depart Lootsberg Pass	15:30
Arrive at Ganora	16:15

9.2 Directions

After departing Bethulie, turn west onto the R701 for approximately 60 km. Turn left (south) onto the N1 and travel 44 km to Colesberg. Where the N1 intersects the N9 south of the town, turn left onto the N9 south. Continue on the N9 for 59 km to the town of Noupoort. Continue past Noupoort on the N9 for approximately 15 km to the top of the Carlton Heights Pass (Stops 3-1 to 3-5). After departing Carlton Heights, continue traveling south on the N9 for ~26 km to Middelburg, where we will stop for lunch. Depart Middelburg, traveling south on the N9 toward Graaff-Reinet for approximately 50 km. When cresting Lootsberg Pass turn right into the parking area at the top of the pass. After returning to the vehicles, continue down the pass for ~9 km. Approximately 1 km before reaching the turn-off to Cradock (R61) on the left, turn right onto the gravel road to Nieu Bethesda (the road is sometimes referred to as 'Bethesda Way'). This road crosses a railway line after ~1 km. Continue on the road for ~21 km until reaching the gate of the Ganora Guest Farm on the left. This will be our accommodation for the next two nights.

9.3 Relevant Background

The Carlton Heights locality is situated along the N9 (Fig. 32), approximately 155 km from Bethulie and 60 km from Lootsberg Pass. This locality has played an accessory role in the development of the extinction model because of the low number of vertebrates recovered from the area and the predominance of sandstone-rich exposures of the Katberg Formation. Known vertebrate remains collected from the immediate area (pers. comm. M. Day, 2014) include a specimen previously assigned to the genus *Dicynodon* (*Daptocephalus?*), and at least 10 fossils assigned to the genus *Lystrosaurus*, but unidentified at species level. Steiner *et al.* (2003) reported post-cranial material, tentatively assigned to *Dicynodon* (*Daptocephalus?*), from the base of their section at Carlton Heights, near the railroad cut, and an increase in *Lystrosaurus* fossils up-section. Retallack *et al.* (2003) similarly noted the presence of lystrosaurid bones in their section. Yet, there is no record that any of the specimens referred to by these authors were identified to species level, collected and/or curated in any museum collection.

In the absence of reliable biostratigraphic control, Retallack *et al.* (2003; their fig. 4) used the criterion of Smith and Ward, a ~12 m thick, interlaminated succession of mudrock, as the basis to identify the PTB. Their reported section (S31° 17.702', E024° 57.093') is adjacent to the N9, with exposures in a donga that descends to the railroad cut. Their positioning of the PTB in this area (Retallack, pers. comm. 10/2007) is located in the rocks adjacent to the railroad siding, where Gastaldo and Rolerson (2008; their fig. 4B) documented long *Katbergia* burrows.



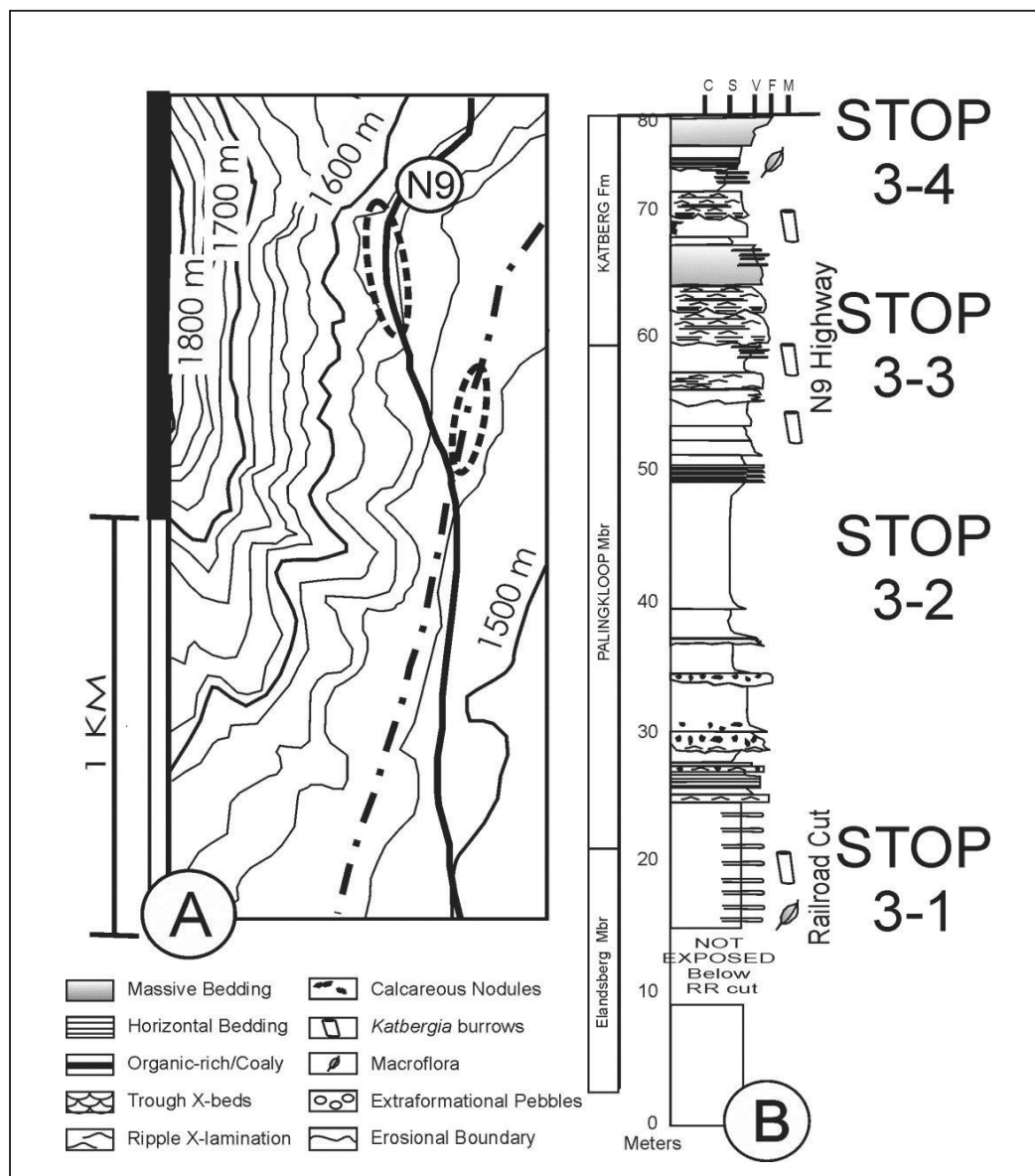


Figure 32.

Map (A) and stratigraphic section (B) for the Carlton Heights locality. The dashed and dotted line sub-parallel to the solid line for the N9 represents the railway line. Stippled ovals represent exposures in the railway cut (Stop 3-1) and road cut (Stops 3-3 and 3-4) along the N9. (Figure from Gastaldo and Rolerson, 2008, *Katbergia* gen. nov., a new trace fossil from Upper Permian and Lower Triassic rocks of the Karoo Basin: Implications for palaeoenvironmental conditions at the P/Tr extinction event: *Palaeontology*, V. 51, pp. 215–229).

Steiner *et al.* (2003) recognised an interbedded succession at the railroad cut that they correlated with the event bed of Smith and Ward (2001). However, they placed the extinction event some 20 m (p. 412) above that proposed by Retallack *et al.* (2003), based on the palynological abundance of fungal spores obtained from a clay-rich bed directly below a sandstone bench assigned to the Katberg Formation. Gastaldo *et al.* (unpublished) collected detrital zircon crystals from similar, clay-rich beds, but these yielded only Carboniferous ages.

Retallack *et al.* (2003) described greenish-grey and reddish-grey mudrock intervals interpreted as various paleosol types (Permian: Som; Triassic: Kuta and Sedibo) with colours not necessarily corresponding to the Permian (green) and Triassic (reddish) paradigm (Table 1). Permian Som paleosols were reported to range in colour between greenish-grey (their data repository) to grey purple (their table 1) to dark red grey (their data repository). In contrast, Triassic Kuta soils range from dark greenish-grey (their table 1) to light bluish grey (their figs. 5, 6), reddish brown (their table 1), and red grey (their data repository). Similarly, the Sedibo paleosol type, which is characterised by exposures at Carlton Heights (Retallack *et al.*, 2003; their fig. 6), is greenish grey to dark greenish grey, with no evidence of extinction-related 'rubification.'

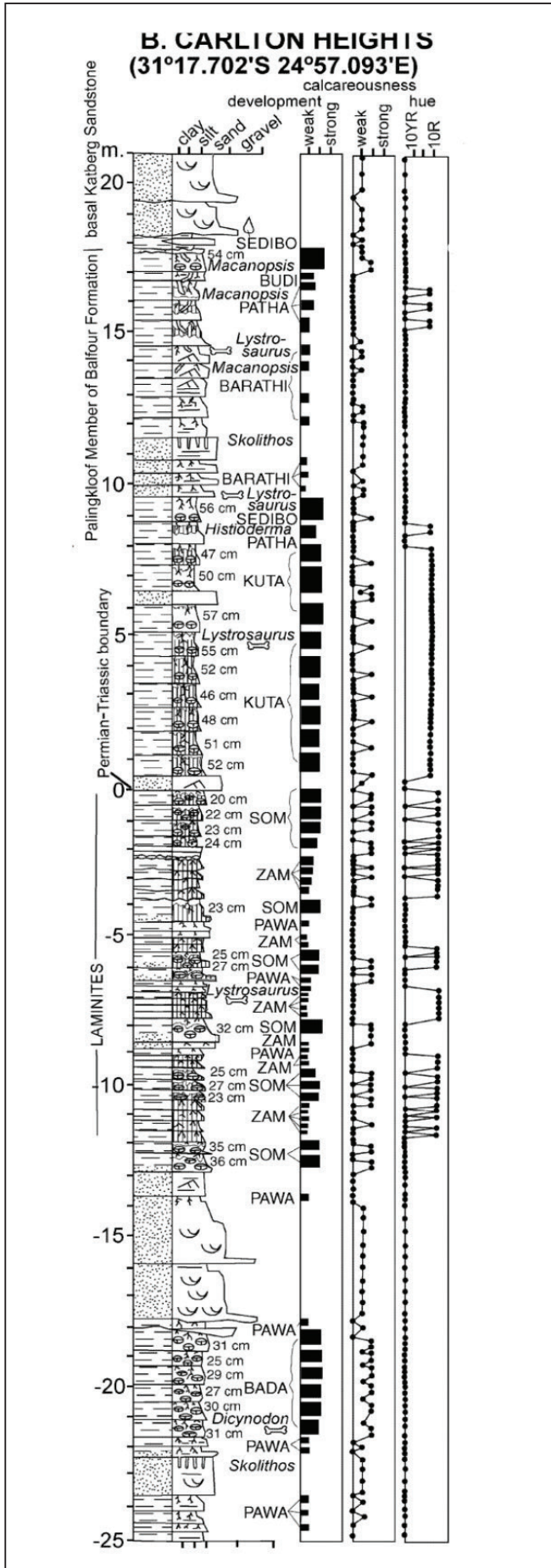


Figure 33. Stratigraphic column reported by Retallack *et al.* (2003, their figure 4) from Carlton Heights. The section shows the position of their pedogenic horizons, as well as their reported degree of development. The section is capped by the thick sandstone beds of the Katberg Formation. (Figure from Retallack *et al.*, 2003, Vertebrate extinction across Permian–Triassic boundary in Karoo Basin, South Africa: Geological Society of America Bulletin, v. 115, pp. 1133–1152. Reprinted with permission from GSA).

Recently, the $\delta^{13}\text{C}_{\text{carb}}$ paleosol data of Ward *et al.* (2000, 2005) have been called into question by Tabor *et al.* (2007) and Gastaldo and Rolerson (2008). These authors demonstrated that many carbonate cements in the soil nodules used in previous analyses (MacLeod *et al.*, 2000; Ward *et al.*, 2005), both below and above the PTB at Carlton Heights and elsewhere (e.g. Wapadsberg Pass —Reid *et al.*, 2006) reflected early diagenetic precipitation of carbonate under conditions of saturated wetland soils. Such carbonate precipitation is mediated bacterially and occurs in a closed system, with carbon contributed from methanogenesis rather than having formed in an open system, interpreted as having been in atmospheric equilibrium.

Smith and Ward (2001) first associated characteristic subhorizontal burrows (<2 cm wide) exclusively with the extinction interval. They considered these to resemble callianassid shrimp burrows, while Retallack *et al.* (2003) referred them to the ichnogenus *Macanopsis*. Gastaldo and Rolerson (2008), in a detailed study undertaken at Carlton Heights, demonstrated that the burrows did not resemble either of these ichnogenera, and they assigned it to a new ichnotaxon, *Katbergia carltonichnus*. In conjunction with stable isotope geochemistry of carbonate cements from nodules surrounding these sigmoidal burrows, Gastaldo and Rolerson (2008) demonstrated that mineral precipitation occurred under saturated sediment conditions (following the observation of Tabor *et al.* [2007] from the same locality) in mudrocks that were deposited in floodplains, with high water tables. The burrows, their association with the encasing sediments, and stable isotope geochemical data are all indicative of wet, rather than arid conditions.

Pace *et al.* (2009) proposed a lithostratigraphic framework for the lower exposures of the Katberg Formation at Carlton Heights. They attempted to account for the PTB scenario vs. discrepancies in field data at the locality, which included the presence of two types of pedogenic nodules and the relationship between Vertisol remnants in intraformational conglomerates, sandy bedforms, sandstone sheets, and bioturbated overbank interfluvial paleosols. According to this model, thick lenticular sandy bedforms and floodplain fines accumulated in vertically stacked beds, with little evidence of erosion. They considered this characteristic of a rapidly aggrading system, with bioturbated inceptisols representing brief periods of landscape equilibrium. The sediment fill in *Katbergia* burrows and their relationship with calcareous pedogenic nodules are indicative of high water tables, where inceptisols were overprinted as gleysols (Gastaldo and Rolerson 2008).

In contrast, the remains of calcic Vertisols (Gastaldo *et al.*, 2013) are present only as erosional remnants in lenses of nodular intraformational conglomerate that drape unconformities, bounding sandstone sheets at the base. Here, and elsewhere in the region, evidence of any *in situ* Calcisols/ Vertisols preserved in the stratigraphy, indicating that entire landscapes had developed under drier climatic conditions, were scavenged during subsequent periods of regional degradation, when disequilibrium returned to the fluvial profile. The largest clasts of these landscapes, primarily carbonate nodules and intraformational mud clasts, were deposited in channel lags, while the finer floodplain sediments were re-entrained and redeposited elsewhere in the system. Therefore, Pace *et al.* (2009) concluded that while a braidplain-dominated landscape of the lower Katberg Formation could have been induced by tectonic processes, sediment accumulation was strongly influenced also by severe climatic oscillations.

CARLTON HEIGHTS

Stop 3-1: Railroad Exposure

We will be required to scale the fence and walk to the railroad cut at the foot of the mountain. Exposure below this cutting is limited and dominated by greenish-grey siltstone. Steiner *et al.* (2003) considered the bedded siltstone exposed in this cutting as part of a 15 m interval of laminated to massive maroon mudstone that they, as did Retallack *et al.* (2003, pers. comm. 10/2007), correlated with the “event beds”

Table 1.
Summary descriptions of the paleosols recognised by Retallack *et al.* (2003, their table 1).

Pedotype	Description
<i>Lystrosaurus</i> AZ paleosols	
Barathi	Bedded olive brown shale with fine root traces
Budi	Bedded green-grey sandstone with root traces and burrows
Karie	Reddish brown (2.5YR) with deep, well-focused calcareous nodules (Bk)
Kuta	Grey surface (A) over reddish brown (2.5YR), with shallow, well-focused calcareous nodules (Bk)
Patha	Reddish brown (2.5YR), with relict bedding, root traces, and burrows
Sedibo	Greenish grey, with deep, well-focused calcareous nodules (Bk)

(Table 1. Continued)

<i>Daptocephalus</i> AZ palesols	
Bada	Grey siltstone, with shallow and scattered calcareous nodules and rhizoconcretions (Bk)
Du	Bedded blue-grey sandstone with fine root traces
Hom	White sandstone, with shallow and scattered calcareous nodules and rhizoconcretions (Bk)
Pawa	Bedded blue-grey shale, with fine root traces
Som	Grey siltstone surface (A) over purple (10R) siltstone, with shallow calcareous nodules (Bk)
Zam	Bedded purple-grey (10R) siltstone, with fine root traces and burrows

(and biozone contact) of Ward *et al.* (2000). We documented thinly bedded and stacked horizontal beds of siltstone at this exposure, but also noted several thin to medium lenticular sand- and siltstone beds that are reminiscent of channel-fill processes. The reported stratigraphic position and thickness for this laminated interval differ between the various authors, with Gastaldo and Rolerson (2008) placing the base of this interval at a much greater stratigraphic distance below the Katberg Formation (Fig. 32) than either Steiner *et al.* (2003, their fig.2) or Retallack *et al.* (2003, their fig 4). The first *Katbergia* burrows have been reported from these exposures (Gastaldo and Rolerson, 2008).

Stop 3-2: Section

We will walk up the main gully section (referred to as VW donga by Pace *et al.*, 2009) to the N9 to gain an overview of the Carlton Heights section. The siltstones exposed below the N9 are commonly bedded and we have documented several intervals of thickly laminated and very thinly bedded siltstone. Laterally restricted horizons, containing large pedogenic nodules occur throughout the section. This is an opportune moment to look for the various pedogenic horizons described by Retallack *et al.* (2003) from the greenish-grey and reddish-grey mudrock intervals exposed at Carlton Heights (Fig. 33). Greenish-grey bedded siltstones, with red, mottled horizons, become more abundant to the top as the N9 is approached.

Stop 3-3: *Katbergia* burrows, the Fungal Spike and Detrital Zircons

We will need to cross the N9 and go behind the barrier to look for composite paleosols with *Katbergia* burrows, in both green-grey and greyish-red mudrock, described by Gastaldo and Rolerson (2008). *Katbergia* burrows exhibit a consistent diameter of 1–2 cm throughout recoverable lengths of 5 to >40 cm. They are cylindrical to ovate in cross section when completely infilled, but can be flattened when fill is incomplete. Complete burrows display sigmoidal geometry, exhibiting a soft S-shape as they descend into the substrate. They terminate



Figure 34.

Image showing the location of the “fungal spike horizon” reported by Steiner *et al.* (2003, their fig. 4). (Figure from an article published in *Palaeogeography, Palaeoclimatology, Palaeoecology*, v. 194, Steiner *et al.*, Fungal abundance spike and the Permian–Triassic boundary in the Karoo Supergroup (South Africa), p. 405–414, Copyright Elsevier, 2003).

in slightly enlarged chambers, but no tapering of the burrow diameter has been observed in either distal or proximal regions. Burrows are inclined in the substrate where the angle ranges between 20 and 30 degrees, but there is no evidence of branching. The Karoo burrows were filled by passive means; therefore, the casting lithology is a record of which sediments were deposited after the burrow had been abandoned. Detailed analysis of scratch marks preserved on the burrow walls indicates that the substrate in which the burrow was excavated was firm enough to maintain a constant cylindrical diameter, as well as allowing for the preservation of a three-fold set of scratch marks along the entire burrow length. The physical conditions necessary to excavate and maintain *Katbergia* burrows preclude saturated sediment and a high water table. There is no physical evidence within any bioturbated siltstone interval for coeval desiccation cracks that would reflect that dry periods had affected the burrowers. Such features occur either below or above the bioturbated zones (Pace *et al.* 2009). Therefore, colonisation of a playa-lake setting cannot be corroborated.

Steiner *et al.* (2003) reported a palynoflora dominated by the fungal cell remains of *Reduviasporonites* and abundant recycled woody material from a 1 m interval below the base of the sandstone bench exposed in the road cut (Fig. 34). This thin-bedded burrowed unit is overlain by a thin (5 cm thick), very fine-grained clay-rich layer, approximately 0.5 m below the base of the sandstone channel-fill, which is laterally continuous at outcrop scale (Fig. 35). Steiner *et al.* (2003) described it as being predominantly composed of the clay minerals illite and illite-smectite (also with quartz, low albite, gypsum, chlorite, mica, and jarosite). Kamo (unpublished) recovered a small suite of zircons from this clay-dominated interval (interpreted to be tuffite). We obtained three ID-TIMS ages on screened, chemically abraded zircons, using the ET535 spike. One Early Carboniferous (Serpukovian, 319.83 ± 0.69) and two Permian (Asselian, 296.14 ± 0.48 ; and Kungurian/Roadian, 270.58 ± 0.53) ages were found for individual grains. Therefore, the recognition of tuffite deposits in the Katberg Formation indicates that volcanic activity and reworking of ashfall deposits continued, but provided no means to constrain geochronologically the age of the *Lystrosaurus* AZ.

Stop 3-4: Lower Katberg Formation sedimentology

The Katberg Formation is approximately 270 m thick at Carlton Heights and consists of fine- to medium-grained sandstone that is typically multistoried and laterally extensive. These sandstones often weather to form resistant benches up to 4 m thick, with intervening, slope-forming siltstone. The field party will walk to the north end of the road cut to climb to the top of the sandstone bench in order to investigate lithofacies relationships. Delegates may decide also to assess the outcrop from the opposite side of the road.

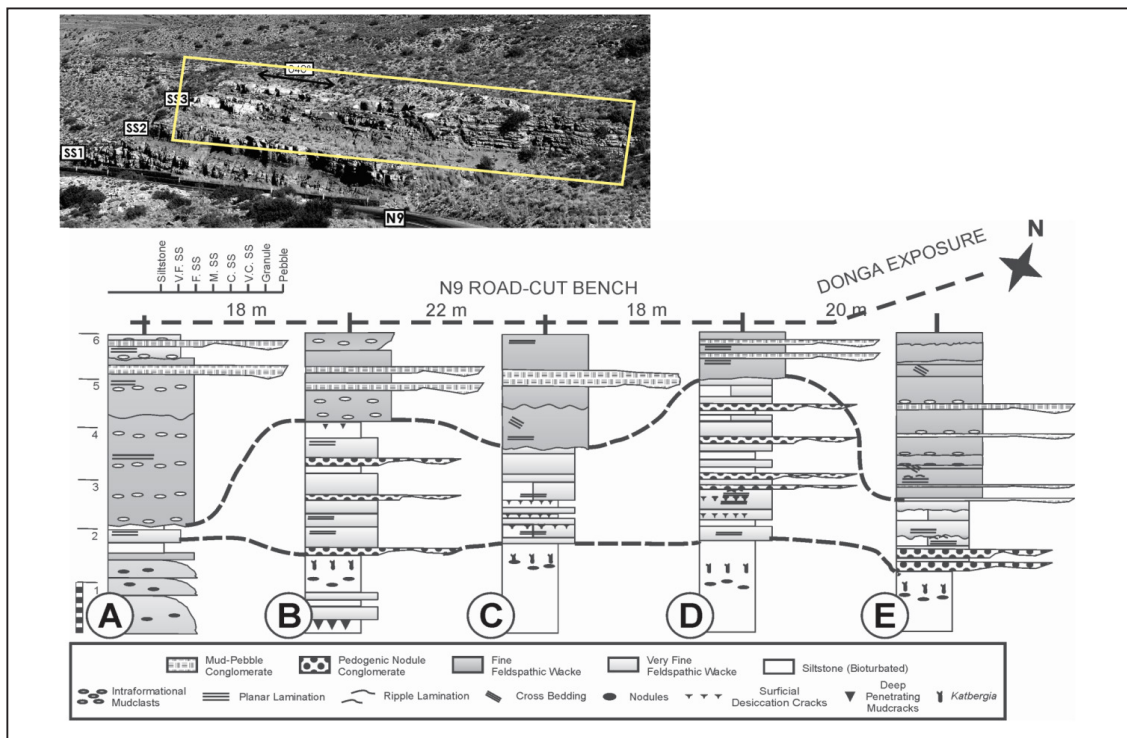


Figure 35.

Five short stratigraphic sections measured from the upper sandstone bench exposed in the N9 road cut (see blocked area in inset photograph). Columns are arranged from southwest (A) to northeast (D), with section E measured in the donga exposure orientated at an angle to the road cut. (Figure adapted from Pace *et al.*, 2009, Early Triassic aggradational and degradational landscapes of the Karoo Basin and evidence for climate oscillation following the P–Tr event: *Journal of Sedimentary Research*, v. 79, p. 316–331).

Recurrent deep (up to 3 m) incisions and the resultant erosional contacts in the section produce vertical and lateral variability in this lithofacies association (Fig. 35). Pace *et al.* (2009) distinguished between two types of sandstone lithofacies associations from these exposures. Lenticular bodies of fine-grained feldspathic greywacke (1–3 m thick) and mudpebble conglomerate overlie extensively scoured bounding surfaces, and represent the most common and resistant rocks of this succession. Downstream accretion bars with trough cross-bedding were documented in these sandstones. Some of these lenticular sandstones are en echelon stacked (multilateral channel geometries), but most show a succession-dominated vertical stacking pattern. The intervening *Katbergia*-bioturbated paleosols are sporadically present, depending on the degree of sandstone incision. Dispersed *in situ* carbonate nodules commonly occur along single horizons, while isolated deep-penetrating mudcracks (at least 10 cm depth) occur sporadically beneath thin sandstone lenses.

Basal nodular conglomerate and very fine-grained sandstone sheets occur in some of the siltstone units, but are exposed only in areas where incision has not been pervasive. These sandstones occur as medium thick (0.05–0.3 m) laminated sheets, in sharp contact with underlying and overlying units. Beds are laterally extensive, traced over distances up to 75 m, and form stacked packages up to 2 m thick. Basal scouring into the underlying units is up to 0.5 m deep. Horizontal, planar cross-bedding and ripple cross-lamination are common, with occasional centimetre-scale shallow desiccation cracks on upper bed surfaces.

Complete genetic sequences are rare in the study area as a result of the omnipresence of laterally extensive erosional scours. Nevertheless, it is clear that these sequences consist of stacked upward-fining cycles, and lateral comparison of these show them to consist of (1) a basal nodular conglomerate overlying an erosional contact that, in turn is (2) overlain by very fine-grained feldspathic wacke sheets and stacked, lenticular fine-grained feldspathic wacke, that (3) fines upward into a *Katbergia*-bioturbated nodule-bearing paleosol.

Stop 3-5: Multistoried Katberg Sandstones

Macroscale analysis indicates that extensive lateral variation occurs throughout the 100 m vertical section studied (Pace *et al.*, 2009). Incisions, similar to those observed in the road-cut-bench exposures are pervasive and often cut into siltstone units and sandstone units of varying thickness, which results in sandstone bodies that amalgamate when traced laterally. For instance, northeast of the main donga and roadside cut, a nodular conglomerate-filled incision occurs, the base of which cuts down 3 m into the underlying very fine-grained feldspathic wacke (Fig. 36). When traced laterally, this unit pinches out over a distance of 200 m and is overlain by fine-grained feldspathic wacke along third-order bounding surfaces. Nodular conglomerate reappears numerous times in medium (10–30 cm) thick, laterally isolated lenses along the same bounding surface. This results in a seemingly continuous series of lenticular, stacked beds of fine-grained feldspathic wacke that are best observed in the exposures in the new road cut to the north.

Similar to earlier workers, Pace *et al.* (2009) interpreted the depositional setting to represent a braided (anabranching) system because of its relatively coarse grain size, infrequent mudstone drapes and trough fills, which result in an absence of fining-up cycles, a rarity of ripples, and low variance in internal palaeocurrent data (Johnson *et al.* 2006).

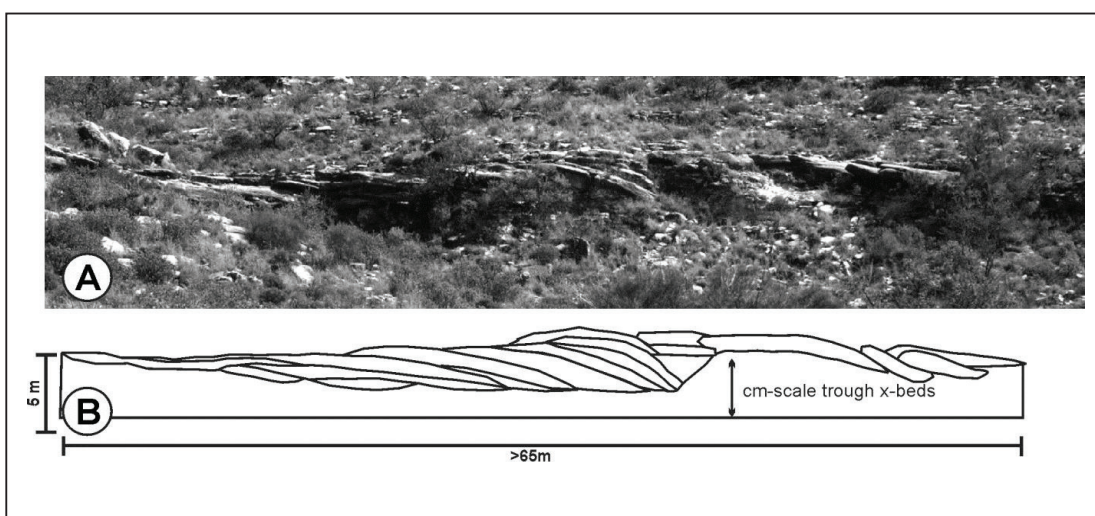


Figure 36. Laterally accreted beds of pebble nodular conglomerates that outcrop above the N9 road cut. The erosive basal bounding surface of the conglomerate incises up to three metres into the underlying very fine sandstone. (Figure adapted from Pace *et al.*, 2009, Early Triassic aggradational and degradational landscapes of the Karoo Basin and evidence for climate oscillation following the P–Tr event: *Journal of Sedimentary Research*, v. 79, p. 316–331).

LOOTSBERG PASS

Stop 3-6: Overview of Lootsberg Pass area

Lootsberg Pass is sometimes referred to as a single section or as representing a group of localities that include (from southeast to northwest) New Wapadsberg Pass, Old Wapadsberg Pass, (new) Lootsberg Pass, Tweefontein, and Old Lootsberg Pass (Fig. 37). Lootsberg Pass has been proposed as the type section of the *Lystrosaurus* AZ (Groenewald and Kitching, 1995), and for the Lootsbergian land-vertebrate faunachron of Lucas *et al.* (2007; Lucas 2009, 2010). The sections published by Ward *et al.*, (2000, 2005), Smith and Ward (2001), and Retallack *et al.* (2003) were measured in the main northeast-orientated river gully near the foot of the pass (also refer to the PTB reported by Retallack *et al.*, 2003, their fig. 3A). Several fossils collected from (new) Lootsberg Pass, incorporated into Smith and Botha-Brink (2014, supplementary material), originate from the rock exposures adjacent to this gully.

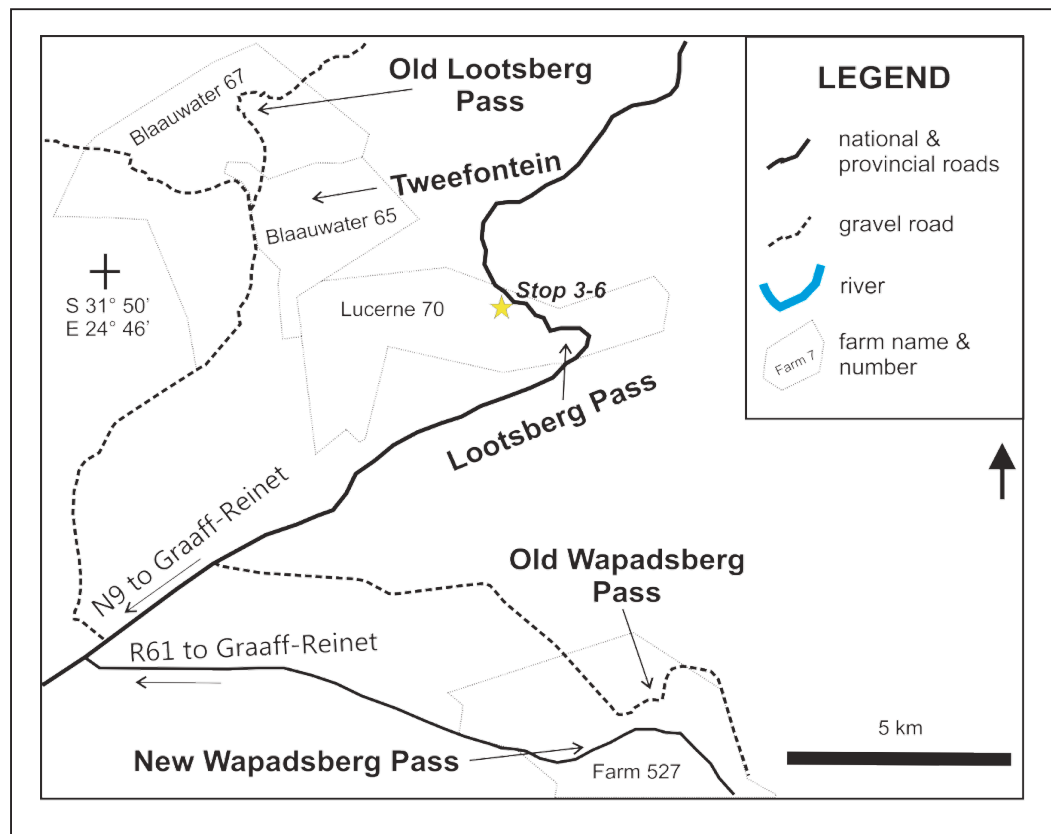


Figure 37.

Map showing the position of the reported boundary localities in the Lootsberg area. Stop 3-6 allows a panoramic view of Lootsberg Pass, and the Old and New Wapadsberg passes.

10.25 AUGUST (DAY 4): OLD LOOTSBERG PASS

Day 4 will be a long day of walking over rough terrain. Please ensure that you wear suitable shoes and dress for both warm and cold weather.

10.1 Timetable

Depart Ganora	08:15
Stop 4-1 (arrival and orientation)	9:00
Stop 4-2 (porcellanite)	9:30
Stop 4-3 (zone of reverse polarity)	10:30
Stop 4-4 (point bar)	11:15
Stop 4-5 (PTB)	12:00–12:45
Stop 4-6 (datum sandstone)	13:00
Lunch	13:30
Stop 4-7 (plant site)	14:15
Stop 4-8 (Katberg traverse)	15:30
Return to vehicle	16:00
Depart for Ganora	16:45
Arrive at Ganora	17:15

10.2 Directions

Depart from Ganora. At the farm gate turn right (north) onto the gravel road to Middelburg. Continue on this road for 21 km. Just before crossing the railway line, turn left onto the gravel road to Old Lootsberg Pass. Continue on this road for 12 km until you approach the

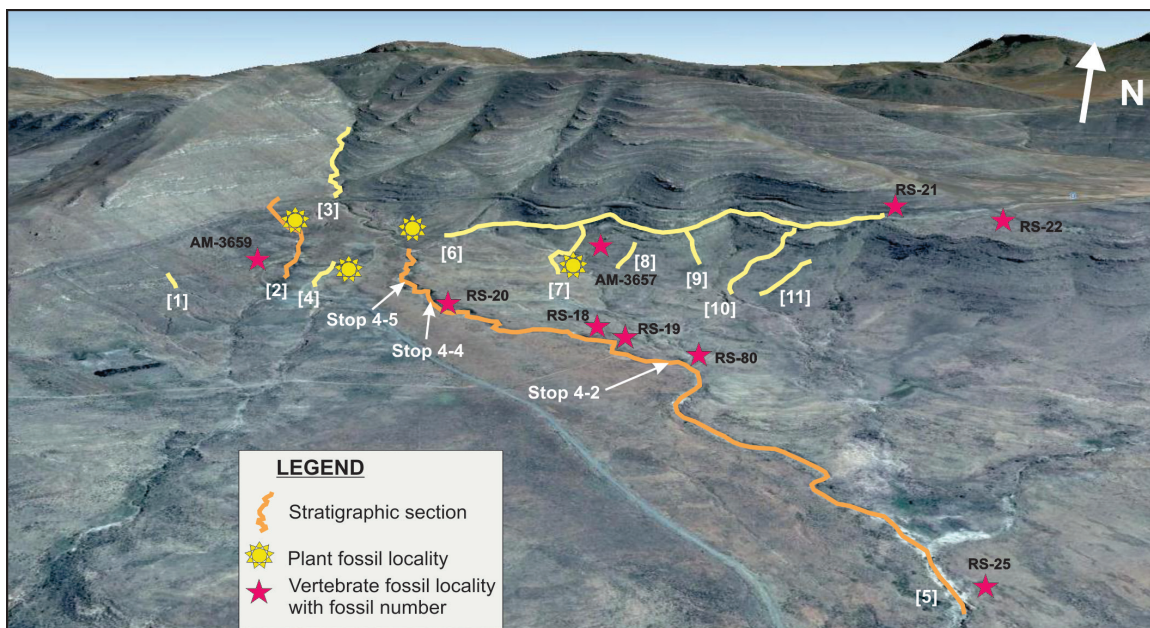


Figure 38.

Google Earth image showing the positions of the sections measured by Gastaldo *et al.* (2015; in review) and Neveling *et al.* (2016). The sections are identified by numbers in square brackets. Darker orange lines represent the sections used to construct the combined section in Fig. 39. Yellow stars represent the plant fossil localities reported by Gastaldo *et al.* (2015) and red stars represent the positions of vertebrate fossils recorded by Smith and Botha-Brink (2014) and Gastaldo *et al.* (2015).



Blaauwater homestead. Turn off onto the gravel trackway to the right, just before the homestead, to go to Old Lootsberg Pass. The pass is no longer in use and access to the old road and locality is gained with the permission of the farm owner at Blaauwater. At the end of the day, we will retrace our route back to Ganora.

10.3 Relevant Background

The Old Lootsberg Pass and Tweefontein localities are referred to by Ward *et al.* (2000, 2005), Smith and Ward (2001), and Smith and Botha-Brink (2014), but little detail information is available for these localities. The exposures at Old Lootsberg Pass are largely restricted to road cuttings, dongas, and other isolated outcrops. The exact position of the section described by Ward *et al.* (2005) is not defined clearly, but their GPS coordinates place the base near the railroad tracks in the Katberg Formation. We have studied this area extensively and measured 11 sections over a ~1 km transect across the locality (Fig. 38). These sections were correlated by laterally tracing sandstone-bounding surfaces in the field to develop a robust lithostratigraphic framework, allowing us to test lateral facies continuity and or variability (Neveling *et al.*, 2016; Gastaldo *et al.*, in review).

Where possible, samples for magnetic polarity stratigraphy were collected by drilling oriented cores in competent rocks at more than 70 stratigraphic horizons (Fig. 39). Typically, seven to twelve independently oriented drill samples were obtained from each suitable bed in the Old Lootsberg Pass section. Most sampled beds are exposed in the main donga, where the section was measured and described. Most sampled beds are medium- to coarse-grained siltstone and very fine sandstones. Several nodular (concretions) horizons in fine siltstone–mudstone were sampled also.

Stop 4-1: Orientation

All the Old Lootsberg Pass sections are located on the farm Blaauwater 67 (Fig. 37). A combined, representative section of 150 m (Fig. 39) was constructed for Old Lootsberg Pass, using two (sections two and five) of the eleven stratigraphic sections measured at this locality. Stop 4-1 coincides with the base of this section, which consists of ~12 m of moderately sorted, fine- to very fine-grained wacke. The bedload deposits are organised into decimetre-scale massive, planar, and lenticular beds that fine upward to thin- to medium-thick, low-angle and trough cross-bed sets. The upper bounding surface of this sandstone can be walked laterally for more than 2 km to the southeast, which allows for correlation with one of the two Tweefontein localities, located on the neighbouring farm Blaauwater 65.

Stop 4-2: Early Changhsingian Porcellanite

The yellowish-grey (5Y 7/2) barforms of the basal sandstone are overlain by coarse to fine, olive-grey (5Y 5/2) channel-fill siltstone in which a laminated bluish-white (5B 9/1) porcellanite occurs. Quartz-rich fine sand-and-silt and volcanogenic clasts occur within a thin-bedded siltstone interval from which a suite of Early Changhsingian zircons is reported (see star in Fig. 39). These resistant beds differ in colour from the surrounding olive-grey siltstone, and are bluish (5B 9/1) or very light grey (N8) to white (N9). Centimetre-scale intervals, consisting of millimetre- and sub-millimetre-scale cross-beds and starved ripples, contorted beds, and micro-scale ball-and-pillow structures, which can be accompanied by minimum bioturbation, characterise the lower part of the succession. A population of euhedral, elongate, and pristine zircons comes from a thin (3 cm) unit comprised of coarse to fine silt fining-up intervals of more homogenous nature. X-ray fluorescence (XRF) data (Steiner *et al.*, 2003) from each bed indicate a high percentage of SiO₂ (78–80%), and moderate percentages of Al₂O₃ (11%) and Na₂O (5%), and low percentages of CaO (1.3%), K₂O (1.3%), and FeO (1%). There is no geochemical difference in major elemental concentration between any well-silicified beds in the porcellanite interval (Lipshultz *et al.*, 2015).

The porcellanite, or silicified ash layer, contains abundant unaltered, euhedral, elongate, equant, and multifaceted zircon grains. U-Pb analyses of 11 single grains yielded data for four that are interpreted as antecrysts, or inherited because of post-depositional sedimentary recycling or inclusion during magmatic ascent and/or emplacement. The data for the remaining seven grains have overlapping ²⁰⁶Pb/²³⁸U ages that together have a weighted mean age of 253.48 ± 0.15 Ma (2σ; mean square of weighted deviates, MSWD = 0.47), interpreted as the best age estimate of the main zircon population. This maximum depositional age estimate places the porcellanite in the early part of the Changhsingian (254.2–251.9 Ma; Fig. 3). This is substantially older than the age of 251.9 Ma reported for the marine extinction event (Burgess *et al.*, 2014). It is also much younger than the Wuchiapingian (255.22 ± 0.16 Ma) age reported from the base of the *Daptocephalus* AZ (Rubidge *et al.*, 2013). As the early Changhsingian age reported from this section occurs in the uppermost part (~60 m from the top) of the *Daptocephalus* AZ, which is reported to be ~500 m thick in this part of the basin (Kitching, 1995; Viglietti *et al.*, 2016), Gastaldo *et al.* (2015) supported by palaeomagnetic data, concluded that there was an extremely low probability that the faunal turnover between the *Daptocephalus* and *Lystrorhynchus* AZs represented the terrestrial expression of the marine mass extinction event.

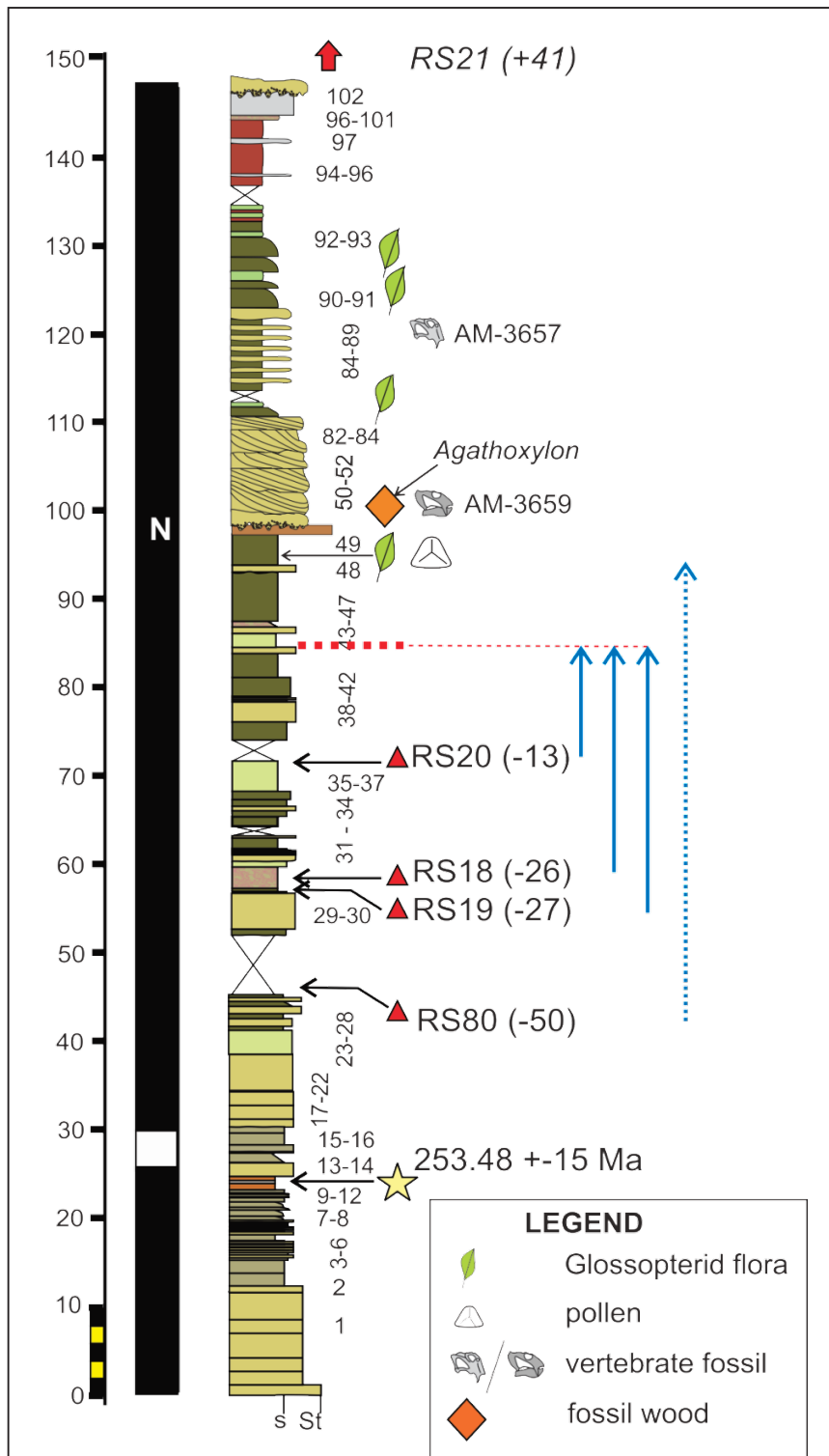


Figure 39. Combined stratigraphic section for Old Lootsberg Pass (also refer to Fig. 38). The numbers next to lithologies refer to palaeomagnetic collecting locations, with the results summarised in the bar on the left. RS-numbers refer to fossils collected by Smith and Botha-Brink (2014, supplementary material) and located using the locality database of Smith (pers. comm., 02/2014), while associated numbers in brackets refer to the reported stratigraphic distance relative to their PTB. Blue arrows on the right show how Gastaldo *et al.* (2015) determined an approximate position for the biozone contact, based on these data. The dotted red line is the proposed position of biozone contact (Gastaldo *et al.*, 2015). Porcellanite reported by Gastaldo *et al.* (2015) represented by yellow star. (From Gastaldo *et al.*, 2015, Is the vertebrate-defined Permian-Triassic boundary in the Karoo Basin, South Africa, the terrestrial expression of the end-Permian marine event?: *Geology*, V. 43, p. 939–942. Reprinted with permission from GSA).

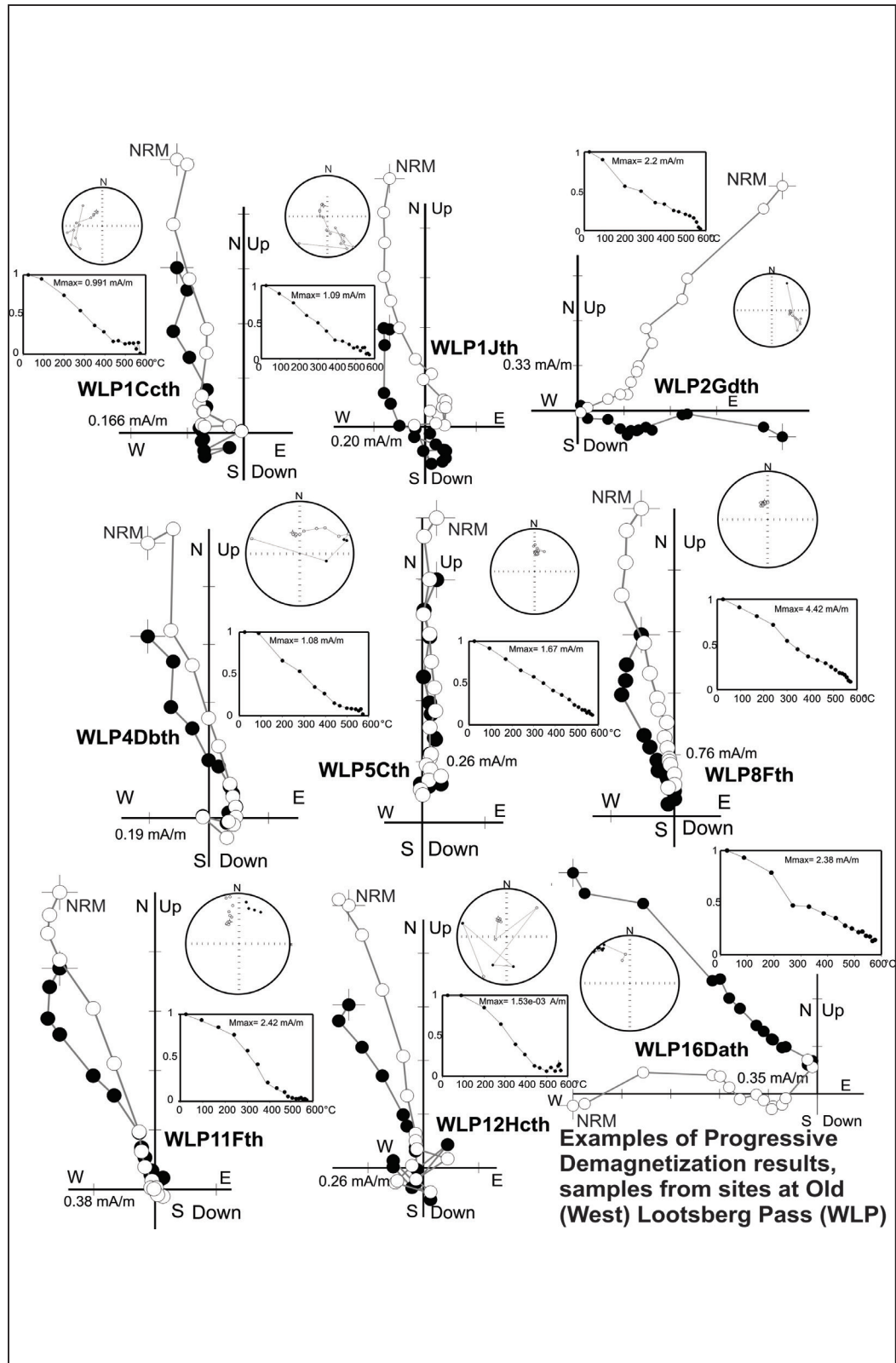


Figure 40. Orthogonal progressive demagnetisation diagrams (Zijderveld, 1967) showing the end point of the magnetisation vector plotted onto the horizontal (filled symbols) and vertical (open symbols) planes (NS–EW, EW–Up/Dn) for individual specimens from samples from selected sites from the Old Lootsberg Pass (West Lootsberg Pass, WLP) locality that have been subjected to alternating field (AF) or thermal demagnetisation. Also shown are normalised intensity decay plots indicating response to progressive treatment and stereographic projections of the magnetisation vector measured at each step. All diagrams in geographic coordinates with identical axes orientations.

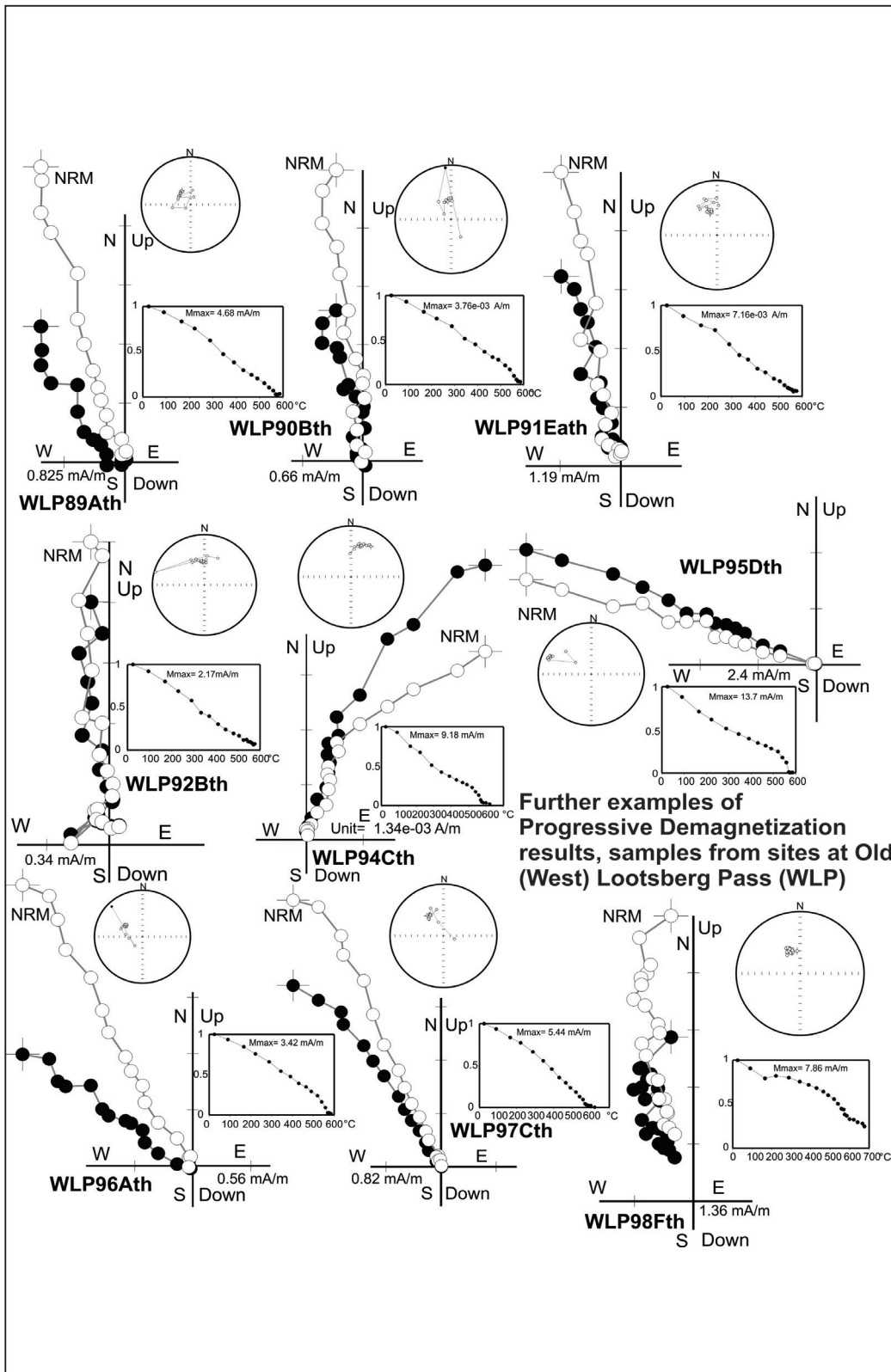


Figure 41.

Orthogonal progressive demagnetisation diagrams (Zijderveld, 1967) showing the end point of the magnetisation vector plotted onto the horizontal (filled symbols) and vertical (open symbols) planes (NS–EW, EW–Up/Dn) for individual specimens from samples from selected sites from the Old Lootsberg Pass (West Lootsberg Pass, WLP) locality that have been subjected to alternating field (AF) or thermal demagnetisation. Also shown are normalised intensity decay plots indicating response to progressive treatment and stereographic projections of the magnetisation vector measured at each step. All diagrams in geographic coordinates with identical axes orientations.



Stop 4-3: Interval of reversed polarity

The palaeomagnetic record of the Old Lootsberg Pass section, which now includes over 150 discrete sampling sites, is dominated by normal polarity magnetisations (Fig. 40, 41). For most sites, the demagnetisation response is well defined and magnetisations of normal polarity persist to laboratory unblocking temperatures close to 580 °C, the maximum for magnetite, or even higher, when haematite is a substantial carrier of the remanence. Typical initial natural remanent magnetisation (NRM) intensities for these rocks are low and range from ~1 to 5 mA/m, when magnetite is the dominant carrier, and higher (10 to 50 mA/m) when haematite is an important remanence carrier. In many instances, there is no hint of the isolation of any magnetisation of opposite polarity. Three sampling efforts were conducted in one horizon, a sequence of ~0.25 to 0.33 m thick beds in olive-green siltstone, stratigraphically some 5 m above the porcellanite bed that has yielded and early Changhsingian depositional age. This horizon has yielded consistently demagnetisation data showing dual component behaviour, with unblocking of a normal polarity remanence to 425–450 °C and, thereupon, the isolation of a south-southeast, moderate to steep positive inclination (reverse polarity) remanence (Figure 42). We interpret this observation to indicate that, for rocks typical of the Old Lootsberg Pass section, any remanence that persists above a laboratory unblocking temperature of approximately 425–450 °C has an antiquity that is older than the timing of the Karoo Large Igneous Province magmatism and, therefore, is likely primary.

Two Karoo sills are exposed in the general Old Lootsberg Pass area and both yield typical north-northwest-directed, steeply negative inclination (normal polarity) magnetisations.

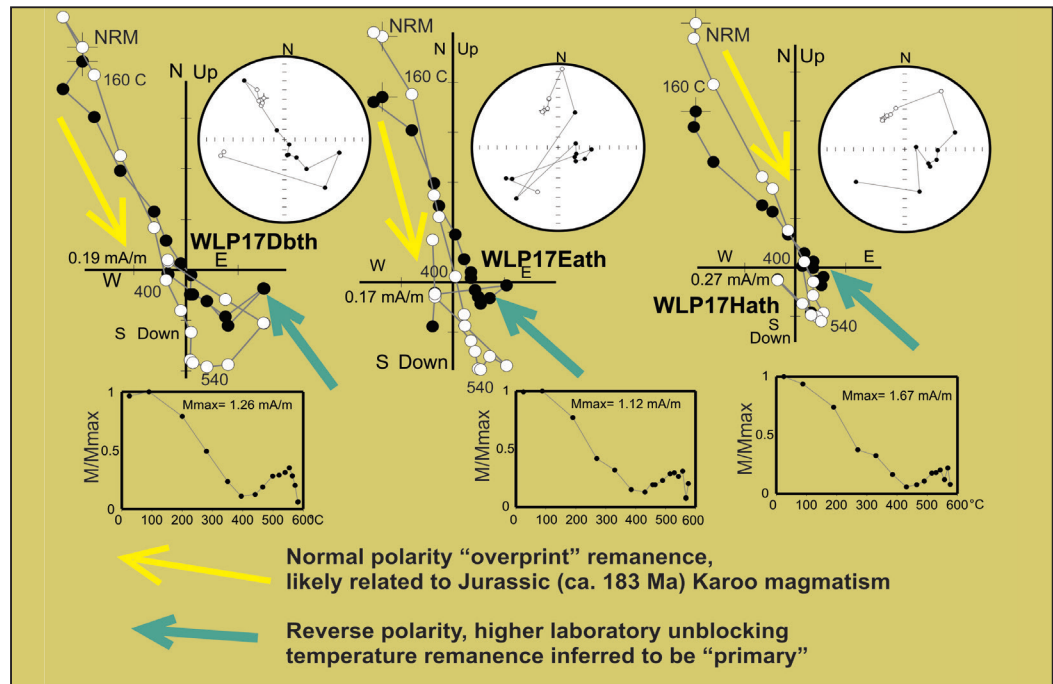


Figure 42. Orthogonal progressive demagnetisation diagrams (Zijderveld, 1967) showing the end point of the magnetisation vector plotted onto the horizontal (filled symbols) and vertical (open symbols) planes (NS–EW, EW–Up/Dn) for individual specimens from samples from site WLP 17 from the Old Lootsberg Pass (West Lootsberg Pass, WLP) locality that have been subjected to thermal demagnetisation. Also shown are normalised intensity decay plots indicating response to progressive treatment and stereographic projections of the magnetisation vector measured at each step. All diagrams in geographic coordinates with identical axes orientations. This site, which has been resampled two additional times, shows clear evidence of the presence of an acceptably well-defined reverse polarity magnetisation in these rocks, the first such demonstrated in the Lootsberg Pass area.

Stop 4-4: Laterally Accreted Bedsets

It is generally accepted that the Balfour Formation, up to the base of the Palingkloof Member, was deposited in a meandering fluvial setting, but exposures of channel deposits in the Elandsberg Member tend to be restricted to isolated outcrops, making architectural element analysis impossible. Laterally accreted bedsets at Stop 4-4 are interpreted to represent lateral accretion in a meandering fluvial environment.

Stop 4-5: Biostratigraphically derived PTB.

There are no lithostratigraphic data available to help locate the purported PTB. The exact position of the sections presented in Ward *et al.* (2000, 2005) and Smith and Ward (2001) are unclear and a repeat stratigraphy could not be located. The lithology bears no resemblance to the sequence reported by Smith and Botha-Brink (2014) and exhibit significant lateral variation (see Stop 4-7).

Prospecting by both Smith and Botha-Brink (2014, supplementary data) and our team yielded an extremely low number of fossils for this locality. Only five specimens (RS 18, RS 19, RS 20, RS 25, RS 80) have been reported next to the main donga section and two (RS 21, RS 22) from the exposures at the top of the pass (Fig. 38; Smith and Botha-Brink, 2014, supplementary material). Gastaldo *et al.* (in review) reported another three *in situ* fossils (AM3657, AM3659, SAM-PK-K8626) recovered from their sections, while the Smith and Botha-Brink (2014) dataset also included another four fossils (RS 15, RS 16, RS 17, RS 81), recovered from exposures further to the south that are equivalent to the lower half of the main section presented here. The density and stratigraphic position of these vertebrates are insufficient to pinpoint the biozone contact.

In an effort to compare our results with the published data, the supplementary data provided by Smith and Botha-Brink (2014) were used to calculate the stratigraphic position of the reported biostratigraphic contact. Using the GPS database provided by R.M.H. Smith, four of the *Daptocephalus* AZ fossils collected next to the main donga were located and traced into our section. Based on their reported stratigraphic distances from the PTB, we calculated and measured the stratigraphic distance to the purported biozone contact (Fig. 39). Three of these fossils (RS 18–20) converge on the same thick interval of stacked, lenticular beds of dark-grey coarse siltstone, which was used to denote the biozone boundary by Gastaldo *et al.* (2015). The stratigraphic data provided for RS 80 suggests that this boundary can be moved <10 m higher (Fig. 39). We do not rule out the possibility that this biozone placement can be incorrect and consider it possible that the boundary, as traditionally defined, can be moved up 30–40 m (see Stop 4-8). Nevertheless, the movement of the biozone contact metres higher still has no impact on the high stratigraphic placement of the porcellanite (Stop 4-2), or on the presence of a glossopterid fauna in the lowermost *Lystrosaurus* AZ (Stops 4-7 and 4-8).

Stop 4-6: Multistoried sandstone

Here, the first evidence of a pebble nodular conglomerate (and by implication regional degradation) is associated with thick sandstone at a stratigraphic height of ~100 m in the section (Fig. 39). This thick sandstone is multistoried, consisting of two stacked channel-fills, and can be traced across exposures at Old Lootsberg Pass for a distance of >0.5 km (Fig. 43). It attains a maximum thickness >11 m, thins to the east and west to <0.5 m, after which it pinches out laterally into greyish-red (east) or olive-grey (west) siltstone. Pebble nodular conglomerate lag deposits intermittently overlie the basal contact of both fill complexes, and consist of small, centimetre-scale carbonate-cemented nodules and mudclasts, as well as rarer bone fragments. Clasts are set in a matrix of very fine-grained sandstone and coarse siltstone. The lags are calcareous cemented and weather moderately yellowish brown (10YR 5/4). The fine to very fine sandstone that makes up the bulk of the channel-fills are organised into decimetre-scale massive, planar, and lenticular beds that fine upward into thin to medium, trough cross-beds. Ripple lamination occurs on laminar bedform surfaces.

Permineralised wood (see Stop 4-7) and a dicynodontoid skull fragment (AM 3659) were collected from the conglomerate lag in the western part of the transect. The large-diameter canines displayed by the latter are normally associated with latest Permian taxa (B. de Klerk and C. Kammerer, pers. comm. 9/2013), but the specimen is extremely poorly preserved and only can be assigned to Dicynontoidea indeterminately, based on its size, labial fossa, and the absence of a post-canine crest (C. Kammerer, writ. comm. 3 February 2016). Several taxa possess this suite of characters and overall general morphology, and possible affinities include *Dicynodon*, *Daptocephalus*, and *Lystrosaurus maccaigi* (Kammerer *et al.*, 2011), but can also include *Dinanomodon* and *Lystrosaurus curvatus* (C. Kammerer, written comm. 3 February 2016). Most of these are *Daptocephalus* AZ fauna, while *L. curvatus* is reportedly restricted to an extremely thin interval overlapping the biozone boundary.

Stop 4-7: Plant Fossil Locality

Fossil plants were collected from six sites in the strata above the PTB, as defined by vertebrate data (see Stop 4-5). Of these sites, four are within 10 m below the laterally traceable, intraformational conglomerate-bearing sandstone that conforms to post-extinction lithologies, and two occur >20 m above it (Fig 43). All collections are *Glossopteris*-dominated and several occur with the typical Permian sphenophyll, *Trizygia speciosa* (Fig. 44). There is no taphonomic evidence indicating any reworking of leaves (DiMichele and Gastaldo, 2008). A characteristic Permian palynoflora of moderate diversity, collected at this stop is consistent with the macrofloral record (glossopterids: *Protohaploxylinus limpidus*, *Striatopodocarpites cancellatus*, and *Weylandites lucifer*; trizygioid sphenophytes: *Columnisporites*). The palynoflora (Fig. 45) includes an array of other gymnosperm, peltasperm, corystosperm, and conifer pollen not found in regional, time-equivalent macrofloral records, but that appear in Karoo floras considered to be of Triassic age (Anderson and Anderson, 1985). Woody trunk



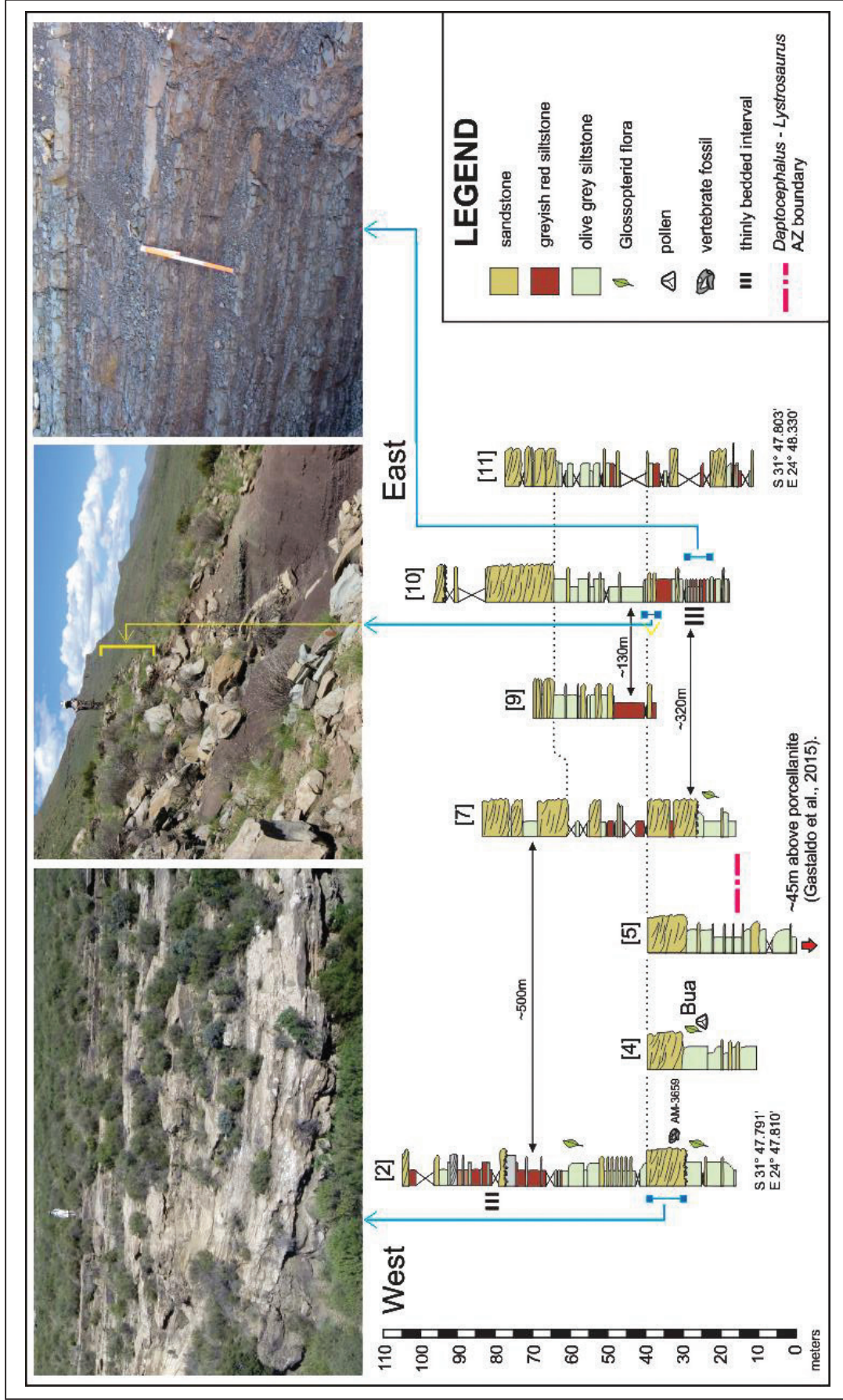


Figure 43.

Seven (of eleven) stratigraphic sections (identified by number), with palaeontological data, measured at the Old Lootsberg Pass locality and correlated by tracing bounding surfaces in the field. The lateral distances between selected sections are depicted by the double arrows. Photographs at the top of the figure show how channel-fills pinch out laterally and the lateral relationship with very thinly bedded siltstones.

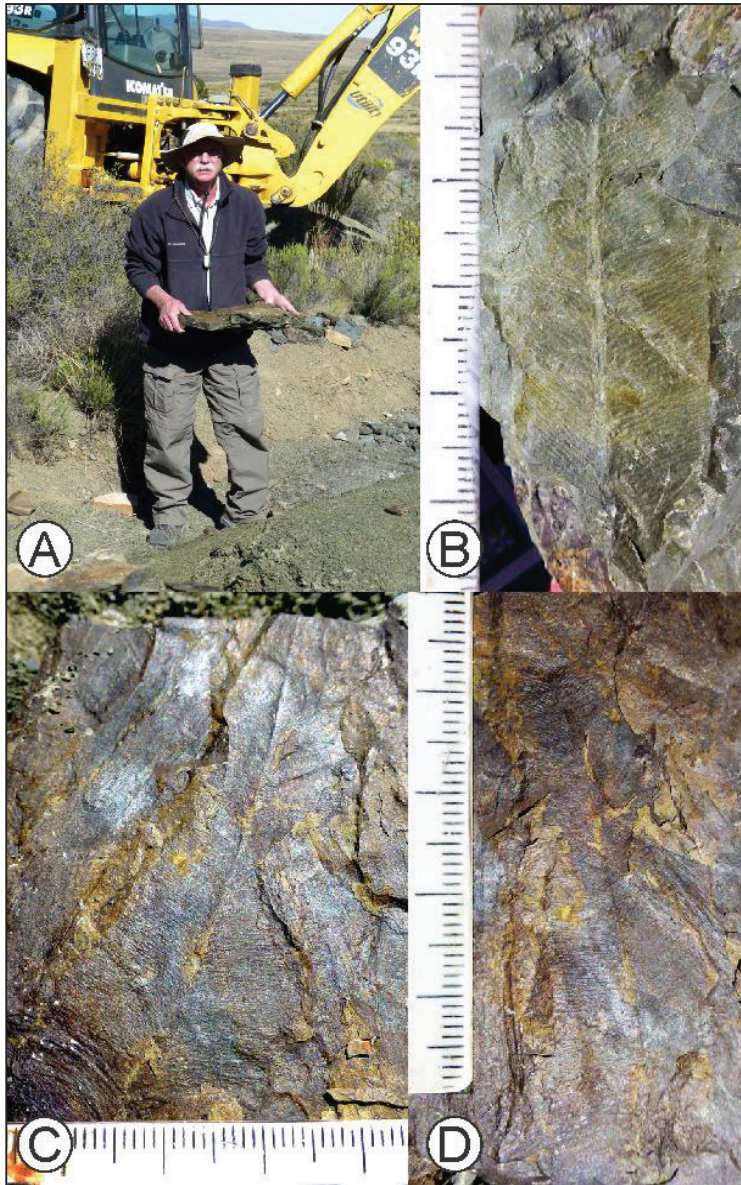


Figure 44.
Glossopteris leaf impressions
collected at Old Lootsberg Pass.

segments (>0.5 m diameter) recovered from the overlying sandstone (Fig. 39), display well-preserved growth rings and have been assigned to the long-ranging Permian–Triassic gymnosperm wood, *Agathoxylon africanum* (Bamford, 1999).

Stop 4-8: Traverse of Katberg Formation

The lithologies overlying the pebble nodular conglomerate-bearing sandstone vary laterally from east to west (Fig. 43). In the east, fossiliferous greyish-red siltstone directly overlies the sandstone body and is intercalated with thin- to medium-bedded, cross-bedded sandstone, without evidence of pebble nodular conglomerate lags. The siltstone colour changes to olive grey higher in this area, with an increasing proportion of channel-sandstone architectures and an increased frequency of thick, cross-bedded pebble-nodular conglomerate channel lags exposed along the Old Lootsberg Pass road.

In contrast, fossiliferous olive-grey siltstone overlies sandstone bodies to the west. An increasing proportion of reddish-grey siltstone is recorded up-section, which forms a much thicker interval here than in the east. Very thin-bedded greenish-grey and greyish-red siltstone, similar to the lithofacies association C of Smith and Botha-Brink (2014), is restricted to two outcrops separated by ~50 m of section (Fig. 43). In both instances, these outcrops are laterally equivalent to thick channel sandstone, thereby corroborating observations first made at Bethulie. A bluish-grey (5B 5/1) wacke, with carbonate-cemented lenticular lag deposits is stratigraphically higher — a facies that becomes more common.

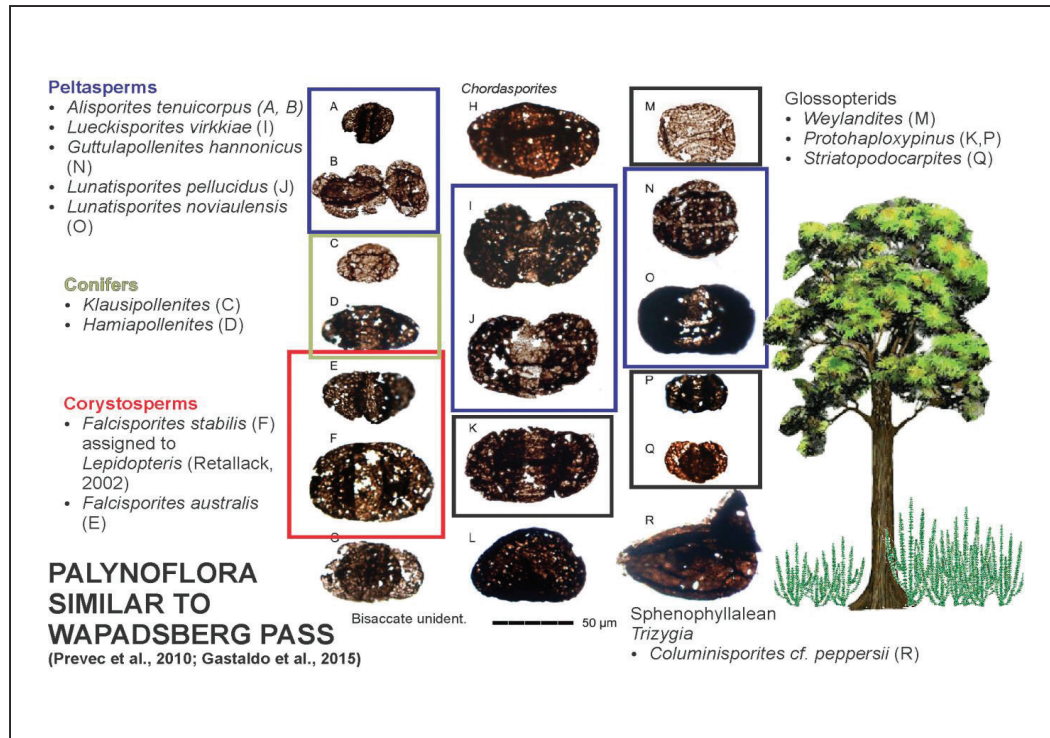


Figure 45. Old Lootsberg Pass palynoflora, with pollen genera assigned to their known parent plant group.

The lateral colour variation displayed by the massive siltstone over a short (<1 km) lateral distance is incompatible with the proposed aeolian origin, which implies blanket deposition (Gastaldo and Neveling, 2016). Instead, the colour does not necessarily reflect primary coloration but alteration, indicative of varying local pedogenic conditions on the ancient floodplain. The spatial variation in colour, along with the spatial variation in the occurrence of intraformational conglomerate also merits a review of the definition of the base of the Katberg Formation, as well as its merit as a stratigraphic marker. If the presence of the intraformational conglomerates, comprised of pedogenic glaeboles, is a distinctive feature of the Katberg Formation (Botha and Smith, 2006; Smith and Botha-Brink, 2014), the base of this formation can be placed at the multistory sandstone at ~100 m (Stop 4-6) in our stratigraphic section. However, this association is not exclusive to this horizon and recent work has shown that it appears much earlier in the stratigraphy (unpublished). If an approach that is more traditional is taken, whereby the base of the formation is defined as the point where the sandstone content increases rapidly (Groenewald, 1996), the lithostratigraphic contact varies by as much as 60 m over a transect of 500 m at the Old Lootsberg Pass locality (Fig. 43). Therefore, it is unwise to use this contact, which represents a transitional landscape, for any regional correlation.

11. 26 AUGUST (DAY 5): WAPADSBERG PASS AND COMMANDO DRIFT

11.1 Timetable

Depart Ganora	08:30
Arrive at New Wapadsberg Pass	9:00
Depart New Wapadsberg Pass	10:30
Arrive at Cradock	11:30
Lunch	12:00
Depart Cradock	13:30
Arrive at Commando Drift	14:00
Depart Commando Drift	15:00
Arrive at Cradock	15:30

11.2 Directions

Depart from Ganora. At farm gate, turn right (north) onto the gravel road to Middelburg. Continue on this road for 22 km until the junction with the N9. Turn right onto the N9 toward Graaff-Reinet. Continue for 1 km and turn left onto the R61 toward Cradock. After 8 km, stop at the base of the Wapadsberg Pass. Delegates walk up the section to re-join the vehicle at the top of the pass. Continue on the R61 for 100 km to Cradock until a T-junction is reached. Turn right onto the N10 and travel toward Cradock for 4 km. Follow the N10 traffic through Cradock. Turn right into Mark Street where the DIE TUISHUISIE is located at No. 36, 30 m from the intersection with Voortrekker Street. After lunch, the vehicle will depart Cradock, starting out south on the N10. While still within the borders of the town, turn left onto the turn-off to Tarkastad (R61). Continue on the R61 for approximately 7 km until reaching the turn-off (to the right) to Commando Drift Dam (it is also an alternative route to Tarkastad). Continue on this road for 30 km until reaching a turn-off to the Commando Drift Dam on the left.

Stop 5-1 Orientation, Changhsingian paleosols, and a *Glossopteris megaflorea*

At a stratigraphic position ~70 m below the vertebrate-defined boundary, as identified at Old Wapadsberg Pass ~1 km to the northeast (Smith and Botha-Brink, 2014, their fig. 3C), is a succession of greenish-grey mudrock in which at least two paleosols occur (Gastaldo *et al.*, 2014). Paleosol profiles are defined by the presence of chambered *Vertebraria*, the roots of glossopterid shrubs and trees, and immature

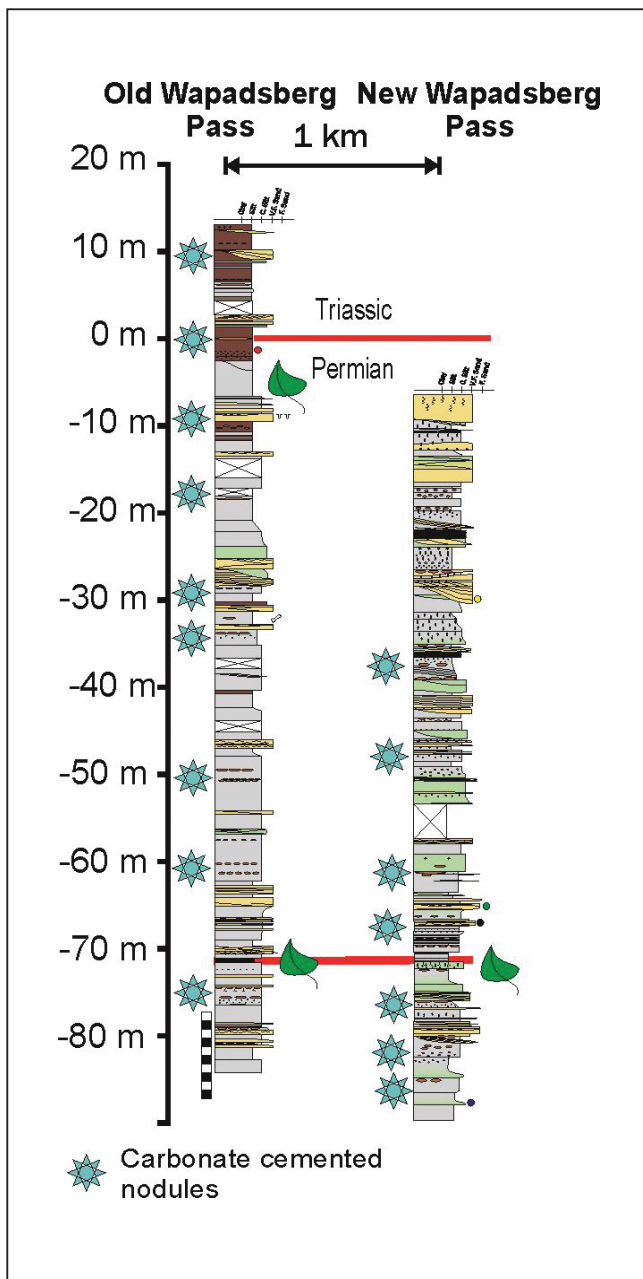


Figure 46. Comparative stratigraphic columns for the Old Wapadsberg Pass and New Wapadsberg Pass. The sections were correlated by tracing bounding surfaces for channel-fills, which confirmed that the devitrified claystone, with plant material, extends laterally for more than 2 km. (Figure from Gastaldo *et al.*, 2014, Latest Permian paleosols from Wapadsberg Pass, South Africa: Implications for Changhsingian climate. Geological Society of America Bulletin, v.126, pp. 665–679. Supplemental data. Reprinted with permission from GSA).



geochemical soil profiles. Defining the upper contact of each paleosol is a moderately to well preserved *Glossopteris* megafloora, in which there is evidence for plant-insect interactions, and a palynological assemblage (Prevec *et al.*, 2010). The palynospectrum is similar to that at Old Lootsberg Pass (Gastaldo *et al.*, 2015), assigned a Changhsingian age, and is correlative with the *Protohaploxylinus microcorpus* biozone of Western (Price, 1997) and Eastern Australia (Morante, 1995; Metcalfe *et al.*, 2015). The Global Boundary Stratotype and Point (GSSP) defined PTB is located in the lower part of the overlying *Kraeuselisporites saeptatus* palynology zone (Metcalfe *et al.*, 2008; Gortler *et al.*, 2009), which has not been encountered yet in the Karoo Basin.

Each soil profile is no more than 30 cm in thickness, and soil molecular weathering indices (base loss, clayeyness, salinisation, mineral maturity) indicate that these developed under high water table conditions. CIA-K values range from 73 to 87, with maxima occurring where preserved O-horizons exist. These proxies reflect soil formation under warm, humid, and probably seasonally wet conditions. One unusual aspect of these paleosols is the presence of detrital, devitrified claystone, as granule- to cobble-sized clasts, interpreted to be of volcanogenic origin (Gastaldo *et al.*, 2014). Detrital zircon crystals have been recovered from these devitrified claystones here and in correlative stratigraphic positions at Old Wapadsberg Pass. High-resolution, U-Pb ID-TIMS analyses of 36 single zircon crystals (23 in 2007–2008; 13 in 2010) yield ages ranging from Cambrian (526.9 ± 0.9 Ma) to Early Triassic (251.8 ± 0.038 Ma; unpublished data). Coney *et al.* (2007) and McKay *et al.* (2015) reported similar age estimates from detrital zircon in the Karoo Basin using ID-TIMS and SHRIMP-RG (Sensitive High Resolution Ion Microprobe-Reverse Geometry), respectively. To date, though, a suite of concordant single crystal ages, similar to that reported by Gastaldo *et al.* (2015) at Old Lootsberg Pass, has not been identified. This claystone can be traced to Old Wapadsberg Pass by following the bounding surfaces of sandstone channel-fills over two kilometre (Fig. 46). Several vertebrate fossils have been collected from Old Wapadsberg Pass (Smith and Botha-Brink, 2014).

We have reviewed the positions of individual fossils localities at Old Wapadsberg, located by using GPS coordinates provided by Smith (pers. comm., February 2014), and visited selected localities in the field. For these localities, we recorded the altitude with a Garmin Map62S, with barometric altimeter, to determine elevation relationships. This review indicated that at least two *Daptocephalus* AZ specimens (RS 174, previously identified as *Dicynodon lacerticeps*, and RS 175, *Lystrosaurus maccaigi*), collected at the top of the pass, overlap the stratigraphic ranges of *Lystrosaurus* AZ faunal elements, including *L. murrayi*, by more than 30 m (Fig. 47). These data suggest that vertebrate taxon ranges for the contact interval between the *Daptocephalus* and *Lystrosaurus* AZ need to be reassessed. These relationships also raise questions about the proposed phased and near coeval extinction of the *Daptocephalus* AZ fauna and, instead, suggest that the former fauna co-existed with the fauna of the overlying *Lystrosaurus* AZ for a much longer time than is currently assumed.

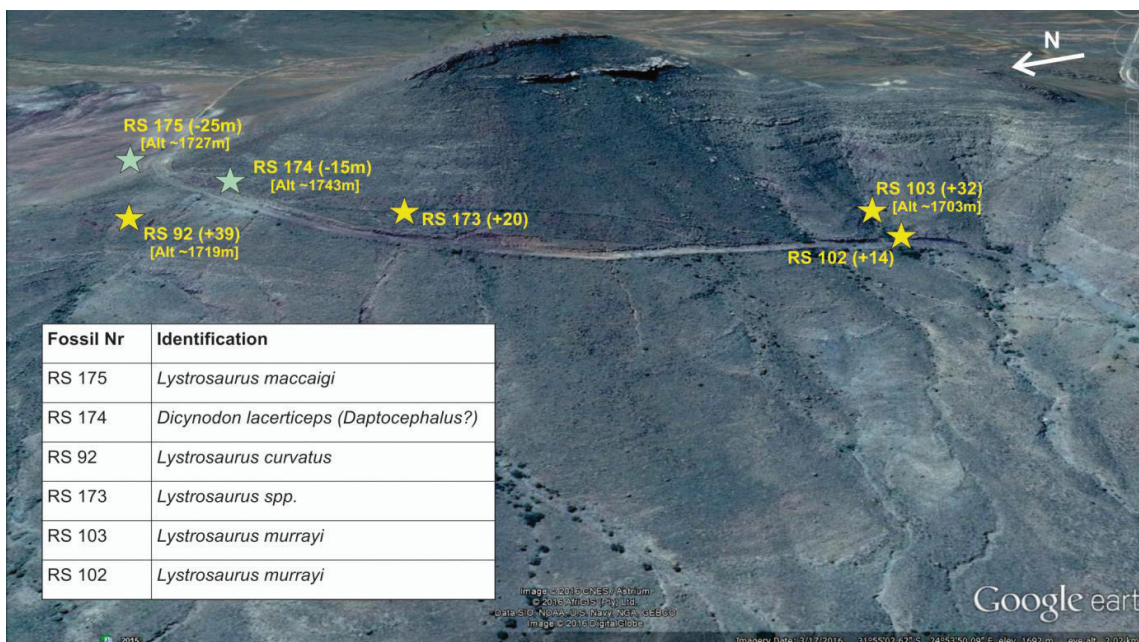


Figure 47. Google Earth image showing the distribution of selected fossil localities at Old Wapadsberg Pass (view to the east), indicating greater biozone overlap than currently proposed in extinction models. Green stars represent *Daptocephalus* AZ fossils and yellow stars *Lystrosaurus* AZ fossils. RS-numbers refer to fossil numbers, while numbers in brackets indicate the reported position of each specimen relative to the PTB (Smith and Botha-Brink, 2014, supplementary material) and the numbers in square brackets indicate the altitude measured with a Garmin Map62S with barometric altimeter.

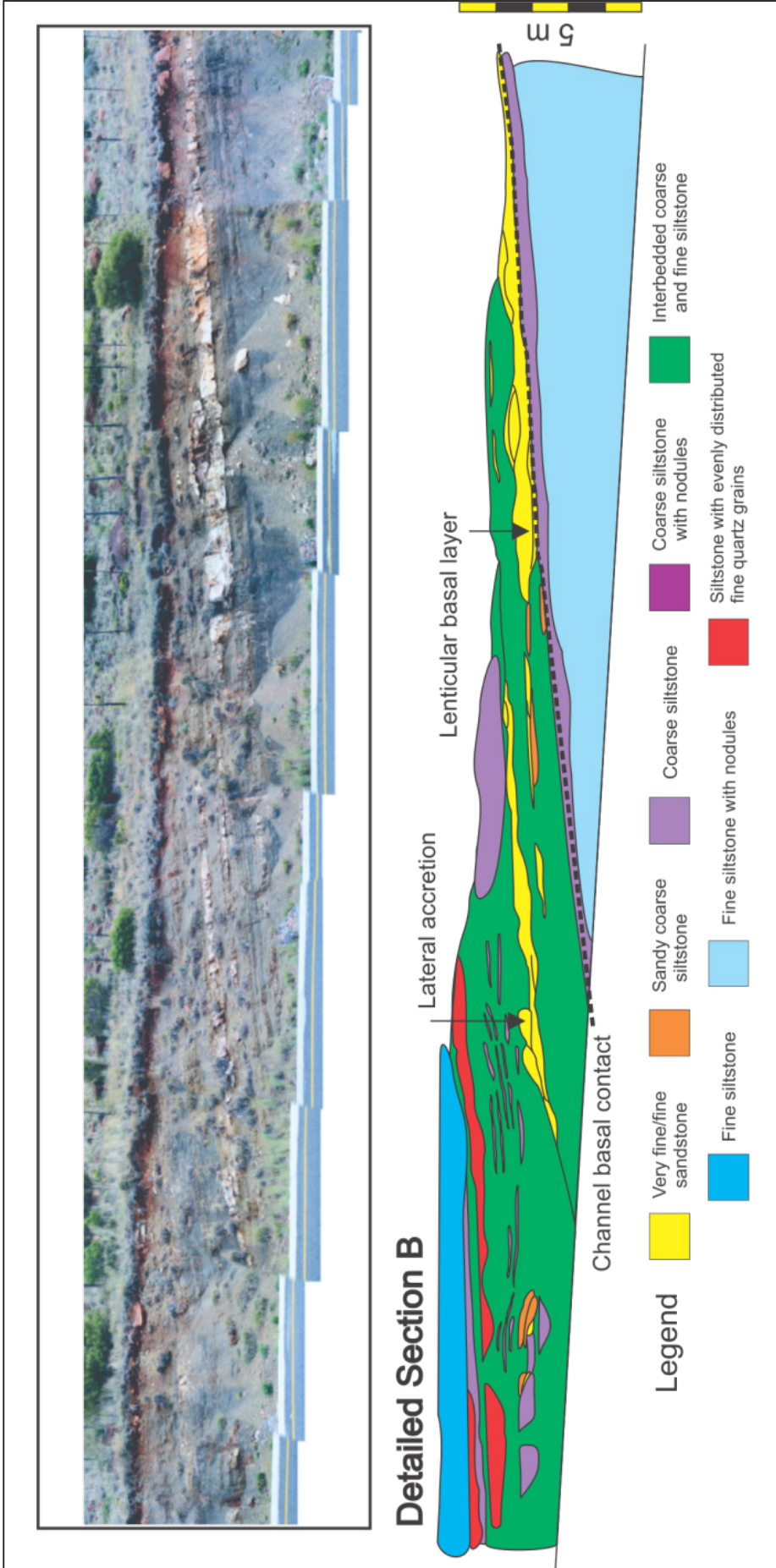


Figure 48.

The lower exposures at New Wapadtsberg Pass contain several channel-fills that display high suspension to bedload ratios. Two channel units can be seen here, incising into underlying channel-fill sequences. These channel-fills are characterised by a bedload sequence ~1 m in thickness, followed by fine- to coarse-siltstone suspension-load deposits. Sandstone beds are laterally offset and separated by southeast-dipping accretionary bounding surfaces.



Stop 5-2 Geometrically Spaced, Pedogenic Nodules

At a stratigraphic position ~10 m above the stacked, aggradational paleosols, are two laterally continuous beds, in which vertical roots are enveloped in calcite-cemented nodules (Prevec *et al.*, 2010; Gastaldo *et al.*, 2014). These nodules are spaced geometrically along the road cut exposure and have been interpreted to mark a transition from a standing body of water, wherein a lithofacies dominated by thinly laminated, greenish-grey (10Y 5/2) siltstone is found, to another set of paleosols. However, these paleosols differ from those in which *Glossopteris* flora is preserved lower in the interval, preserving the only stable isotopic chemistries attributable to calcite precipitation in atmospheric equilibrium with pCO₂ (Gastaldo *et al.*, 2014). Our estimates of Changhsingian pCO₂ from these nodules range from lows of between 500 and 900 ppmV and highs of between 1200 and 1900 ppmV. All other stable isotopic analyses (Fig. 13) of calcite cements from carbonate-cemented nodules or concretions yield δ¹³C values, either reflecting possibly well-drained conditions (41 m below the vertebrate-defined PTB) or values too negative for precipitation under well-drained conditions.

Stop 5-3 Fine-grained Fluvial Architectural Elements

A series of stacked channels can be seen exposed (Fig. 48) along the R61, ~50 m below the vertebrate-defined PTB, with the uppermost fluvial deposits having been subjected to metamorphism in response to dolerite intrusion. This fluvial system and its correlative exposed in Old Wapadsberg Pass should mark the reported changeover from deep, meandering channels in the Beaufort Group to low-sinuosity channel systems prior to, and following, the turnover in vertebrate faunas (Ward *et al.*, 2000).

Each channel form is defined by an arcuate lower contact, which is overlain by thin, <5 m thick very fine to fine lithic wacke, or sandy coarse siltstone, bedload deposits. The remainder of the channel-fill complex consists of fining-up successions of sandy coarse or coarse siltstone overlain by fine siltstone. In several instances, small, non-carbonate cemented nodules also occur. Occasionally, thin (<5 cm) discontinuous beds of white claystone are encountered, from which zircon crystals have been recovered. A U-Pb ID-TIMS age estimate of a population of seven grains assembled from a number of beds is 252.0 ± 0.5 Ma (Chizinski *et al.*, 2013; unpublished data).

Analyses of photomosaics reveal that at least four channel forms are superposed and imbricated in the section unaffected by metamorphic-grade alteration. Fluvial architectural elements are dominated by suspension-load, channel-fill deposits in the lower channel forms, whereas there is an increasing proportion of fine-grained bedload higher in the section. Here, barforms, with thicknesses ranging between 1 and 3 m, become more prominent, although the grain size of the sand component does not change. The lateral relationships of each margin in superposed channel forms indicate that these likely represent a single aggradational system that migrated across the floodplain. An increasing proportion of bedload higher in the stratigraphy signals a greater competence in the river system, which is related to water availability and discharge rate, or available outcrop. The current model for these rocks that transition the vertebrate-defined boundary envisions a landscape of increasing aridity, or seasonal aridity (Smith and Botha-Brink, 2014; Rubidge *et al.*, 2016). An increase in well-developed, sandy barforms, in which there is no evidence of periodic drying (e.g. mudcracks, desiccation cracks on bounding surfaces), indicates that sufficient water was available in these channels and the prevailing climate was not arid.

Stop 5-4: Commando Drift

ATTENTION: A steep topographic gradient is a feature of this locality, upward of 30 degrees, as you approach the summit. The stratigraphy is dominated by weathered siltstone scree, making ascent troublesome at times, and slippery. Caution should be exercised when ascending and descending this outcrop.

The locality is removed from the other PTB sites used to construct the model by a 125 km, straight-line distance from Old Lootsberg Pass on Blaauwater farm. It plays a central role in the Ward *et al.* (2005) model by reason of the reported magnetic polarity data of De Kock and Kirschvink (2004). By now, the stratigraphic distribution of lithofacies should be more than familiar, with greenish-grey siltstone and yellow-grey wacke dominating the lowest exposed rocks with a transition to reddish-grey and mottled greenish-grey siltstone higher in the section. A thick, trough cross-bedded fine to very fine, greyish-yellow wacke, in which channel-lag conglomerate of intraformational mudclasts (both greenish- and reddish-grey colour), caps the hill. To date, though, we have found no intraformational pedogenic nodule lithology as float. This is ascribed to there being only a thin, 5 cm thick, pedogenic nodular conglomerate lag deposit preserved above the contact with the capping sandstone body, which is reported to be the Katberg Formation.

De Kock and Kirschvink (2004) reported the presence of a reverse polarity magnetozone over ~80 m of stratigraphic section in the lowest sandstone–mudrock succession dominated by greenish-grey siltstone (Fig. 49). These rocks are overlain by a magnetozone of normal polarity that is illustrated to be dominated by siltstone and is reddish grey in colour. It is within the normal polarity interval, where the PTB is interpreted to be located, associated with the “event bed” of interlaminated greenish- and reddish-grey siltstone. That horizon is reported also to be at the Last Appearance Datum of *Dicynodon* (*Daptocephalus*), which both occur below the erosional base of an overlying sheet sandstone body. In addition, De Kock and Kirschvink (2004) reported a lithostratigraphic “PTB” where the first reddish-grey beds appear in which the End Permian Paleosol (EPP) is placed, and which is >10 m below the interlaminated unit of the reverse polarity magnetozone.

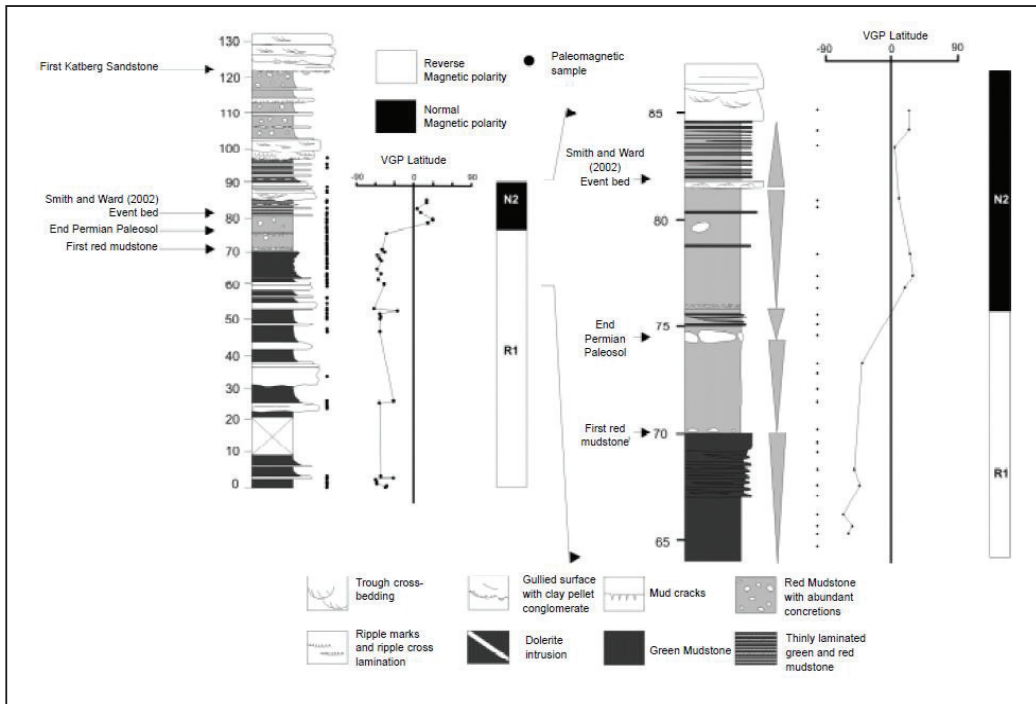


Figure 49.

Palaeomagnetic data reported from Commando Drift. (Figure from an article published in *Gondwana Research*, v. 7, De Kock and Kirschvink, Palaeomagnetic constraints on the Permian-Triassic boundary in terrestrial strata of the Karoo Supergroup, South Africa: implications for causes of the end-Permian extinction event, p.175-183, Reprinted with permission, Copyright Elsevier, 2004).

Both *Dicynodon* (*Daptocephalus*?) and *Lystrorhynchus* are recorded from the immediate vicinity (Fig. 50). It is not known whether the vertebrates in the collection of the Evolutionary Studies Institute (labelled with the prefix BP) and those collected by Groenewald (GHG) from this area (Fig. 50) form part of the database of Smith and Botha-Brink (2014), but it represents the only available palaeontological evidence on which the biozone boundary can be based, specifically at the Commando Drift section. Based on elevation, the localities yielding *Dicynodon* (*Daptocephalus*) and *Lystrorhynchus* show broad overlap, with the former occurring up to an elevation of ~1132 m (GHG 248), while *Lystrorhynchus* has been reported from elevations between ~1 010 m (GHG 292) and ~1 210 m (GHG 258). However, it is not clear whether this represents broad stratigraphic overlap, as the beds dip slightly to the west.

The exact geographic position of the base of the coarse stratigraphic section (De Kock and Kirschvink, 2004) and the GPS coordinates of the sites cored are unreported. These unknowns make it difficult to pinpoint exactly the relationship between the vertebrate collections and their stratigraphy. These relationships are important because De Kock and Kirschvink (2004) identified a different magnetostratigraphic (within the reverse polarity green mudstone-dominated magnetozone) and biostratigraphic (LAD of *Dicynodon* at the "event" bed) placement of the extinction event. These horizons differ by ~15 m, and our estimate of the highest occurrence of "*Dicynodon*" (GHG 248 is roughly equivalent to our palaeomagnetic sample P26) is only 20 m below the basal contact of the capping sandstone unit. This contrasts with the LAD of *Dicynodon* (*Daptocephalus*) reported by De Kock and Kirschvink (2004) >30 m below the basal contact of the capping sandstone. This is at a stratigraphic position, where we have found an ~1 m thick interval consisting of decimetre-scale beds of light-olive coarse siltstone, mottled reddish grey, with *Katbergia* burrows, and reddish-grey fine siltstone.

Ward *et al.* (2005) used the stratigraphy of De Kock and Kirschvink, (2004) and correlated the laminated "event bed" with similar lithofacies at West (Old) and East (New) Lootsberg Pass and Carlton Heights (Fig. 11). By extension, their magnetic polarity record is used to anchor the base of a composite magnetostratigraphic section, which is used to correlate with the marine record. In principle, the approach taken by Ward *et al.* (2005) is acceptable, but only if there is a clear demonstration of the antiquity (i.e. early acquisition) of the magnetisations characteristic of these rocks. The De Kock and Kirschvink (2004) contribution provides no evidence that reverse polarity magnetisations exist in the rocks sampled at this section and that such magnetisations can be adequately resolved in progressive demagnetisation, using either alternating field or thermal methods. We have carried out preliminary resampling of much of the Commando Drift section, along a slightly different traverse than that used by De Kock and Kirschvink (2004) and, to date, have only been able to resolve magnetisations of normal polarity in progressive thermal demagnetisation. Again, from the above, the delegates will note that this section lies directly above a regionally extensive Karoo dolerite sill.

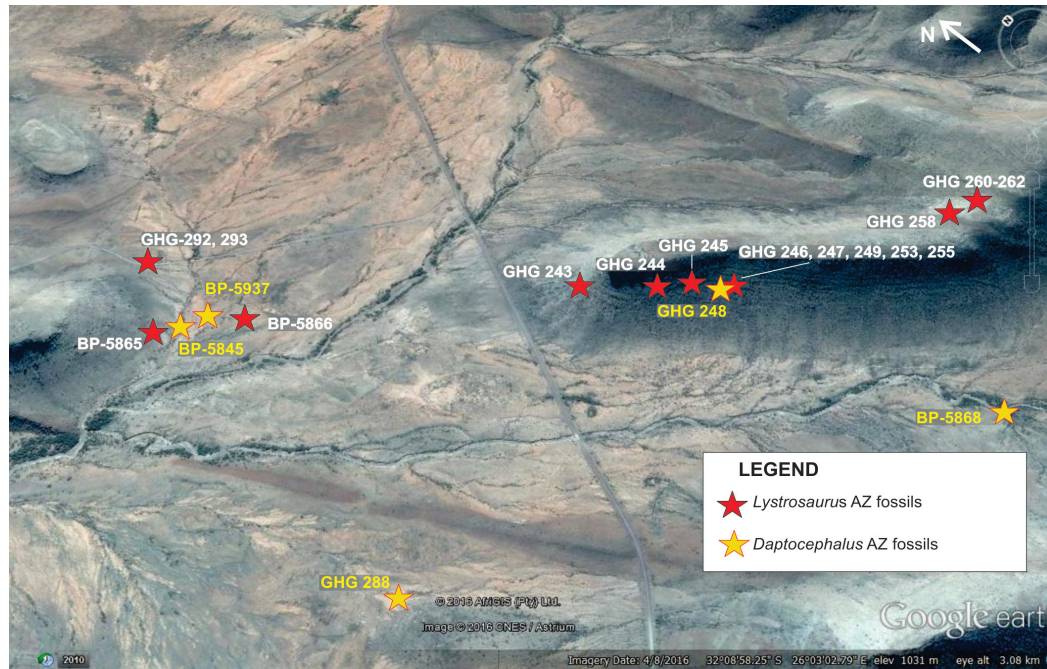


Figure 50. Oblique Google Earth image of Commando Drift, showing the distribution of vertebrate fossil material collected by the Evolutionary Studies Institute (BP-numbers) and Gideon Groenewald (GHG-numbers, constructed using data from the CGS fossil database).

12. 27 AUGUST (DAY 6): CRADOCK TO CAPE TOWN

12.1 Timetable

Depart Cradock	08:30
Graaff-Reinet	10:00
De Rust	12:30
Oudtshoorn (lunch)	13:00-14:00
Ladismith	15:00
Ashton	16:45
Worcester	17:30
Arrive at Cape Town	18:30

12.2 Directions

Depart from Cradock, traveling north on the N10 for 4 km, before turning left onto the R61 to Graaff-Reinet. After 71 km, you will reach a T-junction with the N9. Turn left toward Graaff-Reinet (47 km) and continue south on the N9 past Aberdeen (56 km) and Willowmore (96 km). Approximately 38 km past Willowmore, turn right onto the R341 to Oudtshoorn. After 67 km, you will reach a T-junction at the town of De Rust. Turn left onto the N12 and continue for ~35 km to Oudtshoorn. Continue through Oudtshoorn and travel on the R62 past Calitzdorp (50 km), Ladismith (49 km), Barrydale (77 km), Montagu (60 km), and Ashton (10 km). The R62 becomes the R60 as you travel through Ashton and continue to Robertson (20 km) and Worcester (50 km). At Worcester, turn left onto the N1 (south) and continue for 104 km to Cape Town.

12.3 General Geology

The Camdeboo plain, south of Graaff-Reinet, is underlain primarily by the Middleton Formation, which consists of stacked, upward-fining fluvial cycles, with the proportion of mudstone increasing to the top of the formation. Travelling south from Aberdeen, it is noticeable that tectonic activity related to the formation of the Cape Fold Belt has had an increasing effect on the Karoo Basin fill. Thereafter, the Koonap Formation (lowermost unit of the Beaufort Group) and the formations of the Ecca Group crop out in increasingly narrower bands as we approach the Cape Fold Mountains. We cross the contact of the Dwyka Group with the Witteberg Group of the Cape Supergroup at the southern end of the Beervlei Dam, north of Willowmore.

South of Willowmore, the landscape is formed largely by the Table Mountain and Bokkeveld groups. The valley along which the R341 runs is underlain by the relatively soft sediments of the Bokkeveld Group, which comprises cyclic alterations of fine sandstone and mudrock. The large red hills in this valley consist of remnants of the Uitenhage Group. The red-stained conglomerates of the Enon Formation consist of subrounded pebbles and cobbles of quartzite, and, occasionally, slate, derived from the Cape Supergroup rocks. The cobbles are packed by a sand and siltstone matrix, bounded by limonite cement. Pebbles are often imbricated and most beds dip gently toward the north. Exposures of the Enon Formation in the Oudtshoorn Basin often weather to form small caves, associated with honeycombing.

The Kirkwood Formation crops out to the north of the R34, between Oudtshoorn and Calitzdorp. It consists of coarse- to medium-grained olive sandstone, interbedded with red and greenish-grey siltstones. It accumulated in a predominantly meandering fluvial environment and contains the remains of a dinosaur-dominated fauna (Shone, 2006).

Uplift and deposition during the Late Mesozoic resulted in valley-fill, with a valley floor at much higher elevation than current levels. Erosion during the Cenozoic resulted in deep incision of these valleys down to a newly established base level, giving rise to the formation of fluvial peneplains. Remnants of these once extensive fluvial peneplains are preserved as horizontal terraces along the sides of the major valleys of the region (Toerien, 1979). These Late Miocene to Late Pliocene terrace deposits are typically 8–20 m thick and composed of subrounded gravel and coarse-grained sands. In the Oudtshoorn Basin these features are commonly ferruginised and/or capped by weathering-resistant silcrete, which contributes to their preservation to the present day.



13. ACKNOWLEDGEMENTS

We would like to express our appreciation of the assistance received from various colleagues who have helped to improve our understanding of the terrestrial end-Permian model of the Karoo Basin. In particular, we wish to thank Dr Rose Prevec of The Albany Museum, Rhodes University, for countless hours of palaeontological exploration and collection that has helped to better circumscribe the biostratigraphic ranges of critical taxa; Dr Marion Bamford, Evolutionary Studies Institute, University of the Witwatersrand, for her insight into the collections of permineralised wood; Dr Cindy Looy, University of California-Berkeley, for palynological analyses; Dr Sandra Kamo, Jack Satterly Geochronology Laboratory, University of Toronto, for her tireless efforts to obtain robust, high-resolution U-Pb ID-TIMS age estimates; Dr Billy de Klerk, The Albany Museum, Rhodes University, Dr Christian Kammerer and Dr Jorg Fröbisch, Museum für Naturkunde, Berlin, and Dr Ken Angielczyk, Chicago Field Museum for assistance with vertebrate specimen identification; Dr Neil Tabor, Southern Methodist University, for collaborative efforts to unravel the carbon and oxygen stable-isotopic Karoo records; and Dr Darby Dyar, Mt. Holyoke College, for Mössbauer spectrographic analyses. In addition, we acknowledge the assistance of B.J. Lycka and M.U. Anekwe with MS/AMS measurements in the University of Texas at Dallas laboratory facility, and of K. Able with IRM acquisition data. J.W. Geissman is fully responsible for all remanence measurements in the UTD laboratory.

We acknowledge the field and laboratory assistance of the following Colby College undergraduate students who have undertaken parts of this project as independent research or as honours theses, namely, R. Selover '04, S. Gray '05, D. Pace '06, M. Rolerson '06, L. Masters '06, S. Weeks '06, C. Kit Clark '08, S. Newbury '08, S. Reid '08, C. Knight '10, A. Pludow '11, C. Kapupu '12, N. Katsiaticas '12, T. Chizinski '14, M. Langwenya '14, K. Spencer '14, S. Cusack '15, J. Li '16, K. Lipshultz '16, T. Sasajima '16, O. Battifarano '17, and A. Churchill '17. V. Nxumalo of the Council for Geoscience, as well as Council for Geoscience interns A. Ndhukwani, and S. Makubalo, participated in the field work.

We thank R.H.M. Smith for providing an original vertebrate database, including global positioning system (GPS) coordinates of all the specimens. We acknowledge the contribution of D. Grobbelaar of the Council for Geoscience who compiled the route maps used in this document.

The authors appreciate the hospitality and kindness shown to them over the past decade by Justin and Liesl Kingwill, Blaauwater Farm; JP and Hester Steynberg, Ganora Guest Farm; Phillip Looock, Quaggas Fontein; Sarel Theron, Bethel; Pieter Erasmus, Carlton Heights; Fourie Schoeman, Commando Drif.

JWG acknowledges the faculty start-up funding from UTD. Student participation was supported by the Selover Family student-research endowment and Barrett T. Dixon Geology Research and Internship Fund for undergraduate experiences in the Department of Geology, Colby College. The authors' research efforts were supported in part, by the Council for Geoscience (South Africa); NSF EAR 0417317, 0749895, 0934077, and 1123570; the Whipple-Coddington Endowment, Colby College; and a Fulbright Scholar Award from the U.S. Department of State to RAG in the Department of Geology, Rhodes University, Grahamstown.

14. LITERATURE CITATIONS

- Abdala, F., Cisneros, J.C., and Smith, R.M.H., 2006, Faunal Aggregation in the Early Triassic Karoo Basin: Earliest Evidence of Shelter-sharing Behavior among Tetrapods?: *PALAIOS*, v. 21, p. 507-512.
- Alley, N.F., 1998, Cainozoic stratigraphy, palaeoenvironments and geological evolution of the Lake Eyre Basin, *Palaeogeography, Palaeoclimatology, Palaeoecology*, v. 144, p. 239-263.
- Anderson, J.M., and Anderson, H.M., 1985, Palaeoflora of southern Africa. Prodomus of South African megafloa. Devonian to Lower Cretaceous: Balkema, Rotterdam, 416 p.
- Anderson, J.M., and Cruickshank, A.R.I., 1978, The biostratigraphy of the Permian and the Triassic. Part 5. A review of the classification and distribution of Permo–Triassic tetrapods: *Palaeontologia africana*, v. 21, p. 15–44.
- Angielczyk, K.D., and Kurkin, A.A., 2003, Has the utility of *Dicynodon* for Late Permian terrestrial biostratigraphy been overstated?: *Geology*, v. 31, p. 363-366.
- Askin, R.A., 1998, Floral trends in the Gondwana high latitudes – Palynological evidence from the Transantarctic mountains: *Journal of African Earth Sciences*, v. 27, p. 12-13.
- Awatar, R., Tewari, R., Agnihotri, D., Chatterjee, S., Pillai, S.S.K., and Meena, K.L., 2014, Late Permian and Triassic palynomorphs from the Allan Hills, central Transantarctic Mountains, South Victoria Land, Antarctica: *Current Science*, v. 7, p. 988-996.
- Ballard, M.M, Van der Voo, R. and Hällich, I.W., 1986, Remagnetizations in Late Permian and Early Triassic rocks from southern Africa and their implications for Pangea reconstructions, *Earth and Planetary Science Letters*, v. 79, p. 412-418.
- Bamford, M.K., 1999, Permo–Triassic fossil woods from the South African Karoo Basin: *Palaeontologica africana*, v. 35, p. 25-40.
- Bate, K.J., & Malan, J.A., 1992, Tectonostratigraphic evolution of the Algoa, Gamtoos and Pletmos Basins, offshore South Africa: in de Wit, M.J., and Ransome, I.G.D., eds., *Inversion Tectonics of the Cape Fold Belt, Karoo and Cretaceous Basins of Southern Africa*, A.A. Balkema, Rotterdam. p. 61-73
- Battail, B., 1993, On the biostratigraphy of the Triassic therapsid bearing formations: in Lucas, S.G. and Morales, M., eds., *The Nonmarine Triassic*, New Mexico Museum of Natural History & Science Bulletin, v. 3, p. 31-35.
- Battifarano, O.K., Churchill, A.N., Gastaldo, R.A., Neveling, J., and Geissman, J.W., 2015, Lithostratigraphy and lateral variation in vertebrate biostratigraphy near the Permian–Triassic Boundary at Bethulie, South Africa: *Geological Society of America Abstracts with Programs*. 47 (7), p.570
- Behrensmeier, A.K., Kidwell, S.M., and Gastaldo, R.A., 2000, Taphonomy and Paleobiology: *Paleobiology*, v. 26, p. 103-147.
- Benton, M.J. and Newell, A.J., 2014. Impacts of global warming on Permo–Triassic terrestrial ecosystems: *Gondwana Research*, v. 25, p. 1308-1337.
- Boonstra, L.D. 1969. The fauna of the Tapinocephalus Zone (Beaufort Beds of the Karoo): *Annals of the South African Museum*, v. 56, 73 p.
- Botha, J., and Smith, R.H.M., 2006, Rapid vertebrate recuperation in the Karoo Basin of South Africa following the End-Permian extinction: *Journal of African Earth Sciences*, v. 45, p. 502-514.
- Botha, J., and Smith, R.H.M., 2007, *Lystrosaurus* species composition across the Permo–Triassic boundary in the Karoo Basin of South Africa: *Lethaia*, v. 40, p. 125–137.
- Botha-Brink, J., Huttenlocker, A.K., and Modesto, S.P., 2014, Vertebrate Paleontology of Nooitgedacht 68: A *Lystrosaurus maccaigi*-rich Permo–Triassic Boundary Locality in South Africa: in Kammerer, C.F., Angielczyk, K.D., and Fröbisch, J., eds., *Early Evolutionary History of the Synapsida, Vertebrate Paleobiology and Paleoanthropology*: Springer, Dordrecht, p. 289-304.
- Botha-Brink, J., Codron, D., Huttenlocker, A.K. Angielczyk, K.D. and Ruta, M., 2016, Breeding Young as a Survival Strategy during Earth's Greatest Mass Extinction: *Sci. Rep.* 6, 24053; doi: 10.1038/srep24053.
- Broom, R., 1906, On the Permian and Triassic Faunas of South Africa: *Geological Magazine (Decade V)*, v. 3, p. 29-30.
- Broom, R., 1907, On the geological horizons of the vertebrate genera of the Karoo Formation: *Records of the Albany Museum*, v. 2, p. 156-163.
- Broom, R., 1909, An attempt to determine the horizons of the fossil vertebrates of the Karoo: *Annals of the South African Museum*, v. 7, p. 285-289.



- Broom, R., 1911, On some New South African Permian Reptiles: Proceedings of the Zoological Society of London, v. 81, p. 1073-1082.
- Broom, R., 1932, The mammal-like reptiles of South Africa: London, Witherby, 376 p.
- Burgess, S.D., and Bowring, S.A., 2015, High-precision geochronology confirms voluminous magmatism before, during, and after Earth's most severe extinction: Science advances, v. 1, p. e1500470.
- Burgess, S.D., Bowring, S. and Shen, S.Z., 2014, High-precision timeline for Earth's most severe extinction: Proceedings of the National Academy of Sciences, v. 111, p. 3316-3321.
- Catuneanu, O., Hancox, P.J., Cairncross, B., and Rubidge, B.S., 2002, Foredeep submarine fans and forebulge deltas: orogenic offloading in the underfilled Karoo Basin: Journal of African Earth Sciences, v. 35, p. 489-502.
- Catuneanu, O., Hancox, P.J., and Rubidge, B.S., 1998, Reciprocal flexural behaviour and contrasting stratigraphies: a new basin development model for the Karoo retroarc foreland system, South Africa: Basin Research, v. 10, p. 417-139.
- Catuneanu, O., Wopfner, H., Eriksson, P.G., Cairncross, B., Rubidge, B.S., Smith, R.M.H., and Hancox, P.J., 2005. The Karoo basins of south-central Africa: Journal of African Earth Sciences, v. 43, p. 211-253.
- Cerling, T.E., 1991, Carbon dioxide in the atmosphere: evidence from Cenozoic and Mesozoic paleosols. American Journal of Science, v. 291, p. 377-400.
- Chevallier, L. and Woodford, A., 1999, Morpho-tectonics and mechanism of emplacement of the dolerite rings and sill of the western Karoo, South Africa: South African Journal of Geology, v. 102, no. 1, p. 43-54.
- Chizinski, T., Gastaldo, R.A., and Neveling, J., 2013, The Fluvial Sequence of a Latest Changhsingian, Pre-PT Extinction River Complex, Eastern Cape Province, South Africa: Geological Society of America, Abstracts with Program, v. 45, p. 127.
- Colbert, E.H., 1969, Gondwanaland and the distribution of Triassic tetrapods: Gondwana Stratigraphy, Paris: I.U.G.S. Symposium, Buenos Aires, 1970, UNESCO, p. 355-374.
- Cole, D.I., 1992, Evolution and development of the Karoo Basin: in De Wit, M.J., and Ransome, I.G.D., eds., Inversion Tectonics of the Cape Fold Belt, Karoo and Cretaceous Basins of Southern Africa: Balkema, Rotterdam, p. 87-99.
- Collinson, J.W., Hammer, W.R., Askin, R.A., and Elliot, D.H., 2006, Permian-Triassic boundary in the Central Transantarctic Mountains, Antarctica: Geological Society of America Bulletin, v. 118, p. 747-763.
- Coney, L. Reimold, W.U., Hancox, J., Mader, D., Koeberl, C., McDonald, I., Struk, U., Vajda, V., and Kamo, S.L., 2007, Geochemical and mineralogical investigation of the Permian-Triassic boundary in the continental realm of the southern Karoo Basin, South Africa: Paleoworld, v. 16, p. 67-104.
- Connell, S.D., Kim, W., Smith, G.A., and Paola, C., 2012, Stratigraphic architecture of an experimental basin with interacting drainages: Journal of Sedimentary Research, v. 82, p. 326-344.
- Cooper, M.R., 1982, A Mid-Permian to Earliest Jurassic tetrapod biostratigraphy and its significance: Arnoldia Zimbabwe, v. 7, p. 77-103.
- Cosgriff, J.W., 1965, A new genus of temnospondyli from the Triassic of Western Australia: Journal of the Royal Society of Western Australia, v. 48, p. 65-90.
- Cosgriff, J.W., 1984, The temnospondyl labyrinthodonts of the earliest Triassic: Journal of Vertebrate Paleontology, v. 4, p. 30-46.
- Cosgriff, J.W., and Zawiskie, J.M., 1979, A new species of the Rhytidosteoidea from the *Lystrosaurus* Zone and a review of the Rhytidosteoidea: Palaeontologia africana, v. 22, p. 1-27.
- Cox, C.B., 1967, Changes in terrestrial vertebrate faunas during the Mesozoic: Geological Society, London, Special Publications, v. 2, p. 77-89.
- Day, M.O., Ramezani, J., Bowring, S.A., Sadler, P.M., Erwin, D.H., Abdala, F., and Rubidge, B.S., 2015, When and how did the terrestrial mid-Permian mass extinction occur? Evidence from the tetrapod record of the Karoo Basin, South Africa: Proceedings Royal Society B, v. 282, 20150834.
- De Beer, C.H., 1990, Simultaneous folding in the western and southern branches of the Cape Fold Belt: South African Journal Geology, v. 93, p. 583-591.
- De Beer, C.H., 1998, Structure of the Cape Fold Belt in the Ceres Arc: Council for Geoscience Bulletin, v. 123, 93 p.
- De Beer, C.H., 2002. The stratigraphy, lithology and structure of the Table Mountain Group. In, K. Pietersen, K. and Parsons, R., eds., A Synthesis of the Hydrogeology of the Table Mountain Group—Formation of a Research Strategy: Water Research Commission, WRC Report No. TT 158/01, p. 8-18.

- De Kock, M.O., and Kirschvink, J.L., 2004, Paleomagnetic constraints on the Permian-Triassic boundary in terrestrial strata of the Karoo Supergroup, South Africa: implications for causes of the end-Permian extinction event: *Gondwana Research*, v. 7, p.175-183.
- De Wit, M.C.J., 1999, Post-Gondwana drainage and the development of diamond placers in Western South Africa: *Economic Geology*, v. 97, p. 721-740.
- De Wit, M.J. and Ransome, I.G.D., 1992, Regional inversion tectonics along the southern margin of Gondwana. in de Wit, M.J., and Ransome, I.G.D., eds., *Inversion Tectonics of the Cape Fold Belt, Karoo and Cretaceous Basins of Southern Africa*: A.A. Balkema, Rotterdam, p. 15-22, A.A..
- Dimichele, W.A., and Gastaldo, R.A., 2008, Plant Paleocology in Deep Time: *Annals of the Missouri Botanical Garden*, v. 95, p. 144-198.
- Dingle, R.V., 1978, South Africa: in Moullade, M. and Nairn, A.E.M., eds., *The Phanerozoic Geology of the World II, The Mesozoic A*: Amsterdam: Elsevier, p. 401-434.
- Doucouré, C.M., and De Wit, M.J., 2003, Old inherited origin for the present near-bimodal topography of Africa: *Journal of African Earth Sciences*, v. 36, p. 371-388.
- Dyke, N.D., and Channel, J.E.T., 1996, *Magnetic Stratigraphy*: San Diego, Academic Press, 346 p.
- Efremov, J.A., 1940, Taphonomy: New branch of paleontology: *Pan-American Geology*, v. 74, p. 81-93.
- Erwin, D.H., 2006. *Extinction: how life on earth nearly ended 250 million years ago*. Princeton University Press, 296 p.
- Erwin, D.H., Bowring, S.A. and Yugan, J., 2002, End-Permian mass extinctions: a review: *Geological Society of America Special Papers*, v. 356, p. 363-384.
- Everitt, C.W.F., and Clegg, J.A., 1962, A field test of paleomagnetic stability: *Royal Astronomical Society Geophysical Journal*, v. 6, p. 312-319.
- Fisher, R.A., 1953, Dispersion on a sphere: *Proceedings of the Royal Society of London*, v. A217, p. 295-305.
- Foster, C.B., 1982, Spore-pollen assemblages of the Bowen Basin, Queensland (Australia): Their relationship to the Permian/Triassic boundary: *Review of Palaeobotany and Palynology*, v. 36, p. 165-183.
- Foster, C.B. and N.W. Archbold, 2001, Chronologic anchor points for the Permian Early Triassic of the eastern Australian basins: in Weiss, R.H., ed. *Contributions to Geology and Palaeontology of Gondwana in honour of Helmut Wopfner*: Geological Institute, University of Cologne, Germany, p. 175-199.
- Gastaldo, R.A., Adendorff, R., Bamford, M.K., Labandeira, Neveling, J., and Sims, H.J., 2005, Taphonomic Trends of Macrofloral Assemblages Across the Permian-Triassic Boundary, Karoo Basin, South Africa: *PALAIOS*, v. 20, p. 478-497.
- Gastaldo, R.A. and Demko, T.M., 2011, The relationship between continental landscape evolution and the plant-fossil record: Long term hydrologic controls on preservation: in Allison, P.A., and Bottjer, D.J., eds., *Taphonomy, Second Edition: Processes and Bias Through Time: Topics in Geobiology*, v. 32, p. 249-286.
- Gastaldo, R.A., Knight, C.L., Neveling, J. and Tabor, N.J., 2014. Latest Permian paleosols from Wapadsberg Pass, South Africa: Implications for Changhsingian climate. *Geological Society of America Bulletin*, V. 126, p. 665-679.
- Gastaldo, R.A., Kamo, S.L., Neveling, J., Geissman, J.W., Bamford, M. and Looy, C.V., 2015, Is the vertebrate-defined Permian-Triassic boundary in the Karoo Basin, South Africa, the terrestrial expression of the end-Permian marine event?: *Geology*, v. 43, p. 939-942.
- Gastaldo, R.A. and Neveling, J., 2012, The terrestrial Permian-Triassic boundary event is a nonevent: *REPLY*. *Geology*, v. 40, p. e257.
- Gastaldo, R.A., and Neveling, J., 2016, Comment on "Anatomy of a mass extinction: Sedimentological and taphonomic evidence for drought-induced die-offs at the Permo-Triassic boundary in the main Karoo Basin, South Africa" by R.M.H. Smith and J. Botha-Brink, *Palaeogeography, Palaeoclimatology, Palaeoecology*, v. 396, p. 99-118.
- Gastaldo, R.A., Neveling, J., Clark, C.K. and Newbury, S.S., 2009, The terrestrial Permian-Triassic boundary event bed is a nonevent: *Geology*, v. 37, p. 199-202.
- Gastaldo, R.A., Neveling, J., Looy, C.V., Bamford, M.K., Kamo, S.L., and Geissman, J.W., in review, Paleontology of the Blaauwater 67 and 65 Farms, South Africa: Testing the *Daptocephalus/Lystrosaurus* Biozone Boundary in a Stratigraphic Framework: *PALAIOS*.
- Gastaldo, R.A., Pludow, B.A., and Neveling, J., 2013, Mud aggregates from the Katberg Formation, South Africa: Additional evidence for Early Triassic degradational landscapes: *Journal of Sedimentary Research*, v. 83, p. 531-540.
- Gastaldo, R.A. and Rolerson, M.W., 2008. *Katbergia* gen. nov., a new trace fossil from Upper Permian and Lower Triassic rocks of the Karoo Basin: Implications for palaeoenvironmental conditions at the P/Tr extinction event: *Palaeontology*, v. 51, p. 215-229.



- Geissman, J.W., and Ferre, E.C., 2013, Paleomagnetism of Early Jurassic igneous rocks of the Karoo Large Igneous Province, South Africa, and an evaluation of Karoo paleomagnetic data bearing on the recently postulated Jurassic true polar wander event: Geological Society of America Abstracts with Programs, v. 45, p. 811.
- Glen, J.M.G., Nomade, S., Lyons, J.J., Metcalfe, I., Mundil, R., and Renne, P.R., 2009, Magnetostratigraphic correlations of Permian–Triassic marine-to-terrestrial sections from China: *Journal of Asian Earth Sciences*, v. 36, p. 521–540.
- Gorter, J.D., Nicholl, R.S., Metcalfe, I., Willink, R.J., and Ferdinando, D., 2009, The Permian–Triassic Boundary in West Australia – Evidence from the Bonaparte and Northern Perth Basins—Exploration Implications: *APPEA Journal*, 2009, p. 311–336.
- Gray, S.W., Neveling, J., and Gastaldo, R.A., 2004, Search for the Elusive Permian–Triassic “Laminites” in the Karoo Basin, South Africa: Geological Society of America Abstracts with Program, v. 36, n. 5, p. 74.
- Gresse, P.G., Theron, J.N., Fitch, F.J., and Miller, J.A., 1992, Tectonic inversion and radiometric resetting of the basement in the Cape Fold Belt: in de Wit, M.J., and Ransome, I.G.D., eds., *Inversion Tectonics of the Cape Fold Belt, Karoo and Cretaceous Basins of Southern Africa*: A.A. Balkema, Rotterdam, p. 217–228.
- Groenewald, G.H., 1989, Stratigrafie en sedimentologie van die Groep Beaufort in die Noordoos-Vrystaat: *Bulletin of the Geological Survey of South Africa*, v. 96, p. 1–62.
- Groenewald, G.H., 1991, Burrow casts from the *Lystrosaurus-Procolophon* Assemblage-zone, Karoo Sequence, South Africa: *Koedoe*, v. 34, p. 13–22.
- Groenewald, G.H., 1996, Stratigraphy of the Tarkastad Subgroup, Karoo Supergroup, South Africa: Unpublished Ph.D. Thesis, University of Port Elizabeth, South Africa, 145 p.
- Groenewald, G.H., and Kitching, J.W., 1995, Biostratigraphy of the *Lystrosaurus* Assemblage Zone: in Rubidge, B.S., ed., *Reptilian Biostratigraphy of the Permian–Triassic Beaufort Group (Karoo Supergroup)*: South Africa Commission on Stratigraphy, Biostratigraphic Series, v. 1, p. 35–39.
- Gurnis, M., Mitrovica, J.X., Ritsema, J., and van Heijst, H.-J., 2000, Constraining mantle density structure using geological evidence of surface uplift rates: The case of the African Superplume: *Geochemistry, Geophysics, Geosystems* 1, Paper No. 1999GC000035.
- Hälbich, I.W., 1983, A tectogenesis of the Cape Fold Belt: in Söhnge, A.P.G., and Hälbich, I.W., eds., *Geodynamics of the Cape Fold Belt*: Geological Society of South Africa, Special Publication 12, p. 165–175.
- Hälbich, I.W., and Swart, J., 1983, Structural zoning and dynamic history of the cover rocks of the Cape Fold Belt: in Söhnge, A.P.G., and Hälbich, I.W., eds., *Geodynamics of the Cape Fold Belt*: Geological Society of South Africa, Special Publication 12, p. 75–100.
- Hancox, P.J., Brandt, D., Reimold, W.U., Koeberl, C. and Neveling, J., 2002, Permian–Triassic boundary in the northwest Karoo Basin: Current stratigraphic placement, implications for basin development models, and the search for evidence of impact: *Geological Society of America, Special Paper* 356, p.429–444.
- Hargraves, R.B., Rehacek, J., and Hooper, P.R., 1997, Palaeomagnetism of the Karoo igneous rocks in southern Africa: *South African Journal of Geology*, v. 100, p. 195–212.
- Helby, R., Morgan, R., and Partridge, A.D., 1987, A palynological zonation of the Australian Mesozoic: *Memoirs of the Association of Australasian Palaeontologists*, v. 4, p. 1–94.
- Hermann, E., Hochuli, P.A., Bucher, H., Vigran, J.O., Weissert, H. and Bernasconi, S.M., 2010. A close-up view of the Permian–Triassic boundary based on expanded organic carbon isotope records from Norway (Trøndelag and Finnmark Platform): *Global and Planetary Change*, v. 74, p. 156–167.
- Hiller, N., and Stavrakis, N., 1984, Permo–Triassic fluvial systems in the southeastern Karoo Basin, South Africa: *Palaeogeography Palaeoclimatology Palaeoecology*, v. 45, p. 1–21.
- Holland, S.M., 2016, The non-uniformity of the fossil record: *Philosophical Transactions of the Royal Society B, Biological Sciences* v. 371, no. 20150130. doi: 10.1098/rstb.2015.0130.
- Holland, S.M., and Patzkowsky, M.E., 2015, The stratigraphy of mass extinction: *Palaeontology*, v. 58, p. 903–924.
- Horacek, M., Povoden, E., Richoz, S. and Brandner, R., 2010, High-resolution carbon isotope changes, litho- and magnetostratigraphy across Permian–Triassic Boundary sections in the Dolomites, N-Italy. New constraints for global correlation: *Palaeogeography, Palaeoclimatology, Palaeoecology*, v. 290, p. 58–64.
- Hotton, N., 1967, Stratigraphy and sedimentation in the Beaufort Series (Permian–Triassic), South Africa, in Teichert, C., ed., *Essays in paleontology and stratigraphy*: University of Kansas Department of Geology Special Publication 2, p. 390–428.

- Jha, N., 2006, Permian palynology from India and Africa: A phytogeographical paradigm: *Journal of the Palaeontological Society of India*, v. 51, p. 43–55.
- Johnson, M.R., 1966, The stratigraphy of the Cape and Karoo Systems in the Eastern Cape Province: Unpublished M.Sc. Thesis, Rhodes University, Grahamstown, South Africa, 76 p.
- Johnson, M.R., 1976, Stratigraphy and sedimentology of the Cape and Karoo Sequences in the Eastern Cape Province: Unpublished Ph.D. Thesis, Rhodes University, Grahamstown, South Africa, 336 p.
- Johnson, M.R., 1991, Sandstone petrography, provenance and plate tectonic setting in Gondwana context of the southeastern Cape–Karoo Basin: *South African Journal of Geology*, v. 94, p. 137–154.
- Johnson, M.R., Van Vuuren, C.J., Visser, J.N.J., Cole, D.I., Wickens H.DE V., Christie, A.D.M., Roberts, D.L., and Brandl, G., 2006, Sedimentary rocks of the Karoo Supergroup: in Johnson, M.R., Anhaeusser, C.R., and Thomas, R.J., eds., *The Geology of South Africa: the Geological Society of South Africa, Johannesburg, and the Council for Geoscience, Pretoria*, p. 461–499.
- Kalandadze, N.N., 1975, The first discovery of *Lystrosaurus* in the European regions of the USSR: *Palaeontological Journal*, v. 9, p. 557–560.
- Kammerer, C.F., Angielczyk, K.D., and Fröbisch, J., 2011, A comprehensive taxonomic revision of *Dicynodon* (Therapsida, Anomodontia) and its implications for dicynodont phylogeny, biogeography, and biostratigraphy: *Journal of Vertebrate Paleontology*, v. 31, p. 1–158.
- Kamo, S.L., Czamanske, G.K., Amelin, Y., Fedorenko, V.A., Davis, D.W. and Trofimov, V.R., 2003, Rapid eruption of Siberian flood–volcanic rocks and evidence for coincidence with the Permian–Triassic boundary and mass extinction at 251 Ma: *Earth and Planetary Science Letters*, v. 214, p.75–91.
- Keyser, A.W., 1979, A review of the biostratigraphy of the Beaufort Group in the Karoo Basin of South Africa: *Geological Society of South Africa, 15th Geocongress, Abstracts, Part 2*, p. 13–31.
- Keyser, A.W., 1981, The stratigraphic distribution of the Dicynodontia of Africa reviewed in a Gondwana context: in Creswell, M.M., and Vella, P., eds., *Gondwana Five: A.A. Balkema, Rotterdam*, p. 61–64.
- Keyser, A.W., and Smith, R.H.M., 1978, Vertebrate Biozonation of the Beaufort Group with Special Reference to the Western Karoo Basin: *Annals of the Geological Survey*, v. 12(1977–1978), p. 1–35.
- King, L.C., 1962, *The Morphology of the Earth: A Study and Synthesis of World Scenery: Oliver & Boyd, Edinburgh*, 799 p.
- King, G.M., and Jenkins, I., 1997, The dicynodont *Lystrosaurus* from the Upper Permian of Zambia: evolutionary and stratigraphical implications: *Palaeontology*, v. 40, p. 149–156.
- Kirschvink, J.L., and Ward, P.D., 1998, Magnetostratigraphy of the Permian/Triassic boundary sediments in the Karoo of South Africa: *Journal of African Earth Sciences* 27(1A), Spec. Abst. Issue Gondwana 10, Events Stratigraphy of Gondwana, 124 p.
- Kitching, J.W., 1971, A short review of the Beaufort zoning in South Africa: in Haughton, S.H., ed., *Second Gondwana Symposium, Proceedings & Papers*, p. 309–312.
- Kitching, J.W., 1977, The distribution of the Karoo vertebrate fauna: *Memoir of the Bernard Price Institute for Palaeontological Research, University of the Witwatersrand*, v. 1, p. 1–131.
- Kitching, J.W., 1978, The stratigraphic distribution and occurrence of South African fossil amphibia in the Beaufort beds: *Palaeontologia africana*, v. 21, p. 101–112.
- Kitching, J.W., 1995, Biostratigraphy of the *Dicynodon* Assemblage Zone: in Rubidge, B.S., ed., *Reptilian Biostratigraphy of the Permian–Triassic Beaufort Group (Karoo Supergroup): South Africa Commission on Stratigraphy, Biostratigraphic Series 1*, p. 29–34.
- Knoll, A.H., Bambach, R.K., Payne, J.L., Pruss, S., and Fischer, W.W., 2007, Paleophysiology and end-Permian mass extinction: *Earth and Planetary Science Letters*, v. 256, p. 295–313.
- Kutty, T.S., 1972, Permian reptilian fauna from India: *Nature*, v. 237, p. 462–463.
- Le Roux, J.P., 1983, Structural evolution of the Kango Group: in Sönghe, A.P.G., and Hälbich, I.W., eds., *Geodynamics of the Cape Fold Belt: Geological Society of South Africa Special Publication 12*, p. 47–56.
- Li, J.L., Gastaldo, R.A., and Neveling, J., 2015, Iron, Climate, and Mass Extinction: Geochemistry of Green-gray and Red-gray Siltstones Straddling the Vertebrate-defined, Permian–Triassic Mass Extinction in South Africa: *Geological Society of America Abstracts with Programs*, v. 47, no. 7, p. 570.
- Lindeque, A., de Wit, M.J., Ryberg, T., Weber, M., and Chevallier, I., 2011, Deep crustal profile across the southern Karoo Basin and Beattie magnetic anomaly, South Africa: An integrated interpretation with tectonic implications: *South African Journal of Geology*, v. 114, p. 265–292.



- Lipshultz, K., Gastaldo, R.A., Kamo, S., Neveling, J., and Geissman, J.W., 2015, Stratigraphic Contextualization of Volcanic Ash Deposited near the Permian–Triassic Boundary in the Karoo Basin, South Africa: *Geological Society of America, Abstracts with Program*, v. 47, no. 7, p. 569.
- Lucas, S.G., 2009, Timing and magnitude of tetrapod extinctions across the Permo–Triassic boundary: *Journal of Asian Earth Sciences*, v. 36, p. 491–502.
- Lucas, S.G., 2010, The Triassic timescale based on nonmarine tetrapod biostratigraphy and biochronology: *Geological Society of London, Special Publications*, v. 334, p. 447–500.
- Lucas, S.G., Hunt, A.P., Heckert, A.B., and Spielmann, J.A., 2007, Global Triassic tetrapod biostratigraphy and biochronology – 2007 status: *New Mexico Museum of Natural History and Science Bulletin*, v. 41, p. 229–240.
- MacLeod, K.G., Smith, R.M., Koch, P.L., and Ward, P.D., 2000, Timing of mammal-like reptile extinctions across the Permian–Triassic boundary in South Africa: *Geology*, v. 28, p. 227–230.
- Marshall, C.R., 1990, Confidence intervals on stratigraphic ranges: *Paleobiology*, v. 16, p. 1–10.
- Marshall, C.R., 2005, Comment on “Abrupt and gradual extinction among Late Permian land vertebrates in the Karoo Basin, South Africa”: *Science*, v. 308, p. 1413b.
- McKay, M.P., Weislogel, A.L., Fildani, A., Brunt, R.L., Hodgson, D.M. and Flint, S.S., 2015, U–Pb zircon tuff geochronology from the Karoo Basin, South Africa: implications of zircon recycling on stratigraphic age controls: *International Geology Review*, v. 57, p. 393–410.
- McLoughlin, S., Lindström, S., and Drinnan, A.N., 1997, Gondwanan floristic and sedimentological trends during the Permian–Triassic transition: new evidence from the Amery Group, northern Prince Charles Mountains, East Antarctica: *Antarctic Science*, v. 9, p. 281–298.
- Metcalfe, I., Nicoll, R.S., and Willink, R.J., 2008, Conodonts from the Permian Triassic transition in Australia and position of the Permian–Triassic boundary: *Australian Journal of Earth Sciences*, v. 55, p. 349–361.
- Metcalfe, I., Crowley, J.L., Nicoll, R.S., & Schmitz, M., 2015, High-precision U–Pb CA–TIMS calibration of Middle Permian to Lower Triassic sequences, mass extinction and extreme climate-change in eastern Australian Gondwana. *Gondwana Research*, v. 28 no. 1, p. 61–81, <http://dx.doi.org/10.1016/j.gr.2014.09.002>.
- Morante, R., 1996, Permian and early Triassic isotopic records of carbon and strontium in Australia and a scenario of events about the Permian–Triassic boundary: *Historical Biology*, v. 11, p. 289–310.
- Mory, A.J., and Backhouse, J., 1997, Permian stratigraphy and palynology of the Carnarvon Basin, western Australia: *Geological Survey of Western Australia, Perth, Report 51*, 37 p.
- Nanson, G.C., Rust, B.R., and Taylor, G., 1986, Coexistent mud braids and anastomosing channels in an arid-zone river: Cooper Creek, central Australia: *Geology*, v. 14, p. 175–178.
- Neveling, J., Hancox, P.J., and Rubidge, B.S., 2005, Biostratigraphy of the lower Burgersdorp Formation (Beaufort Group; Karoo Supergroup) of South Africa – Implications for the stratigraphic ranges of Early Triassic tetrapods: *Palaeontologia africana*, v. 41, p. 81–87.
- Neveling, J., Gastaldo, R.A., Kamo, S.L., Geissman, J.W., Looy, C.V., and Bamford, M.K., 2016, A Review of Stratigraphic, Geochemical, and Paleontologic Correlations Data of the Terrestrial end–Permian record in the Karoo Basin, South Africa: in de Wit, M., and Linol, B., eds., *The Origin and Evolution of the Cape Mountains and Karoo Basin*: Springer Publishing, Chapter 15.
- Newbury, S., Clark, C.K., Gastaldo, R.A., and Neveling, J., 2007, High Resolution Stratigraphy of the Permian–triassic Boundary at Bethulie, Karoo Basin South Africa: *Geological Society of America, Abstracts with Program*, v. 39, p. 148.
- Newton, A.R., Shone, R.W., & Booth, P.W.K., 2006, The Cape Fold Belt: in Johnson, M.R., Anhaeusser, C.R., and Thomas, R.J., eds., *The Geology of South Africa*: Geological Society of South Africa, Johannesburg / Council for Geoscience, Pretoria, p. 521–530.
- Ochev, V.G. and Shishkin, M.A., 1989, On the principles of global correlation of the continental Triassic on the Tetrapods: *Acta Palaeontologica Polonica*, v. 34, no. 2, p. 149–172.
- Ogg, J.G., 2004, Status of divisions of the International Geologic Time Scale: *Lethaia*, v. 37, p. 183–199.
- Opdyke, N.D., and Channel, J.E.T., 1966, *Magnetic Stratigraphy*: Academic Press, San Diego, 346 p.
- Pace, D.W., Gastaldo, R.A., and Neveling, J., 2009, Early Triassic aggradational and degradational landscapes of the Karoo Basin and evidence for climate oscillation following the P–Tr event: *Journal of Sedimentary Research*, v. 79, p. 316–331.
- Partridge, T.C., and Maud, R.R., 1987, Geomorphic evolution of southern Africa since the Mesozoic: *South African Journal of Geology*, v. 90, p. 179–208.

- Paton, D.A., Macdonald, D.I.M., and Underhill, J.R., 2006, Applicability of thin or thick skinned structural models in a region of multiple inversion episodes: Southern South Africa: *Journal of Structural Geology*, v. 28, p. 1933–1947.
- Payne, J.L., and Clapham, M.E., 2012, End-Permian mass extinction in the oceans: an ancient analog for the twenty-first century?: *Annual Review of Earth and Planetary Sciences*, v. 40, p. 89–111.
- Payne, J.L., Lehmann, D.J., Wei, J., Orchard, M.J., Schrag, D.P. and Knoll, A.H., 2004, Large perturbations of the carbon cycle during recovery from the end-Permian extinction: *Science*, v. 305, p. 506–509.
- Plotnick, R.E., Smith, F.A., and Lyons, K., The fossil record of the sixth extinction: *Ecology Letters*, v. 19, p. 546–553.
- Prevec, R., Labandeira, C.C., Neveling, J., Gastaldo, R.A., Looy, C.V., and Bamford, M.K., 2009, Portrait of a Gondwanan Ecosystem: A New Late Permian Locality from Kwazulu-Natal, South Africa: *Review of Palaeobotany and Palynology*, v. 156, p. 454–493.
- Prevec, R., Gastaldo, R.A., Neveling, J., Reid, S.B., and Looy, C.V., 2010, An Autochthonous Glossopterid flora with Latest Permian palynomorphs from the Dicynodon Assemblage Zone of the southern Karoo Basin, South Africa: *Palaeogeography Palaeoclimatology Palaeoecology*, v. 292, p. 381–408.
- Price, P.L., 1997, Permian to Jurassic palynostratigraphic nomenclature of the Bowen and Surat basins. in Green, P.M., ed., *The Surat and Bowen Basins, southeast Queensland*: Queensland Department of Mines and Energy, p. 137–178.
- Reid, S., Gastaldo, R.A., and Neveling, J., 2007, Fluvial Systems and Carbonate Nodules Reveal Late Permian Climate Change at Wapadsberg Pass, Eastern Cape Province, South Africa: *Geological Society of America Abstracts with Programs*, v. 39, no. 6, p. 85.
- Reitz, M.D., Pickering, J.L., Goodbred, S.L., Paola, C., Steckler, M.S., Seeber, L., and Akhter, S.H., 2015, Effects of tectonic deformation and sea level on river path selection: Theory and application to the Ganges-Brahmaputra-Meghna River Delta: *Journal of Geophysical Research: Earth Surface*, v. 120, p.671–689.
- Retallack, G.J., and Krull, E.S., 2006, Carbon isotopic evidence for terminal-Permian methane outbursts and their role in extinctions of animals, plants, coral reefs and peat swamps: in Greb, S., and DiMichele, W.A., eds., *Wetlands through time*: Geological Society of America Special Paper 399, p. 249–268.
- Retallack, G.J., Smith, R.M., and Ward, P.D., 2003, Vertebrate extinction across Permian–Triassic boundary in Karoo Basin, South Africa: *Geological Society of America Bulletin*, v. 115, p. 1133–1152.
- Rey, K., Amiot, R., Fourel, F., Rigaudier, T., Abdala, F., Day, M.O., Fernandez, V., Fluteau, F., France-Lanord, C., Rubidge, B.S., and Smith, R.M., 2015, Global climate perturbations during the Permo-Triassic mass extinctions recorded by continental tetrapods from South Africa: *Gondwana Research* GR-01523. Doi 10.1016/j.gr.2015.09.008
- Romer, A.S., 1966, The Chanares (Argentina) Triassic reptile fauna: *Breviora*, v. 247, p. 1–14.
- Romer, A.S., 1969, The Triassic faunal succession and the Gondwanaland problem: *Gondwana Stratigraphy*, Paris: UNESCO, p. 375–400.
- Roopnarine, P.D., and Angielczyk, K.D., 2015, Community stability and selective extinction during the Permian–Triassic mass extinction: *Science*, v. 350, p. 90–93.
- Roopnarine, P.D., Angielczyk, K.D., Wang, S.C., and Hertog, R., 2007, Trophic network models explain instability of Early Triassic terrestrial communities: *Proceedings of the Royal Society*, v. B274, p. 2077–2086.
- Rubidge, B.S., 2005, Re-uniting lost continents – Fossil reptiles from the ancient Karoo and their wanderlust: *South African Journal of Geology*, v. 108, p. 135–172.
- Rubidge B.S., Day, M.O., Barbolini, N., Hancox, P.J., Choiniere, J., Bamford, M.K., Viglietti, P.A., McPhee, B., and Jirah, S., 2016, Advances in Nonmarine Karoo Biostratigraphy: Significance for Understanding Basin Development: in de Wit, M., and Linol, B., eds., *The Origin and Evolution of the Cape Mountains and Karoo Basin*: Springer Publishing, Chapter 19.
- Rubidge, B.S., Erwin, D.H., Ramezani, J., Bowring, S.A., and de Klerk, W.J., 2013, High-precision temporal calibration of Late Permian vertebrate biostratigraphy: U–Pb zircon constraints from the Karoo Supergroup, South Africa: *Geology*, v. 41, p. 363–366.
- Rubidge, B.S., Johnson, M.R., Kitching, J.W., Smith, R.M.H., Keyser, A.W., and Groenewald, G.H., 1995, An introduction to the biozonation of the Beaufort Group: in Rubidge, B.S., ed., *Biostratigraphy of the Beaufort Group (Karoo Basin)*: South African Committee for Stratigraphy, *Biostratigraphic Series* 1, p. 1–2.
- Rubidge, B.S., Hancox, P.J., and Catuneanu, O., 2000, Sequence analysis of the Ecca–Beaufort contact in the southern Karoo of South Africa: *South African Journal of Geology*, v. 103, p. 81–96.
- Rubidge BS, Hancox PJ, Mason R., 2012, Waterford Formation in the south-eastern Karoo: Implications for basin development. *South African Journal of Science*, v.108 (3/4), Art. #829, 5 pages. [http:// dx.doi.org/10.4102/sajs.v108i3/4.829](http://dx.doi.org/10.4102/sajs.v108i3/4.829).



- Scheffler, K., Buehmann, D., and Schwark, L., 2006, Analysis of late Palaeozoic glacial to postglacial sedimentary successions in South Africa by geochemical proxies – Response to climate evolution and sedimentary environment: *Palaeogeography, Palaeoclimatology, Palaeoecology*, v. 240, p. 184–203.
- Schwindt, D.M., Rampino, M.R., Steiner M., Eshet Y., 2003, Stratigraphy, paleomagnetic results, and preliminary palynology across the Permian–Triassic (P–Tr) boundary at Carlton Heights: in Koerberl, C. and Martinez-Ruiz, F., *Impact markers in the stratigraphic record*: Springer, Heidelberg, p. 280–302.
- Sheldon, N.D., 2005, Do red beds indicate paleoclimatic conditions?: A Permian case study, *Palaeogeography, Palaeoclimatology, Palaeoecology*, v. 228, p. 305–319.
- Shen, S.Z., Crowley, J.L., Wang, Y., Bowring, S.A., Erwin, D.H., Sadler, P.M., Cao, C.Q., Rothman, D.H., Henderson, C.M., Ramezani, J., Zhang, H., Shen, Y., Wang, X.D., Wang, W., Mu, L., Li, W.Z., Tang, Y.G., Liu, X.L., Liu L.J., Zeng, Y., Jiang, Y.F., and Jin, Y.G., 2011, Calibrating the end-Permian mass extinction: *Science*, v. 334, p. 1367–1372.
- Shone, R.W., 2006, Onshore Post-Karoo Mesozoic Deposits: in Johnson, M.R., Anhaeusser, C.R., and Thomas, R.J., eds., *The Geology of South Africa: Geological Society of South Africa, Johannesburg / Council for Geoscience, Pretoria*, p. 541–552.
- Signor, P.W., and Lipps, J.H., 1982, Sampling bias, gradual extinction patterns, and catastrophes in the fossil record: in Silver, L.T., and Schultz, P.H., eds., *Geological implications of impacts of large asteroids and comets on the Earth: Geological Society of America Special Publication*, v. 190, p. 291–296.
- Sixsmith, P.J., Flint, S.S., Wickens, H. de V., and Johnson, S.D., 2004, Anatomy and stratigraphic development of a Basin floor turbidite system in the Laingsburg Formation, Main Karoo Basin, South Africa: *Journal of Sedimentary Research*, v. 74, p. 239–254.
- Smith, R.M.H. 1987, Morphology and Depositional History of exhumed Permian point bars in the southwestern Karoo, South Africa: *Journal of Sedimentary Petrology*, v. 57, no. 1, p. 19–29.
- Smith, R.M.H., 1995, Changing fluvial environments across the Permian–Triassic boundary in the Karoo Basin, South Africa and possible causes of tetrapod extinctions: *Palaeogeography, Palaeoclimatology, Palaeoecology*, v. 117, p. 81–104.
- Smith, R.M.H., and Botha, J., 2005, The recovery of terrestrial vertebrate diversity in the South African Karoo Basin after the end-Permian Extinction: *Compte Rendu Palevol*, v. 4, p. 555–568.
- Smith, R.M.H., and Botha-Brink, J., 2014, Anatomy of a mass extinction: Sedimentological and taphonomic evidence for drought-induced die-offs at the Permo–Triassic boundary in the main Karoo Basin, South Africa: *Palaeogeography, Palaeoclimatology, Palaeoecology*, v. 396, p. 99–118.
- Smith, R.M.H., and Kitching, J.W., 1995, Biostratigraphy of the *Cistecephalus* Assemblage Zone: in Rubidge, B.S., ed., *Reptilian Biostratigraphy of the Permian–Triassic Beaufort Group (Karoo Supergroup): South Africa Commission on Stratigraphy, Biostratigraphic Series 1*, p. 23–28.
- Smith, R.M.H., and Ward, P.D., 2001, Pattern of vertebrate extinctions across an event bed at the Permian–Triassic boundary in the Karoo Basin of South Africa: *Geology*, v. 29, p. 1147–1150.
- Söhnge, A.P.G., 1983, The Cape Fold Belt—Perspective: in Söhnge, A.P.G., and Hälbig, I.W., eds., *Geodynamics of the Cape Fold Belt: A Contribution to the National Geodynamics Programme: Geological Society of South Africa Special Publication 12*, p. 1–6.
- Song, H., Wignall, P.B., Tong, J., and Yin, H., 2013, Two pulses of extinction during the Permian–Triassic crisis: *Nature Geoscience*, v. 6, p. 52–56.
- South African Committee for Stratigraphy, 1980, *Stratigraphy of South Africa. Part 1: Africa, South West Africa/Namibia, and the republics of Bophuthatswana, Transkei and Venda: Geological Survey of South Africa, Handbook 8*, p. 535–548.
- Stankiewicz, J., Ryberg, T., Schulze, A., Lindeque, A., Weber, M.H., and de Wit, M.J., 2007, Initial results from wide-angle seismic refraction lines in the southern Cape: *South African Journal of Geology*, v. 110, p. 407–418.
- Stavrakis, N., 1980, Sedimentation of the Katberg Sandstone and adjacent formation in the southeastern Karoo Basin: *Transactions of the Geological Society of South Africa*, v.83, p.361–374. Stear, W.M. 1985. Comparison of the Bedform Distribution and Dynamics of modern and ancient Sandy Ephemeral Flood Deposits in the southwestern Karoo region, South Africa: *Sedimentary Geology*, v. 45, p. 209–230.
- Steiner, M.B., 2006. The magnetic polarity time scale across the Permian–Triassic boundary: *Geological Society, London, Special Publications*, v. 265, p. 15–38.
- Steiner, M.B., Eshet, YU., Rampino, M.R., and Schwindt, D.M., 2003, Fungal abundance spike and the Permian–Triassic boundary in the Karoo Supergroup (South Africa): *Palaeogeography, Palaeoclimatology, Palaeoecology*, v. 194, p. 405–414.

- Stoops, G., 1989, Relict properties in soils of humid tropical regions with special reference to central Africa: in Bronger, A., and Catt, J.A., eds., *Paleopedology: Nature and Application of Paleosols*: Catena, Berlin, Supplement 16, p. 95-106.
- Straub, K., Paola, C., Kim, W., and Sheets, B., 2013, Experimental investigation of sediment-dominated vs. tectonic-dominated sediment transport systems in subsiding basins: *Journal of Sedimentary Research*, v. 83, p. 1162-1180.
- Szurliés, M., 2007, Latest Permian to Middle Triassic cyclo-magnetostratigraphy from the Central European Basin, Germany: implications for the geomagnetic polarity timescale: *Earth and Planetary Science Letters*, v. 261, p. 602-619.
- Szurliés, M., 2013, Late Permian (Zechstein) magnetostratigraphy in Western and Central Europe, in Gasiewicz, A., and Stowakiewicz, M., (eds.), *Palaeozoic Climate Cycles: Their Evolutionary and Sedimentological Impact*. Geological Society, London, Special Publications, 376, p.73-85, doi: 10.1144/SP376.7.
- Tabor, N.J., Montañez, I.P., Steiner, M. and Schwindt, D., 2007. The $\delta^{13}\text{C}$ values of Permo-Triassic carbonates from South Africa reflect a stinking, sulfurous swamp, not atmospheric conditions: *Palaeogeography, Palaeoclimatology, Palaeoecology*, v. 225, p. 370-381.
- Tankard, A., Welsink, H., Aukes, P., Newton, R., and Stettler, E., 2009, Tectonic evolution of the Cape and Karoo basins of South Africa: *Marine and Petroleum Geology*, v. 26, p. 1379-1412.
- Thamm, A.G. and Johnson M.R., 2006, The Cape Supergroup: in M.R. Johnson, M.R., Anhaeusser, C.R., and Thomas. R.J. (eds.), *The Geology of South Africa*: Geological Society of South Africa, Johannesburg, and Council for Geoscience, Pretoria, p. 443-460,
- Toerien, D.K., 1979, *The Geology of the Oudtshoorn Area (Explanation: Sheet 3322 (1:250 000)*. Geological Survey , 13 p.
- Tooth, S., and Nanson, G.C., 1995, The geomorphology of Australia's fluvial systems: retrospect, perspect and prospect: *Progress in Physical Geography*, v. 19, p. 35-60.
- Turner, B.R., 1999, Tectonostratigraphical development of the Upper Karoo foreland basin: orogenic unloading versus thermally-induced Gondwana rifting: *Journal of African Earth Sciences*, v. 28, p. 215-238.
- Viglietti, P.A., Smith, R.M., Angielczyk, K.D., Kammerer, C.F., Fröbisch, J., and Rubidge, B.S., 2016, The *Daptocephalus* Assemblage Zone (Lopingian), South Africa: A proposed biostratigraphy based on a new compilation of stratigraphic ranges: *Journal of African Earth Sciences*, v. 113, p. 153-164.
- Wang, W., Cao, C.Q., and Wang, Y., 2004, The carbon isotope excursion on GSSP candidate section of Lopingian–Guadalupian boundary: *Earth and Planetary Science Letters*, v. 220, p. 57–67.
- Ward, P.D., Montgomery, D.R. and Smith, R.H.M., 2000, Altered river morphology in South Africa related to the Permian–Triassic extinction: *Science*, v. 289, p. 1740-1743.
- Ward, P.D., Botha, J., Buick, R., De Kock, M.O., Erwin, D.H., Garrison, G.H., Kirschvink, J.L. and Smith, R., 2005, Abrupt and gradual extinction among Late Permian land vertebrates in the Karoo Basin, South Africa: *Science*, v. 307, p. 709-714.
- Ward, P.D., Retallack, G.J., and Smith, R.M.H., 2012, The terrestrial Permian–Triassic boundary event bed is a nonevent: *COMMENT: GEOLOGY*, v. 40, p. e256.
- Watson, D.M.S., 1942, On the Permian and Triassic tetrapods: *Geological Magazine*, v. 79, p. 81-116.
- Wickens, H. de V., 1994, Basin floor fan building turbidites of the southwestern Karoo Basin, Permian Ecca Group, South Africa: PhD thesis (unpublished), University of Port Elizabeth, 233 p.
- Wopfner, H., 2002, Tectonic and climatic events controlling deposition in Tanzanian Karoo basins: *Journal of African Earth Science*, v. 34, p. 167–177.
- Zijderveld, J.D.A., 1967, Demagnetization of rocks: Analysis of results: in Collinson, D.W., Creer, K.M., and Runcorn, S.K., eds., *Methods in Palaeomagnetism*: Elsevier, Amsterdam, p. 254- 286.

